Tectonics, structural analysis and geodynamic evolution of the Maghrebian Flysch Basin and Ligurian Accretionary Complex Units: Examples in the Western Mediterranean Area

A dissertation

submitted to the department of Earth,

Environment and Resourse Sciences

and the committee on graduate studies

of University of Naples, Federico II

Dottorato di Ricerca (ciclo XXVII) in “Scienze della Terra"

Francesco D'Assisi Tramparulo

Tutor: Ph.D. Stefano Vitale

Cotutors: Ph.D. Sabatino Ciarcia

Ph.D. Lorenzo Fedele

Prof. Mohamed Najib Zaghloul

Sommario

Abstract

This work provides a structural study on some successions of the Ligurian Accretionary Complex (LAC; southern Italy), Maghrebian Flysch Basin (MFB; Morocco) and External *Dorsale Calcaire* (Morocco). The LAC Units, cropping out in the southern Apennines include the sedimenary deep basin successions of *Nord-Calabrese*, *Parasicilide and Sicilide*. Presently they are the highest tectonic units of the South Apennine fold and thrust belt. They are all characterized by a polyphasic and progressive deformation related to the Early Miocene inclusion in the tectonic accretionary wedge, by means of a frontal accretion mechanism, with a mean E/SE tectonic vergence. A subsequent deformation stage, associated to the eastward migration of the thrust front, affecting also the Middle-Upper Miocene unconformable wedge-top basin deposits, was characterized by a mean E/NE tectonic transport. In this orogenic phase the Apennine thrust sheet pile, formed by LAC and Apennine Platform Units, tectonically covered the successions located in the westernmost sector of the *Lagonegro-Molise* Basin. Finally a Pliocene-Middle Pleistocene regional fold set deformed the whole orogenic prism, comprised the LAC Units as consequence of a thick-skinned tectonics expressed by means of deeply rooted thrusts in the buried Apulian Platform carbonates. The metamorphic units of LAC, analyzed in this study, are the *Frido* and *Diamante-Terranova* Units, cropping out at *Calabria-Basilicata* boundary and northern *Calabria*, respectively. Both units are characterized by a HP/LT metamorphism reaching pressures of ca. 1.4/1.2 and 1.0 GPa and temperatures of 350-360 and 380 °C, respectively. The HP/LT parageneses include the Fe-carpholite, chlorite and phengite for the *Frido* and glaucophane, lawsonite, epidote and chlorite

for the *Diamante-Terranova* Unit. The tectonic exhumation was recorded by Ca-amphiboles. The P-T-paths, presented below, of both units indicate a cool and rapid exhumation. This is testified also by the preservation of HP/LT mineral parageneses and by non-isothermal exhumation such as marked in the P-T-paths of the *Frido*(this work) and *Diamante-Terranova* (Liberi and Piluso, 2009) Units. These units were subducted in the latest Oligocene and Early Eocene, respectively, with their complete exhumation in the middle Tortonian. The comparable geodynamic evolution of the LAC Units suggests an origin of all successions in a common oceanic domain (Ligurian Ocean) characterized by a western sector floored by oceanic crust (Diamante-Terranova domain), a central sector represented by an Ocean Continent Transition (*Frido* and *Nord-Calabrese* domain) and an eastern area formed by thinned continental crust (*Parasicilide* and *Sicilide* domain).

A further aim of this study is the reconstruction of the tectonic evolution of some successions of the Maghrebian Flysch Basin (MFB) domain (Predorsalian and Massylian Units) and the External *Dorsale Calcaire* in a key area (Chefchaouen) of the Rif chain in the northern Morocco. Maghrebian Flysch Basin successions show a comparable stratigraphy with the sedimentary LAC successions, suggesting paleogeographic continuity between LAC, located to E/NE, and the MFB to the W. The Triassic-Lower Miocene External *Dorsale Calcaire* succession overthrust the Predorsalian Unit through a regional thrust fault well-exposed in Chefchaouen area. The kinematic analysis of this structure and all minor structures in the footwall, indicate a SW-tectonic vergence. The Predorsalian unit in turn overthrust the Massylian succession characterized by a similar progressive deformation. The whole tectonic pile was subsequentely deformed by thrust and folds verging to NW. Like the sedimentary LAC units, the MFB Units were deformed by frontal accretion in the Burdigalian-Langhian time. The External *Dorsale Calcaire* provides a good example of Inversion Tectonics. The Liassic succession (cherty limestones and conglomerates) recorded the extension related to the Jurassic rifting of the Neotethys Domain as normal faulting and veining.The subsequent inclusion of these rocks in the orogenic wedge, which mainly occurred in the Miocene time, deformed the most of pre-orogenic structures in a passive manner, with only few cases of reverse reactivation; whereas, frequently, pre-orogenic normal fault planes show only an indentation of hanging-wall and footwall (buttressing effect). The orogenic deformation includes two main stages; the first tectonic pulse, which occurred during the Burdigalian-Langhian interval, was characterized by a NE-SW shortening and recorded by folds, thrust and back-thrust faults. During this stage the carbonates of the External *Dorsale Calcaire* tectonically covered the Predorsalian succession, producing, in the thrust front, a SW-verging regional fold. The second orogenic deformation, consisting of a NW-SE shortening, was expressed by thrust faults and related folds both verging to NW and SE, which probably occurred in the Late Miocene-Pliocene time.

Riassunto

Questo lavoro fornisce uno studio strutturale sulle successioni del Complesso d'Accrezione Liguride (CAL; Italia meridionale), del Bacino dei Flysch Magrebidi (BFM; Marocco) e della *Dorsale Calcaire* Esterna (Marocco). Le unità del CAL, affioranti in Appennino meridionale, includono le successioni sedimentarie di bacino profondo (Nord-Calabrese, Parasicilide e Sicilide). Attualmente, esse rappresentano le unità più alte della catena appenninica. Queste successioni sono tutte caratterizzate da una deformazione polifasica e progressiva associata al loro inserimento, nel Miocene Inferiore, nel cuneo d'accrezione tettonico, attraverso il meccanismo d'accrezione frontale, con una vergenza tettonica media E/SE. Una fase tettonica successiva, associata alla migrazione verso Est del fronte della catena orogenica, che coinvolge anche i depositi discordanti di tipo *wedge-top basin*, di età Miocene Medio-Superiore, è stata caratterizzata da un trasporto tettonico medio verso E/NE. In questa fase orogenica, la pila di falde tettoniche appenniniche, formata dal CAL e dalle unità di Piattaforma Appenninica, ricopre tettonicamente le successioni poste nel settore più occidentale del Bacino Lagonegrese-Molisano. Infine, pieghe e sovrascorrimenti regionali, di età Pliocene Medio-Pleistocene, hanno deformato l'intero prisma orogenico, comprese le unità del CAL, come conseguenza di una tettonica *thick-skinned* espressa per mezzo di faglie profonde nei carbonati sepolti della Piattaforma Apula. Le unità metamorfiche del CAL, analizzate in questo studio, sono le Unità del Frido e Diamante-Terranova, affioranti rispettivamente al confine calabro-lucano e in Calabria settentrionale. Entrambe sono caratterizzate da un metamorfismo di AP/BT che raggiunge, rispettivamente, pressioni di circa 1.4/1.2 e 1.0 GPa e temperature di

350-360 e 380 °C. Le paragenesi di AP/BT sono rappresentate dalle fasi Fe-carfolite, clorite e fengite per l'Unità del Frido e glaucofane, lawsonite, epidoto e clorite per l'Unità Diamante-Terranova. L'esumazione tettonica è stata registrata dall'anfibolo calcico. I *P-T-path*, presentati in seguito, di entrambe le unità indicano un'esumazione fredda e rapida. Questo è testimoniato anche dalla conservazione delle paragenesi mineralogiche e dall'esumazione non isotermica, evidenziata nei P-T-*path*. Le unità del Frido e Diamante-Terranova probabilmente sono state subdotte, rispettivamente, nel tardo Oligocene e nell'Eocene Inferiore, con la loro completa esumazione nel Tortoniano medio. L'evoluzione geodinamica simile delle unità del CAL, suggerisce un'origine in un dominio oceanico comune (oceano Liguride), caratterizzato da un settore occidentale di crosta oceanica (Ofioliti Calabresi), un settore centrale di transizione oceano-continente (Unità del Frido e Nord-Calabrese) e un dominio orientale formato da crosta continentale assottigliata (Unità Parasicilide e Sicilide).

Altro scopo di questo studio è la ricostruzione dell'evoluzione tettonica di alcune successioni del BFM (*Predorsalian* e *Massylian*) e della *Dorsale Calcaire* Esterna in un'area chiave (Chefchaouen) della catena del Rif nel Marocco settentrionale. Le successioni del BFM mostrano una stratigrafia comparabile con le successioni sedimentarie del CAL, che suggerisce una continuità paleogeografica tra il CAL, collocato a E/NE, e il BFM a Ovest. La successione triassico-miocenica della *Dorsale Calcaire* Esterna ricopre l'Unità *Predorsalian* per mezzo di un sovrascorrimento regionale ben esposto nell'area di *Chefchaouen*. L'analisi cinematica di questa struttura, e di tutte quelle minori presenti nel letto, indica una vergenza tettonica verso SO. Quest'ultima unità, a sua volta, ricopre la successione *Massylian* caratterizzata da una simile deformazione progressiva. Tutta la pila tettonica è stata, infine, deformata da pieghe e sovrascorrimenti vergenti a NO. Come le unità sedimentarie del CAL, le unità del BFM sono state impilate per mezzo di accrezione frontale nel Burdigaliano-Langhiano.

La *Dorsale Calcaire* Esterna, appartenente al dominio interno, rappresenta un buon esempio d’inversione tettonica. La successione liassica (calcari e conglomerati con selce) ha registrato l'estensione relativa al *rifting* giurassico del dominio della Neotetide attraverso faglie normali e vene. La successiva inclusione di queste rocce nel cuneo orogenico, avvenuta principalmente nel Miocene, ha deformato la maggior parte delle strutture pre-orogeniche in modo passivo, con solo pochi casi di riattivazione in senso inverso; mentre, più frequentemente, i piani di faglia normale preorogenici mostrano solo un’indentazione del blocco di tetto e di letto. La deformazione orogenica include due stadi principali; il primo impulso tettonico, avvenuto durante l'intervallo Burdigaliano-Langhiano, fu caratterizzato da un raccorciamento NE-SO e registrato da pieghe, sovrascorrimenti e retro-scorrimenti. Durante questo stadio i carbonati della *Dorsale Calcaire* Esterna hanno ricoperto tettonicamente la successione *Predorsalian*, producendo, a fronte della catena orogenica, una piega regionale vergente a SO. La seconda deformazione orogenica, che consiste in un raccorciamento NO-SE, è stata registrata da sovrascorrimenti e relative pieghe vergenti sia a NO sia a SE, probabilmente avvenuta nel tardo Miocene-Pliocene.

Chapter 1– Introduction and geological setting

1.1. Introduction

The western peri-Mediterranean Alpine chains form a poly-arcuate orogenic belt including Apennines, Calabrian Arc, Maghrebian chains and western Betic Cordillera (Fig. 1). As a whole, these orogens are formed by the superposition of several thrust sheets (amongst others Kornprobst, 1974; Chalouan, 1986; Bonardi et al., 2001; Michard et al., 2002; 2006; 2007; 2014; Guerrera et al., 2005; Handy et al., 2010; Mazzoli and Martin-Algarra 2011; Vitale and Ciarcia, 2013) grouped in three main tectonic complexes: (i) Internal Units; (ii) Maghrebian Flysch and Ligurian Accretionary Complex Units; and (iii) External Units.

Internal Units consist of Paleozoic continental crust, high-grade metamorphic and mantle rocks, and Mesozoic covers characterized by different degrees of metamorphism (e.g. Kornprobst, 1974; Chalouan, 1986; Bonardi et al., 2001). From the first attempts to find a common origin for the Internal Units (e.g. Haccard et al., 1972; Alvarez et al., 1974), now a days two different models are facing. The first model suggests that Internal Units were originated by a common microplate (AlKaPeCa or Mesomediterranean Terrain, Michard et al., 2002; Guerrera et al., 2005; Handy et al., 2010) separated, in the Jurassic-Cretaceous time, from the European plate to the West and the Apulia-African plate to the East by two oceanic branches (e.g. Michard et al., 2002; Handy et al., 2010): W-Ligurian/Betic and E-Ligurian/Maghrebian Flysch Oceans, respectively. The second model was firstly introduced by Boullin (1984) and Knott (1987) and reprised in the last years (e.g. Faccenna et al., 2001; Rossetti et al., 2004; Schettino and Turco, 2011; Vignaroli et al., 2012). This paleogeography envisages the existence of a single ocean (Ligurian Ocean, Knott, 1987; Ligurian Tethys, Schettino and Turco, 2011), with the Internal Units forming the SE margin of the European plate. However in both models, since the (i) Eocene (Vignaroli et al., 2012 and reference therein) and (ii) Early Miocene (Chalouan et al., 2006; Ciarcia et al., 2012), the Ligurian Ocean and Maghrebian Flysch Basin (MFB) successions, respectively, were deformed and tectonically overthrusted by the Internal Units. The migration of different orogenic arcs was mainly driven by the roll-back of the downgoing lithospheres (Malinverno and Ryan, 1986; Faccenna et al., 1996) producing the dispersion of the early internal domain along the western Mediterranean margins (Alvarez et al., 1974). Presently (Fig. 1), Maghrebian Flysch Basin (MFB) and Ligurian Accretionary Complex (LAC) are sandwiched between Internal Units on the top and External Units on the bottom, the latter formed by sedimentary successions deposited onto the continental margins of Adria, Africa and Iberia plates (e.g. Chalouan et al., 2008; Mazzoli and Algarra, 2011; Vitale and Ciarcia, 2013).

Despite of their wide spreading in the all Alpine belts, the MFB and LAC Units were poor-studied from the point of view of deformation, structural setting, kinematics and relationships with the overlaying and underling Internal and External Units, respectively.

In relation to these issues, this work is aimed to provide:

- A structural analysis of the LAC cropping out in the southern Apennines and northern Calabria (i.e. *Frido*, *Nord Calabrese*, *Parasicilide*, *Sicilide* and *Diamante-Terranova* Units).

- Petrographic and micro-structural analyses of metamorphic rocks of *Frido* and *Diamante-Terranova* Units.
- Structural analyses of MFB Units (Massylian and Predorsalian Units) and External *Dorsale Calcaire* succession (Internal domain), cropping out in a key area of Moroccan Rif, located near Chefchaouen.
- Kinematic analysis of the main thrust fault between External *Dorsale Calcaire* (Internal domain) and Predorsalian Units (MFB);

Successively, all structural data will be analyzed and used to reconstruct:

- The deformation evolution of the analyzed successions;
- A geodynamic evolution well-fitting with the peri-Mediterrenean orogenic history. Finally a comparison between the results from the different units located in the southern Apennines, northern *Calabria* and Rif.

In the following chapters, after a geological setting description of the southern Apennines\Calabrian Arc, a review of LAC stratigraphy is described, followed by the description of the petrographic, micro- and meso-structural analyses and the reconstruction of the deformation and geodynamic evolutions. In the second part of the work, Rif chain structure and stratigraphy of Massylian and Predorsalian Units (MFB) and External *Dorsale Calcaire* Unit (Internal Domain) are described, followed by the structural analysis. These results, added to information of the available literature, allowed to reconstruct, such as made before, the deformation and geodynamic evolutions. Finally, a comparison between the deformation evolutions of the analyzed successions is provided.

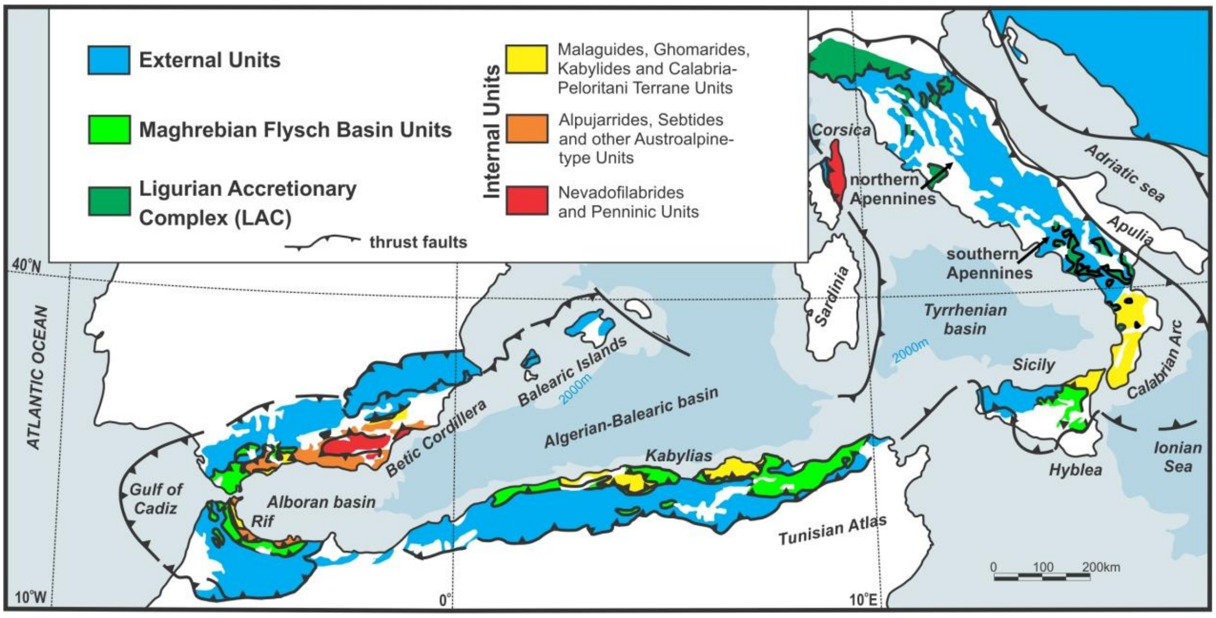

Fig. 1- Schematic tectonic map of the circum-Mediterranean orogenic belts (modified after Mazzoli and Martin-Algarra, 2011).

1.2. Geological setting of the southern Apennines/northern Calabria

Southern Apennines and *Calabria-Peloritani* Terrane (CPT; Figs. 2, 3) are segments of a long peri-Mediterranean orogen which comprises also Alps, Maghrebian chain (Sicily, Tunisia, Algeria and Morocco), Betic Cordillera (southern Spain), Balearic Island and part of Corsica Island (Fig. 1, 3c). These orogenic belts are all defined by the superposition of three tectonic units originated from: (i) internal domains, made of continental crust and sedimentary covers; (ii) oceanic and thinned continental crust and relative sedimentary covers, known as Maghrebian Flysch Basin, to S/SW, and Ligurian domain, to E/NE (e.g., Knott, 1987; Guerrera et al., 2005; Ciarcia et al., 2012); and (iii) external domains represented by African and European margin successions.

Taking into account the analyzed sector, going from northern *Calabria* until to the southern Apennines (Fig. 3a), the structural architecture is characterized by three main tectonic complex: (i) tectonic units formed by Paleozoic continental crust rocks and their Mesozoic covers with different grade and age of metamorphism (*Sila*, *Castagna* and *Bagni* Units; Fig. 2; Amodio-Morelli et al., 1976; Bonardi et al., 2001), referable to Internal Units in analogy with other peri-Mediterranean chains (Guerrera et al. 2005); (ii) Calabrian ophiolites successions, (Fig. 2, 3; *Diamante-Terranova*, *Malvito*, *Gimigliano* and *Frido* Units; Amodio-Morelli et al., 1976; Bonardi et al., 2001; Rossetti et al., 2001, 2004; Liberi et al., 2006; Liberi and Piluso, 2009; Vitale et al., 2013a and references therein) affected by an HP-LT/HP-VLT metamorphism, and sedimentary deep basin successions (Fig. 2, 3a, b; *Nord Calabrese, Parasicilide* and *Sicilide* Units; Selli, 1962; Ogniben, 1969; Bonardi et al., 1988a; Ciarcia et al., 2009;

Vitale et al., 2010, 2011, 2013b; Ciarcia et al., 2012), all together forming the Ligurian Accretionary Complex (LAC); and finally (iii) External Units (Fig. 1), formed by the superposition of covers of Apulian (African) block formed by successions, Mesozoic to Neogene in age (D'Argenio et al., 1973; Bonardi et al., 1988b, 2009; Patacca et al. 1990; Bigi et al., 1992; Cosentino et al., 2003; Patacca and Scandone, 2007), partially detached from their pre-Triassic basement (e.g., Casero et al., 1988; Menardi Noguera and Rea, 2000; Shiner et al., 2004; Cippitelli, 2007).

The building up of the southern Apennines\CPT system consists of two main geodynamic phases (Dewey et al., 1989; Faccenna et al., 2001): (i) Late Oligocene-Middle Miocene trench migration, accompanied by opening of the Ligurian-Provençal back-arc basin and (ii) Tortonian-Pleistocene migration, with opening of the Tyrrhenian back-arc basin (e.g., Roure et al., 1991; Liotta et al., 1998; Carmignani et al., 2001; Mazzoli et al., 2008; Molli, 2008; Mantovani et al., 2009; Carminati et al., 2012; Turco et al., 2012; Vitale and Ciarcia, 2013). The orogenic accretion of the Apennine prism, was characterized by a relatively fast migration of the thrust front-foredeep system (Faccenna et al., 2001; Vitale and Ciarcia, 2013), mainly driven by the eastward retreat of a west-directed oceanic slab (roll-back mechanism; Malinverno and Ryan, 1986; Carminati et al., 2012, and references therein). The development of the Apennine mountain belt and the associated fast E-W opening of the Tyrrhenian Sea (with spreading values up to ~10 cm/yr, Faccenna et al., 2001), compared with the slow N-S convergence between the Eurasian and the African/Adria plates (of the order of ~1 cm/yr; e.g., Mazzoli and Helman, 1994), indicate that a complex pattern of forces controlled the evolution of the proto-Central-Western Mediterranean Sea (e.g., Lustrino et al., 2011). The closure of the oceanic domain (E-Ligurian Ocean; Handy et al., 2010) interposed between the continental paleomargins and the still active subduction of the Ionian lithosphere (Minelli and Faccenna, 2010) allowed the overriding Calabria-Peloritani Terrane (CPT; Fig. 3) (Bonardi et al., 2001) to move E/SE-ward by at least 1000 km from ~30 Ma to the Present (Carminati et al., 2012; Vitale and Ciarcia, 2013) and produced widespread orogenic volcanism since the Eocene-Oligocene (Savelli, 2002) with the maximum development in Miocene time (Lustrino et al., 2009).

The shallow crustal structure of the southern Apennines (Fig. 2) is marked by the superposition, by means of low-angle tectonic contacts, of the Apennine Platform carbonate platform\slope successions; in the hanging wall, and the pelagic successions of *Lagonegro-Molise* Units (Scandone, 1967, 1972; Mostardini and Merlini, 1986) in the footwall. At deepest levels, the Apennine structure is dominated by high-angle normal faults affecting both the buried Apulian Platform and allochtonous successions (Fig. 2). The highest tectonic position, presently, is occupied by the deep basin successions, locally including oceanic to continental lithospheric rocks, forming the LAC (Fig. 1). These units are detached from their pre-Cretaceous successions, (*Nord-Calabrese*, *Parasicilide* and *Sicilide* Unit; Bonardi et al., 1988a; Monaco et al., 1991; Ciarcia et al., 2009, 2012 and references therein); whereas the HP/VLT *Frido Unit* is characterized by an OCT (Ocean Continent Transition) basement, characterized by the juxtaposition of oceanic crust and continental lithosphere materials and by scarcity of effusive rocks, and a meta-sedimentary basin succession (Knott, 1987, 1994; Vitale et al., 2013a). Finally, the LAC is unconformably covered by a Langhian-lowermost Tortonian succession named *Cilento* Group (Amore et al., 1988; Russo et al., 1995), including arenitic and marly deposits of *Pollica* and *San Mauro* Fms. (Ietto et al., 1965), and corresponding to the clastic undifferentiated succession of the *Albidona* Fm., in Lucania region (Selli, 1962; Bonardi et al., 1985). In Calabria-Lucania boundary area further wedge-top basin successions, unconformable on the previous units, and characterized by dominantly coarse-grained clastic deposits, include the Upper Miocene *Perosa* (*sensu* Vezzani,1966) and *Oriolo* Fms. (Selli, 1962; Fig. 2).

In such a geodynamic setting, slices of oceanic and continental crust and related sedimentary cover were subducted, reaching relatively high pressure conditions, and then quickly exhumed, allowing to preserve high pressure-low temperature (HP/LT) metamorphic assemblages (e.g., Stöckhert et al., 1999; Oberhänsli et al., 2001; Rossetti et al., 2004; Iannace et al., 2007; Brun and Faccenna, 2008; Liberi and Piluso, 2009; Vignaroli et al., 2009; Brogi and Giorgetti, 2012). A HP/LT event has been documented in the southern Apennines since the '70s (De Roever, 1972; Spadea, 1976,1982; Lanzafame et al., 1979) within the ophiolitic succession of the *Frido* Unit (Knott, 1987, 1994) cropping out along the northern edge of Calabria (Fig. 2). More recently, Fe-Mg-carpholite-bearing metapelites have been found in Lower Miocene foredeep deposits (Vitale et al. 2013a) stratigraphically overlying carbonate successions of the distal part of the Adria continental paleomargin (*Lungro-Verbicaro* Unit; Iannace et al., 2005, 2007). By means of field structural, stratigraphical analysis and petrological investigations, integrated with micro-structural observations, this chapter aims to provide an interpretation of the tectonic and metamorphic evolution of the Ocean Continent Transition (OCT)-derived *Frido* Unit, of basinal sedimentary deposits of the Ligurian Accretionary Complex (LAC) and of the *Diamante-Terranova* Unit, within the general framework of the southern Apennine/CPT system.

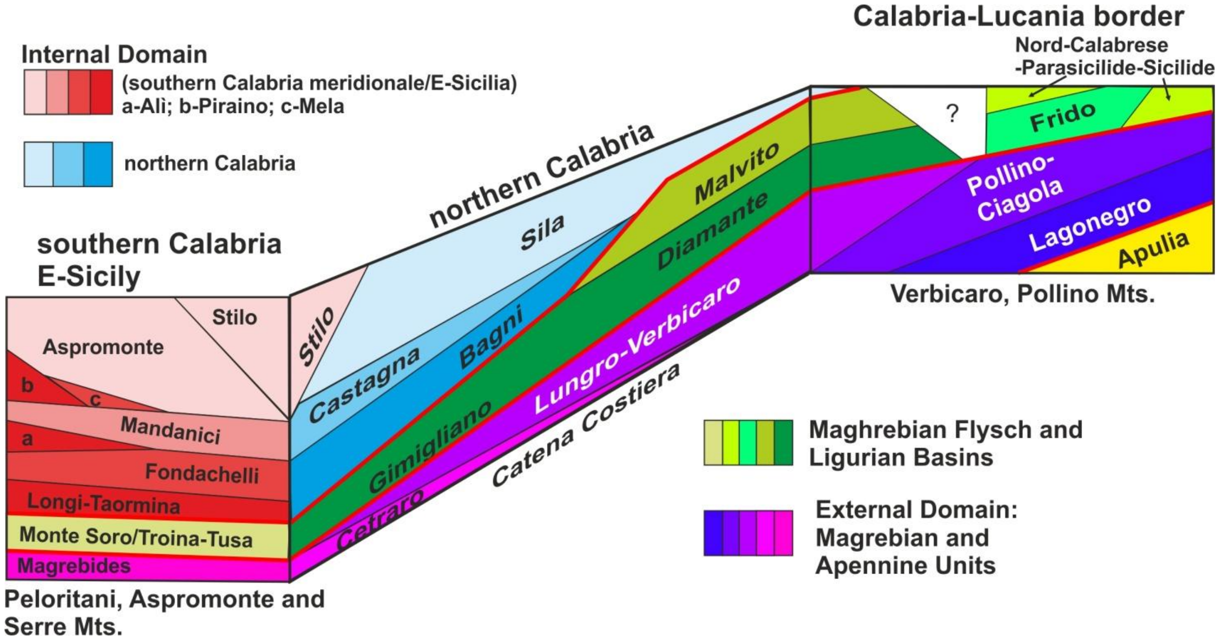

Fig. 2- Tectonic schemefrom the *Calabria-Lucania* border to E-Sicily.

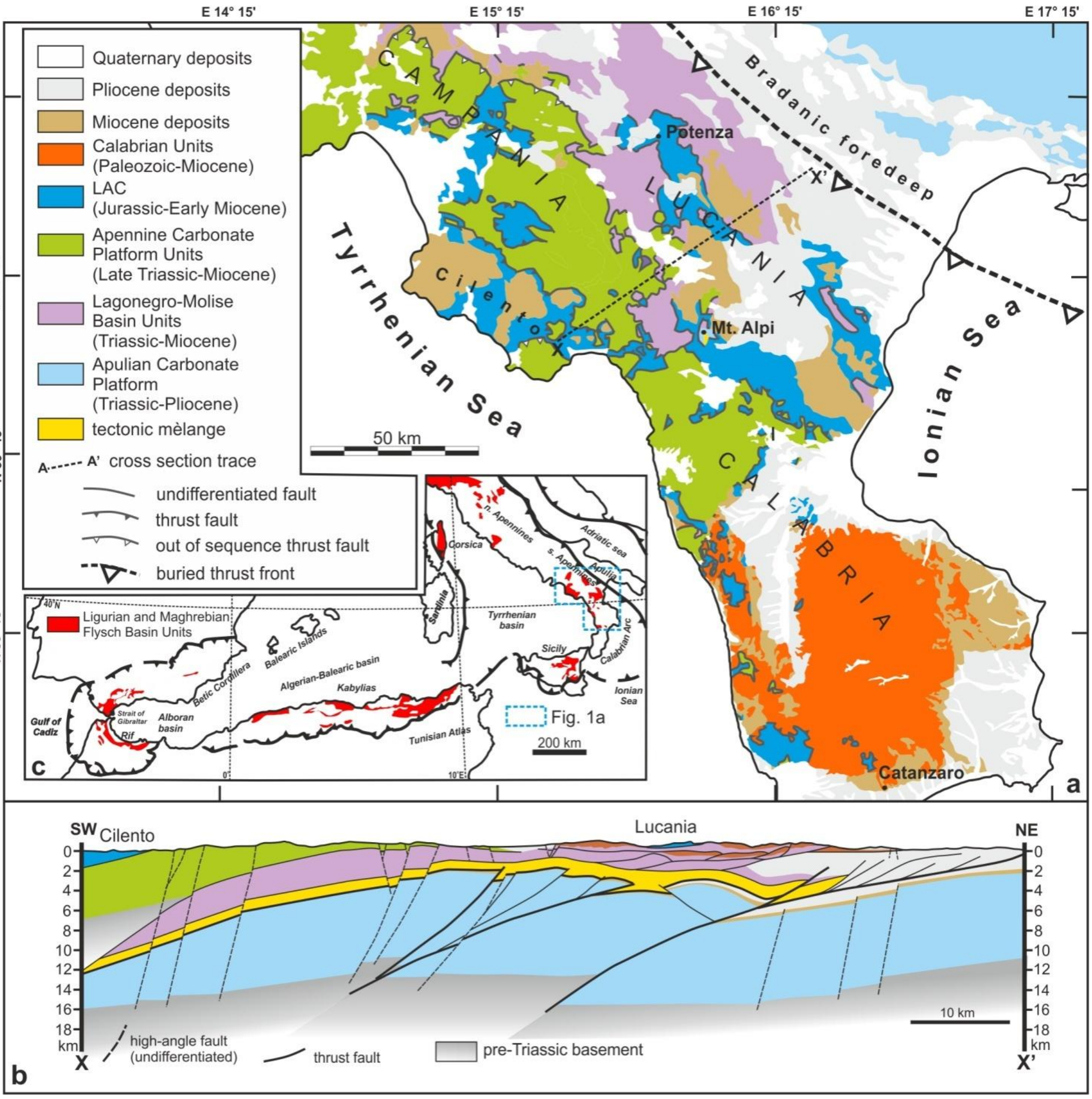

Fig. 3- (a) Geological sketch map of southern sector of the southern Apennines and northern Calabrian Arc (after Amodio-Morelli et al., 1976 and Bonardi et al., 1988b, modified). (b) Cross section (after Mazzoli et al., 2008, modified). (c) Outcrops of Ligurian and Maghrebian Flysch Basin Units in the western-central Mediterranean Alpine belts.

Chapter 2 - LAC: Stratigraphy, tectonic and structural setting

2.1. Introduction

The Ligurian Accretionary Complex (LAC), cropping out in the southern Apennines along the boundary between *Campania*, *Lucania* and *Calabria* regions, is a thrust sheet pile formed by deep basin successions, locally including oceanic to continental lithospheric rocks. It occupies the highest tectonic position (Figs. 2, 3) including *Nord-Calabrese*, *Parasicilide* and *Sicilide* Units (Fig. 3), which were detached from their pre-Cretaceous successions (Bonardi et al., 1988a; Monaco et al., 1991; Ciarcia et al., 2009, 2012 and references therein) and were piled up by means of frontal accretion mechanisms in the Burdigalian time (Ciarcia et al., 2012). The *Frido* Unit (Fig. 4) was affected by HP/VLT metamorphism showing the characters of an OCT (Ocean Continent Transition) basement, covered by a metasedimentary basin succession (Knott, 1987, 1994; Vitale et al., 2013a). It was subducted in the Late Oligocene and successively exhumed and intruded into the tectonic prism before the middle Tortonian.

In the following paragraphs, stratigraphy and the structural analysis will be described for all the units forming the LAC (*Frido*, *Nord Calabrese*, *Parasicilide* and *Sicilide* Units). For the *Frido* Unit, a petrographic analysis will be provided.

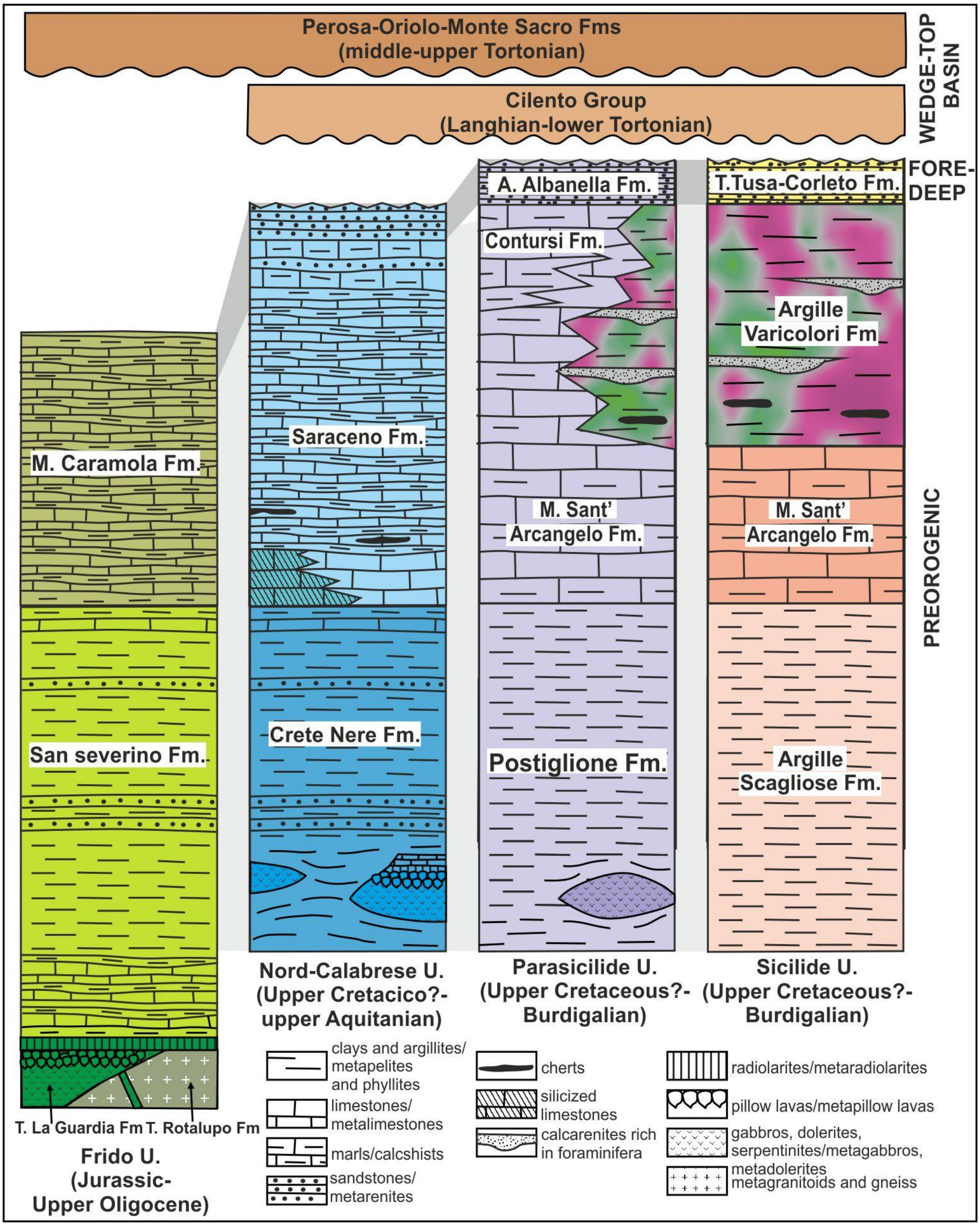

Fig. 4- Schematic stratigraphic logs of LAC successions and Miocene wedge-top basin deposits (modified after Vitale et al., 2013a).

2.2. Stratigraphic setting of LAC in the southern Apennines

The sedimentary rocks of the LAC are characterized by a broadly comparable stratigraphy. The Upper Cretaceous(?)-Middle Eocene successions show mainly argillitic sequences upward passing to calcareous, marly and clayey sequences. The sedimentary pile is topped by foredeep sandstones of Aquitanian-lowermost Burdigalian age for the *Nord-Calabrese* Unit and Burdigalian age for the *Parasicilide* and *Sicilide* Units. These successions were piled up by means of frontal accretion mechanisms in the Burdigalian time (Ciarcia et al., 2012). Presently, the *Parasicilide* Unit crops out mainly in the *Campania* region, whereas the *Nord-Calabrese* Unit is exposed in *Cilento* (southern *Campania*) and, extensively, along the *Calabria-Lucania* border, while the *Sicilide* Unit crops out only in the *Lucania* region (Fig. 5). In contrast to above mentioned units, the *Frido* Unit (Fig. 4) is characterized by a metamorphic and highly deformed succession (Vitale et al., 2013b) consisting of oceanic crustal and continental lithospheric rocks, covered by a deep basin meta-sedimentary succession and finally by Upper Oligocene calcschists (Bonardi et al., 1993; Vitale et al., 2013a). In the geological sketch map shown in Fig. 5, the *Frido* Unit tectonically covers the *Nord-Calabrese* Unit in the SE sector ("*Timpa delle Murgie*" area), whereas it is placed below the *Nord-Calabrese* and *Parasicilide* Units in the NW sector (*Seluci* area). In turn LAC overlays an orogenic wedge formed by Mesozoic-Tertiary successions, more or less detached from their Paleozoic substrate, encompassing both platform carbonates (Apulian and Apennine Platforms Units, Mostardini and Merlini, 1986; Vitale and Ciarcia, 2013) and basin successions (*Lagonegro-Molise* Basin Units, Mostardini and Merlini, 1986; Vitale and Ciarcia, 2013), here named External Units

(Fig. 1) in analogy with thetectonic units occupying the same structural position in other circum-Mediterranean chains (e.g. Guerrera et al., 2005).

In the study area (Fig. 5), also the *Lagonegro-Molise* Basin successions extensively crop out, with the Triassic-Cretaceous lower part mainly exposed in the north-western sector (Mt. *Sirino* area), whereas the Paleogene-Miocene, upper part (*Flysch Rosso*, Numidian sandstones and post-Numidian marls), spread out especially in the south-eastern sector (*i.e. Ferro* River Valley, *Valsinni* ridge and *Rotondella* area; Fig. 5). The LAC Units were studied by several authors (e.g. Selli, 1962; Vezzani, 1968; Ogniben 1969; Bousquet, 1973; Spadea, 1982; Bonardi et al., 1988a; 1993; Knott, 1987, 1994; Monaco et al., 1991; Monaco and Tortorici, 1995; Mazzoli, 1998; Critelli, 1999); however, only in the last years complete studies approaching the stratigraphy and the tectono-metamorphic evolution of the *Nord-Calabrese*, *Parasicilide*, *Sicilide* and the *Frido* successions (Ciarcia et al., 2009; 2012; Vitale et al., 2010, 2011, 2013a, b) were carried out.

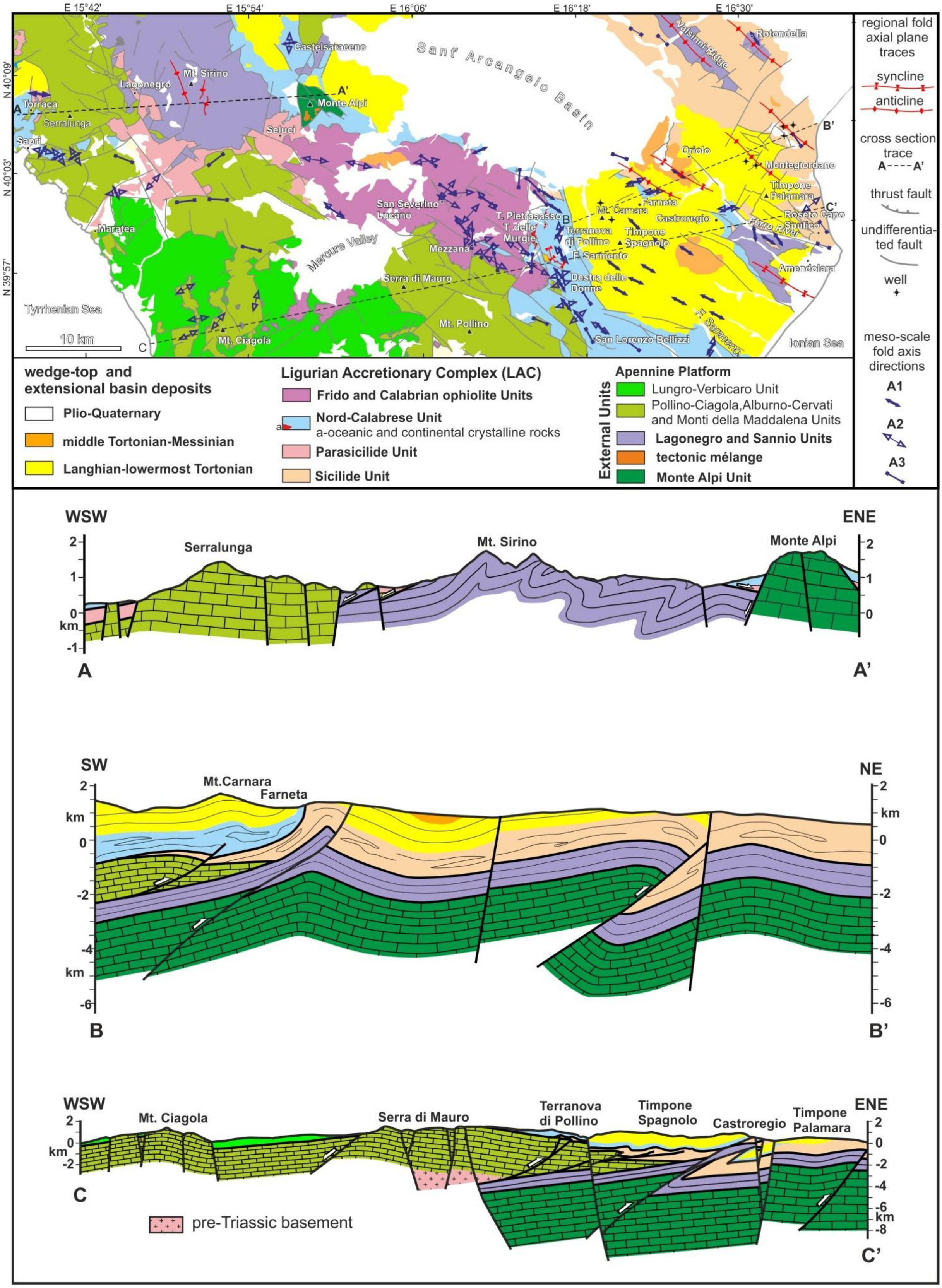

Fig. 5- Geological sketch map and cross-sections of *Calabria-Lucania-Campania* border (modified after Bonardi et al., 1988b; Iannace et al., 2007; ISPRA, 2009; Vitale et al., 2013a).

2.3. *Frido* Unit.

The *Frido* Unit is the only succession of LAC affected by metamorphism. The latter, crops out along the northern edge of *Calabria* region and forms a NW-SE elongated tectonic unit overlying the *Nord-Calabrese* Unit (which is locally exposed in tectonic windows; Fig. 6) in the south-eastern sector of the study area. On the other hand, in the north-western sector (*Seluci* area; Fig. 6) the *Frido* Unit is overlain by the *Nord-Calabrese* and *Parasicilide* Units. In this section stratigraphy, structural analysis and the main petrographic features of the *Frido* Unit rocks will be described.

2.3.1. Stratigraphy

The *Frido* Unit is characterized by four main formations and several sub-units. From bottom to the top it is formed by: (i) the *Timpa della Guardia* Fm., made of oceanic crustal rocks like metagabbros, metadolerites and metapillow lavas (Fig. 4); (ii) the *Timpa Rotalupo* Fm., characterized by continental crustal lithologies and upper mantle rocks, including metagranitoids, gneisses, amphibolites, granofelses and metacarbonates, often cut by basic dykes, plus serpentinized peridotites (Fig. 4). Crystalline rocks are covered by a deep basin sedimentary succession represented by (iii) *San Severino* Fm. (Fig. 4), formed by metaradiolarites, calcschists, phyllites, quartzites and metapelites and finally by (iv) *Monte Caramola* Fm. (Fig. 4), made of calcschists, whose age reaches the Upper Oligocene according to Bonardi et al. (1993). The occurrence of tightly juxtaposed oceanic and continental crust materials and upper mantle rocks, together with the scarcity of effusive rocks, is coherent with the interpretation of the *Frido* succession as originally forming part of an OCT domain, as suggested by Cello and Mazzoli (1998). As reported by several authors, the *Frido* Unit show evidence of an HP/LT metamorphic assemblages, such as aragonite in calcschists (Spadea, 1976) and glaucophane, crossite, lawsonite and Na-pyroxene in the metabasites (including crosscutting dykes; De Roever, 1972; Lanzafame et al., 1979; Spadea, 1982; Monaco et al., 1991; Belviso et al., 2009). The presence of lawsonite and pumpellyite + aragonite or crossite-Mg-riebeckite-aegirine-augite overprints in continental crust rocks (Spadea, 1982) constrained the pressure peak around 0.8-1.0 GPa and ~400-450 °C temperature, with a subsequent re-equilibration at greenschist facies conditions (P ~0.4 GPa and T ~300-350 °C). According to Monaco et al. (1991), a similar P-T evolution was experienced also by the calcschists and metapelites, whereas some metabasites were locally characterized by a very low metamorphic grade.

According to Monaco et al. (1991) and Belviso et al. (2009), the *Frido* Unit is characterized also by several minor units: (i) the *Cropani-Episcopia* sub-unit, including most of the outcrops in the north-western sector (between *Episcopia* and *Seluci*; Fig. 6), is characterized by HP/LT metamorphism marked by the occurrence of Na-amphibole in the metabasites, with temperature estimates as low as 300°C and pressure values as high as 1.3 GPa. Recently, Cristi Sansone et al. (2011) emphasized the presence of dykes intruded in the serpentinized peridotites as an evidence of oceanic crust generated at slow/ultraslow-spreading ridges, well fitting with an OCT domain. Furthermore, the authors recognized a greenschist facies mineral assemblage related to an ocean-floor metamorphism predating the HP/LT tectonic event, rather than to a late overprint associated with decompression, as interpreted by previous authors (e.g. Monaco et al., 1991). Late Oligocene HP/LT metamorphism of the *Frido*

Unit was followed by rapid exhumation during Miocene times (Mazzoli, 1998; Corrado et al., 2010).

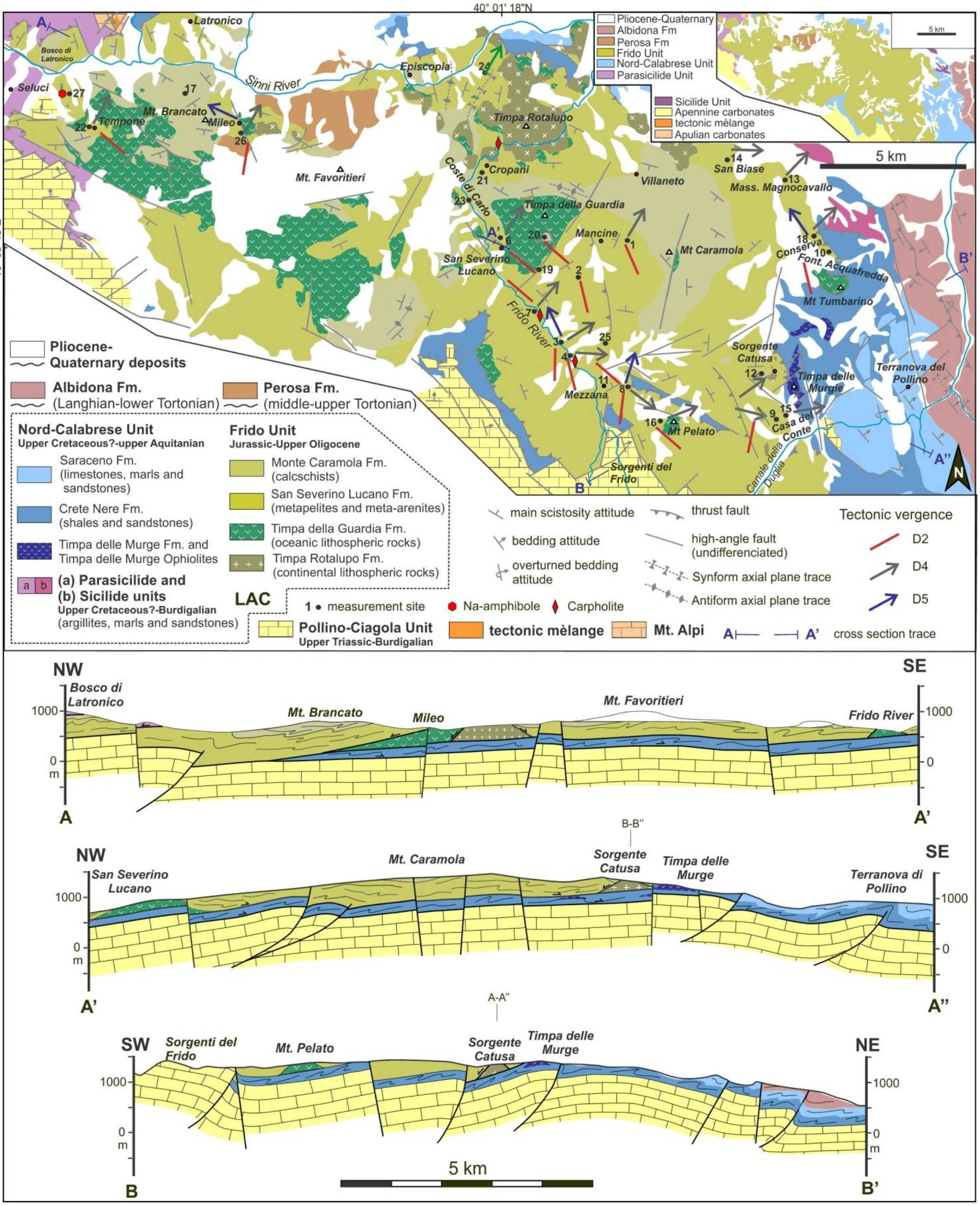

Fig. 6- Geological sketch map and cross-sections of the *Calabria-Lucania* border (from Belviso et al., 2009, modified) and geological cross-sections.

2.3.2. Meso- and micro-scale structural analyses

The rocks of the *Frido* Unit are characterized by a complex deformation pattern produced by the superposition of five deformation stages (Figs. 7-8-9) well-recorded in phyllites, metapelites and calcschists, whereas oceanic and continental basement rocks rarely show evidence of deformation. The latter rocks occur as boudins (up to several hundreds of meters sized) embedded within lesser competent rocks (such as phyllites/metapelites), bounded by extensional brittle-ductile shear zones (Knott, 1994).

The first deformation stage (D_1) produces a foliation (S_1) marked, in phyllites and metapelites, by the isorientation of metamorphic white mica and chlorite in microlithons (Fig. 8a, b), whereas in the calcschists the main foliation (S_1) is defined by recrystallized calcite and thin films of metamorphic white mica with rare relicts of bedding planes (S_0) in the microlithons (Fig. 8e). In the calcschists, the S_1 foliation is enhanced by pressure-solution (Fig. 8c). In this deformation stage no micro- and meso-scale folds were recognized in association with the S_1 foliation. At least two vein sets are hosted in the calcschists, both parallel and oblique to S_1 surfaces (Fig. 8c). Both S_1 and early veins are folded by isoclinal to tight folds (D_2 stage; Fig. 8c, d f). F_2 folds occur mainly in the form of kink bands, observed also in the metabasites (Fig. 7a). In the calcschists, F_2 isoclinal folds are associated with an S_2 foliation parallel to the axial planes, often marked by pressure-solution seams (Fig. 8c), whereas in metapelites and phyllites F_2 folds frequently appear as intrafolial folds with associated a S_2 crenulation cleavage and a CL_2 crenulation lineation. This latter foliation is so intensely developed in these lithotypes that it appears as the main foliation (Figs. 8a, b; 9c, d). A well-developed boudinage affects the metacalcareous and metarenitic layers embedded in the less competent rocks, as well as veins, especially in the stretched limbs of isoclinal F_2 folds (Fig. 8c). Rare pre-buckle thrusts affect competent layers embedded in a pelitic matrix (Fig. 7g). A mineral/stretching lineation (SL_2) is well developed, generally parallel to the F_2 fold axes. Calcite-quartz veins, generally parallel to the S_2 foliation, display at least two generations of fibrous centimeter-sized carpholite crystals generally orthogonal to the host walls (Fig. 7b-f), observed also in quartz veins hosted in massive metalimestones (Fig. 7c). Carpholite crystals appear also with a prismatic habitus (Fig. 7d) or as very thin needles (Fig. 7e). D_3 extensional shear surfaces (ESS) are hosted in metapelites and phyllites (Fig. 9a, b), generally indicating extension both orthogonal and parallel to SL_2. In the Seluci area, metasandstones are characterized by the growth of stilpnomelane and Na-amphibole along the S_2 schistosity (Fig. 7h) and D_3 extensional shear surfaces (Fig. 9a). A fourth deformation stage (D_4) is characterized by late, open to tight F_4 folds with a kink geometry (Fig. 9c-f), locally associated with thrust faults with centimetric to metric displacements. A crenulation cleavage (S_4; Fig. 9c-e) and a crenulation lineation (CL_4) occur in metapelites and phyllites. The S_4 cleavage is enhanced by pressure-solution structures and marked by thin films of opaque and residual minerals (Fig. 9c, d). F_2 and F_4 folds generally show similar axial trends and form a type 3 interference pattern according to Ramsay's classification (Ramsay, 1967). The fifth deformation stage (D_5) produced rare thrust faults (Fig. 9g), generally with displacements of a few centimeters, and associated open to tight F_5 folds, a crenulation lineation (CL_5) and an additional, discontinuously developed, crenulation cleavage (S_5).

The structural survey carried out for Frido unit, in the study area (Fig. 6), reveal a main NW-SE and subordinately NE-SW trends for F_2 fold axes (A_2) and crenulation lineation (CL_2) (Fig. 10b). Poles to F_2 fold axial planes (AP_2) show a scattered distribution (Fig. 10c), whereas poles to S_1 and S_2 foliation planes are broadly distributed along a mean NNE-SSW great circle (Fig. 10a). The stretching lineation SL_2 (Fig. 10d) is dominantly characterized by a NW-SE trend. D_3 extensional shear surfaces (ESS) cut previous structures, indicating extension both orthogonal and parallel to SL_2 stretching lineation (Fig. 10e). F_4 fold axes (A_4) and the crenulation lineation CL_4 are generally slightly plunging with a mean WNW-ESE orientation (Fig. 10f). Poles to AP_4 (Fig. 10g) and to the crenulation foliation S_4 are scattered along a NE-SW mean great circle (Fig. 10h). F_5 fold axes (A_5) and crenulation lineation CL_5 show a mean NE-SW direction (Fig. 10i). Finally, poles to AP_5 are dipping mainly to the NW and secondarily to the SE (Fig. 10j).

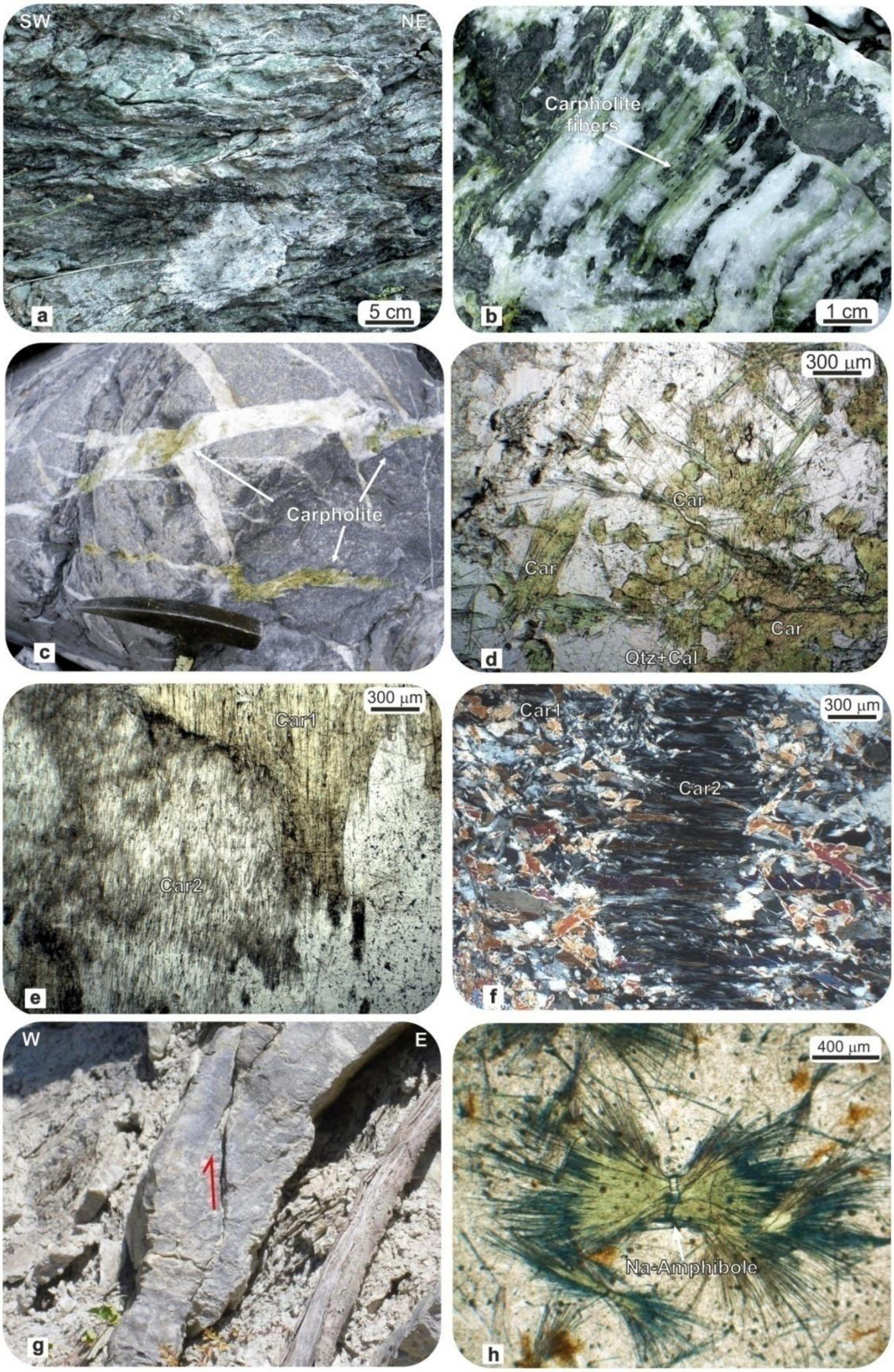
SW
NE
5 cm
a
Carpholite
fibers
1 cm
b
Carpholite
c
300 µm
Car
Car
Car
Qtz+Cal
d
300 µm
Car1
Car2
e
Car1
300 µm
Car2
f
W
E
g
400 µm
Na-Amphibole
h

Fig. 7- Examples of micro- and meso-structures of the *Frido* Unit: (a) F_2 kink folds in metabasites (site 12, *Sorgente Catusa*). (b) Centimeter-sized carpholite fibers within calcite-quartz veins (site 7, *Frido* River). (c) Carpholite-quartz vein lets hosted in massive metalimestone. (d) Thin section microphotograph (plane polarized light) showing fibers and aggregates of carpholite (Car) within a quartz (Qtz) –calcite (Cal) vein. (e-f) Thin section microphotographs (plane polarized light and crossed polars, respectively) showing two generations of carpholite fibers (Car_1 and Car_2; site 7, *Frido* River). (f) Pre-buckle thrust in arenitic layer embedded in pelitic levels (site 11, *Mezzana*). (h) Thin section microphotograph (plane polarized light) showing growth of Na-amphibole on the S_2 foliation in a metaradiolarite sample (site 27, *Seluci*).

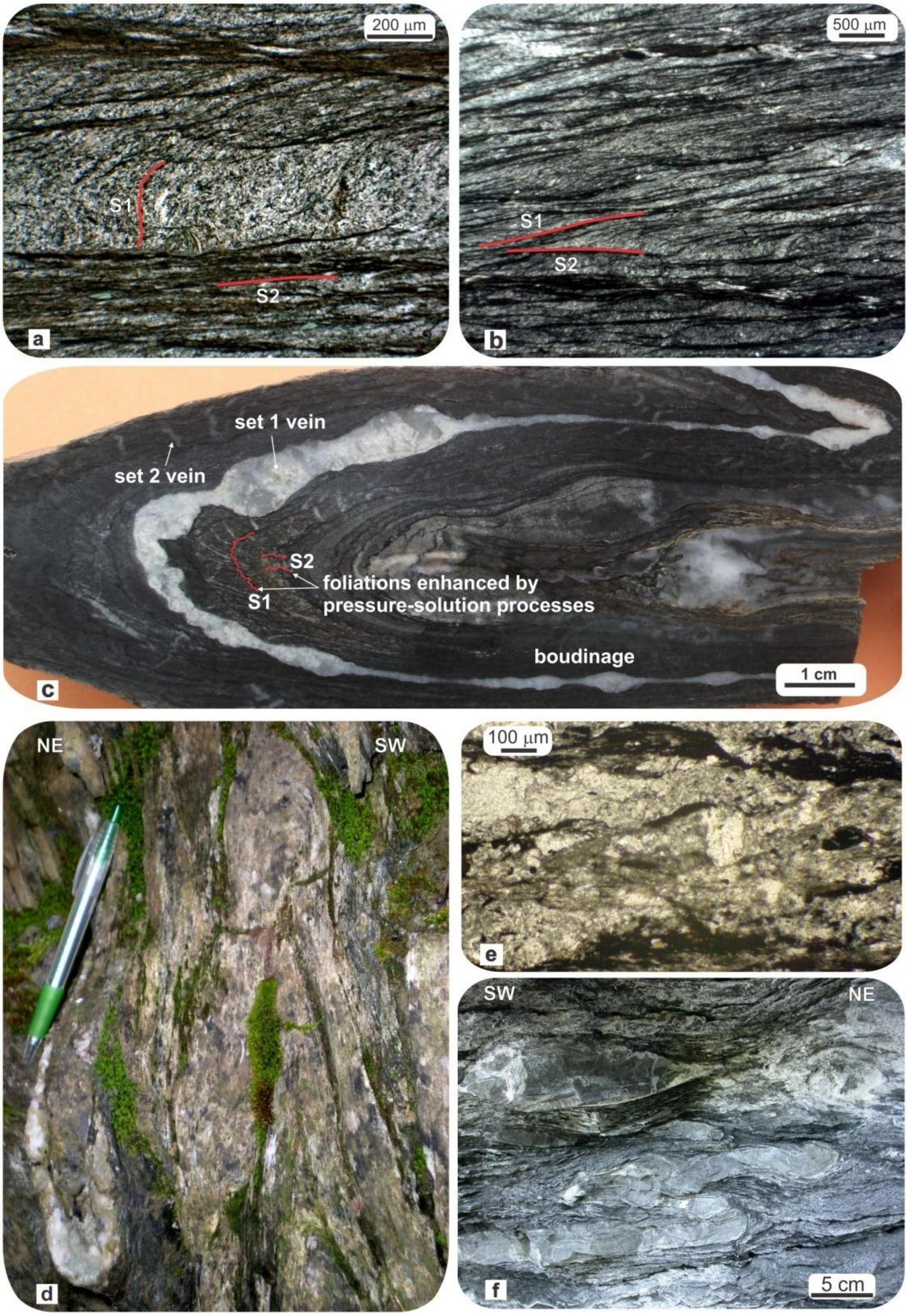
200 µm
S1
S2
a
500 µm
S1
S2
b
set 1 vein
set 2 vein
S2
foliations enhanced by
pressure-solution processes
S1
boudinage
1 cm
c
NE
SW
d
100 µm
e
SW
NE
5 cm
f

Fig. 8- Examples of micro- and meso-structures of the *Frido* Unit: (a) Thin section microphotograph (crossed polars) showing crenulation cleavage S_2 and the relict of foliation S_1 in microlithons within phyllite (site 22, *Tempone*). (b) Thin section microphotograph (crossed polars) showing crenulation cleavage S_2 and the relict offoliation S_1 in microlithons within metapelite (site 12, *Sorgente Catusa*). (c) F_2 isoclinal folds in calcschist sample (site 22, *Tempone*). (d) F_2 isoclinal folds in calcschists (site 22, *Tempone*).(e) Thin section microphotograph of calcschist (site 22, *Tempone*) showing the relict of bedding (S_0) within a microlithon. (f) Boudinated calcareous layer and F_2 intrafolial folds (site 7, *Frido* River).

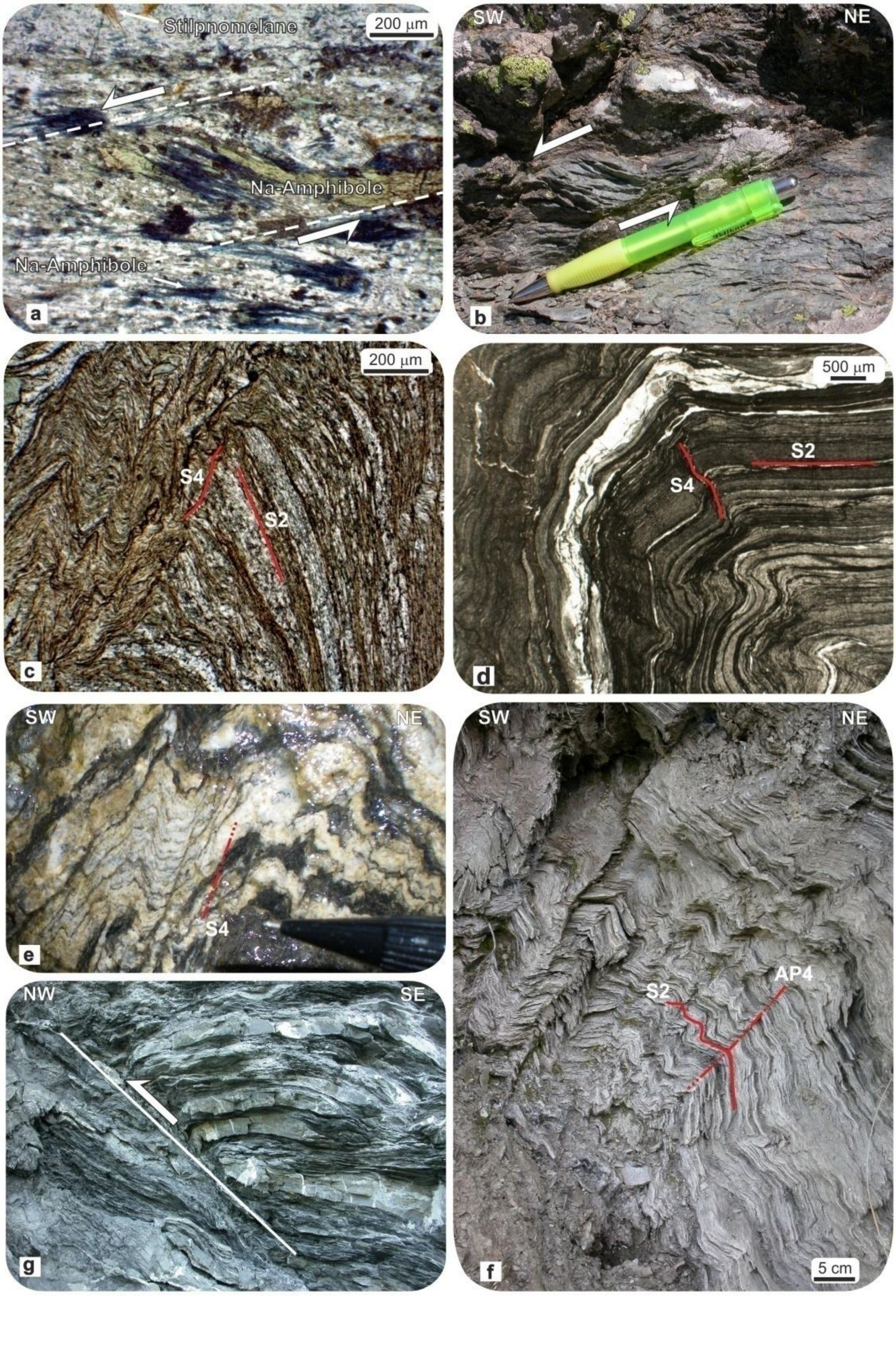
Stilpnomelane
200 µm
Na-Amphibole
Na-Amphibole
a
SW
NE
b
200 µm
S4
S2
c
500 µm
S2
S4
d
SW
NE
S4
e
SW
NE
S2
AP4
5 cm
f
NW
SE
g

Fig. 9- Examples of micro- and meso-structures of the *Frido* Unit: (a) Thin section microphotograph (plane polarized light) of Na-amphibole grown along D_3 extensional shear surfaces in metarenite (site 27, *Seluci*). (b) D_3 extensional shear surfaces in metapelites (site 12, *Sorgente Catusa*). (c-d) Thin section microphotographs (plane polarized light) showing F_4 fold with associated S_4 crenulation cleavage in phyllite (site 22, *Tempone*) and metapelite (site 12, *Sorgente Catusa*) samples, respectively. (e-f) F_4 chevron folds (respectively: site 22, calcschists, *Tempone* and site 7, phyllites, *Frido* River). (g) F_4 fold associated with a thrust fault (site 7, phyllites, *Frido* River).

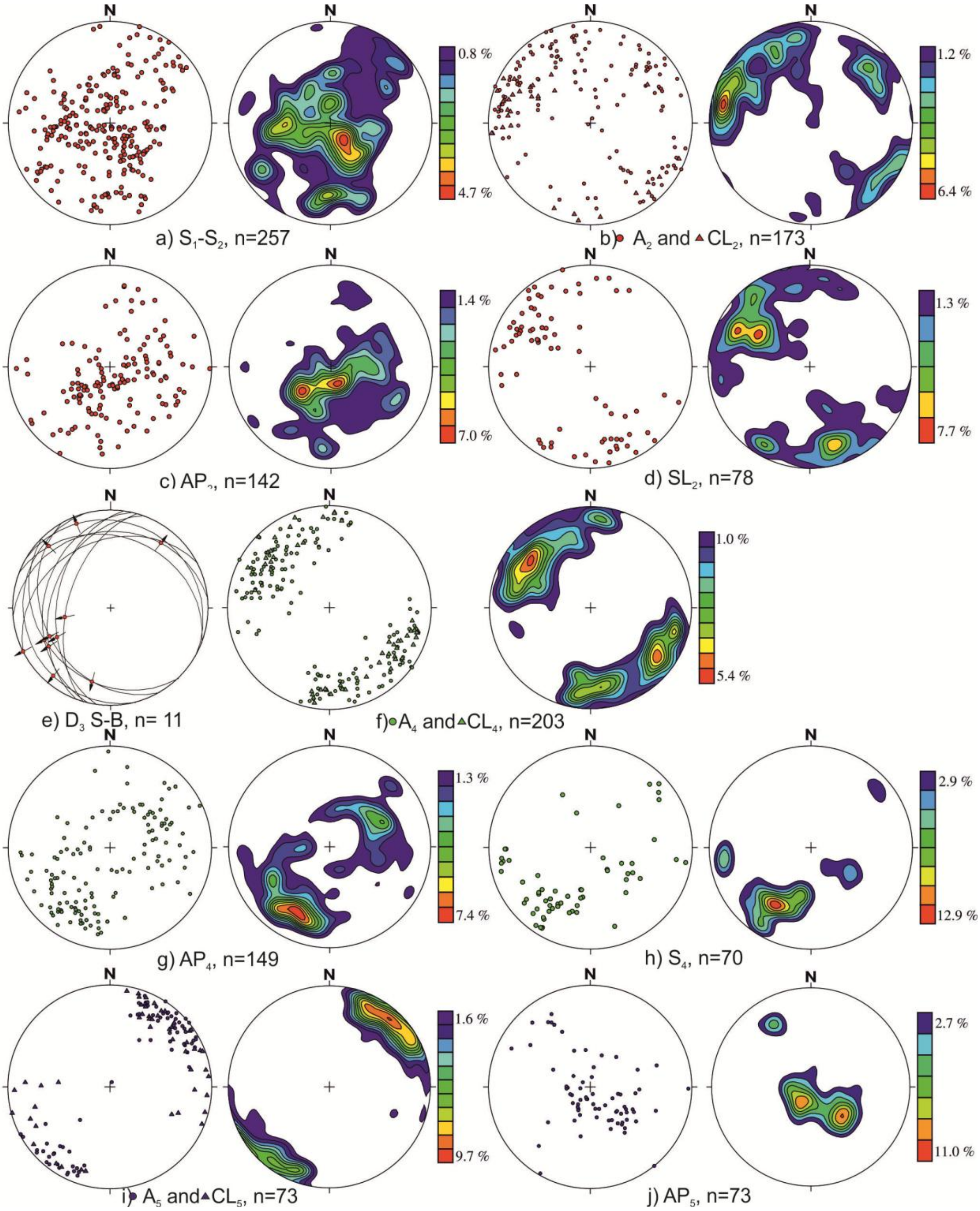

Fig. 10- Stereographic projections and contour plots (equal area net, lower hemisphere) of the analyzed structures.

2.3.3. Petrography of the *Frido* Unit

In order to provide new data about metamorphic evolution of the *Frido* Unit, a petrological analysis on the metasedimentary pelitic succession is presented. For this purpose, representative phyllites, metapelites, calcschists, and meta-sandstone samples were collected from the *Frido* River (site 7), *Sorgente Catusa* (site 12), *Casa del Conte* (site 9), *Tempone* (site 22) and *Seluci* (site 27) localities (Fig. 6). To obtain also information about micro-structures, thin sections were oriented parallel to the main planes of the finite strain ellipsoid, i.e. parallel to the S_2 foliation (plane XY), orthogonal to the foliation and parallel to the available stretching lineation (plane XZ) and orthogonal to the previous planes (plane YZ).

The Frido Unit consists of metabasites occurring as dark-green, metric, generally well-foliated blocks, although massive isotropic bodies are also observed. The original igneous (pillow?) structure, however, is commonly completely obliterated as a result of intense weathering. Mineral parageneses include mainly the relicts of the original igneous phases, namely plagioclase, clinopyroxene and olivine. The latter two are commonly replaced by serpentine-group minerals and chlorite. The groundmass is made up of similar mineral phases, plus oxides mica and quartz. Phyllites and metapelites, object of the petrological investigation, can be distinguished mainly on the basis of their crystal size, with the former characterized by coarser grained minerals, whereas the latter show a distinctively lower crystallinity. The two lithotypes show strongly anisotropic structures and are very similar both in their mineral assemblages (millimetric to centimetric mica and chlorite cleavage domains and microlithons of quartz and albite) and in their intensely foliated fabric with recurrent crenulation lineation and ptygmatic folds. Phyllites typically occur in the north-western (*Tempone*, site 22) and central (*Frido* River, site 7) sectors of the investigated area, whereas the metapelites are commonly found in the south-eastern outcrops (e.g., *Sorgente Catusa* and *Casa del Conte* localities; sites 12 and 9, respectively; Fig. 5). Metapelites are basically characterized by millimetric mica and chlorite (plus clay minerals) cleavage domains and microlithons of quartz (plus feldspars). Phyllites are quite similar -though coarser- in terms of texture and parageneses, although some from the *Frido* River locality (Fig. 6), are occasionally cut by large quartz and calcite veins containing abundant carpholite crystals, occurring both as monomineralic fibrous clusters and as hair-like tiny inclusions in quartz crystals (Fig. 7b-e). Metacarbonates and calcschists display strongly anisotropic and deformed textures basically consisting of carbonate minerals (plus oxides and clay mineral inclusions in the metacarbonates and quartz, feldspars and phyllosilicates in the calcschists). Stylolites and late, undeformed veins of white spatic calcite are also common. Meta-sandstones are commonly intercalated within the phyllite/metapelite and metacarbonate levels (e.g., Mt. *Tumbarino* and *Mezzana* localities; Fig. 6) and are almost entirely made of quartz grains. At the *Seluci* locality (site 27; Fig. 6), sheaf-like aggregates of strongly zoned fibrous sodic amphibole (greenish in the core, blue to violet in the more peripheral zones), titanite and stilpnomelane also occur.

Mineral chemistry analyses were performed on the thin sections by Energy Dispersive Spectrometry at the C.I.S.A.G. (Centro Inter-dipartimentale di Servizi per Analisi Geomineralogiche) of the University of Napoli Federico II. The employed apparatus is an Oxford Instruments Micro analysis Unit equipped with an INCA X-act detector and a JEOLJSM-5310 microscope operating at 15 kV primary beam voltage, 50-100 mA filament current, variable spot size and 50s net acquisition time. Measurements were performed with an INCA X-stream pulse processor. The following standards were used for calibration: diopside (Mg), wollastonite (Ca), anorthoclase (Al, Si), albite (Na), rutile (Ti), almandine (Fe), Cr_2O_3 (Cr), rhodonite (Mn), orthoclase (K), apatite (P), fluorite (F), barite (Ba), strontianite (Sr), zircon (Zr, Hf), synthetic Smithsonian orthophosphates (La, Ce, Nd, Sm, Y), pure vanadium (V), corning glass (Th and U), sphalerite (S, Zn), sodium chloride (Cl), and pollucite (Cs). See Melluso et al. (2010) for full analytical details.

Mineral chemistry analyses of the main occurring phases were performed on selected representative samples of phyllites, metapelites, and metasandstones. The results are briefly summarized here.

The analyzed chlorite crystals are generally Fe-rich (FeO_{TOT}= 26.1-35.0 wt.%; Mg = 8.06-12.6 wt.%) and plot between the amesite and (clinochlore) daphnite end-members (Fig. 11a), although some chemical variability is recorded in both the investigated lithotypes. Metapelites show a slightly narrower range in compositions, with X_{Mg} values between 0.33 and 0.44, coupled with slightly lower Fe (2.27-2.99 a.p.f.u.) and Al^{IV} (1.05-1.36 a.p.f.u.) with respect to phyllites (i.e., X_{Mg} = 0.29-0.44, Fe = 2.46-3.35 a.p.f.u., Al^{IV} = 1.14-1.48 a.p.f.u.). The metapelites from *Casa del Conte* have chlorites with generally lower X_{Mg} (0.33-0.36) and Fe (2.66-2.84 a.p.f.u.) with respect to those from *Sorgente Catusa* (X_{Mg} = 0.33-0.44, Fe basically between 2.60 and 2.99 a.p.f.u.). Chlorite from phyllites displays a more marked compositional variation, with the *Tempone* ones being the Mg-richest (i.e., X_{Mg} up to 0.43).

Analyzed mica crystals record a wide compositional variability. Metapelites generally show large Tschermack (i.e., X_{Mus} = 0.51-0.85 and X_{Cel} = 0.09-0.40) and moderate pyrophillitic substitutions (X_{Prl} = 0.03-0.17), with the *Casa del Conte* samples being more homogeneous (i.e. X_{Mus} = 0.51-0.59, X_{Cel} = 0.30-0.32 and X_{Prl} = 0.11-0.17) with respect to those from *Sorgente Catusa*. Phyllites display an even wider spectrum of mica compositions, with X_{Mus} ranging from 0.38 to 0.85, X_{Cel} from 0.10 to 0.46 and X_{Prl} from 0.01 to 0.17. The three analyzed localities are characterized by a pronounced variability, which is more evident for the mica from the *Tempone* locality, whereas mica crystals analyzed in the *Frido* River locality generally show higher muscovite contents, coupled with smaller substitutions (Fig. 11b).

The analyzed carpholite (Fig. 12a, b) crystals are found in *Frido* River phyllites (site 7; Fig. 6) and show a quite homogeneous, relatively Fe-rich and Mn-poor composition (X_{Fe} = 0.57-0.69, X_{Mg} = 0.29-0.41, X_{Mn} ~0.03). Amphibole crystals found in the meta-sandstones from the *Seluci* area. The structural formulae were calculated on the basis of 23 oxygens. According to the classification scheme proposed by Leake et al. (1997), compositions range from sodic to sodic-calcic amphibole (Fe-richterite, riebeckite and Mg-riebeckite). Sheaf-like aggregates show a marked chemical zonation, with a core-to-rim increase in MgO and decrease in CaO, Na_2O and Al_2O_3. Matrix amphiboles are basically sodic, overlapping the composition of the larger sheaf-like aggregate rims (i.e., MgO = 6.22-8.82 wt. %, CaO = 0.58-1.94 wt.%, Na2O = 6.13-6.97 wt.%, Al_2O_3 = 1.50-2.32wt.%).

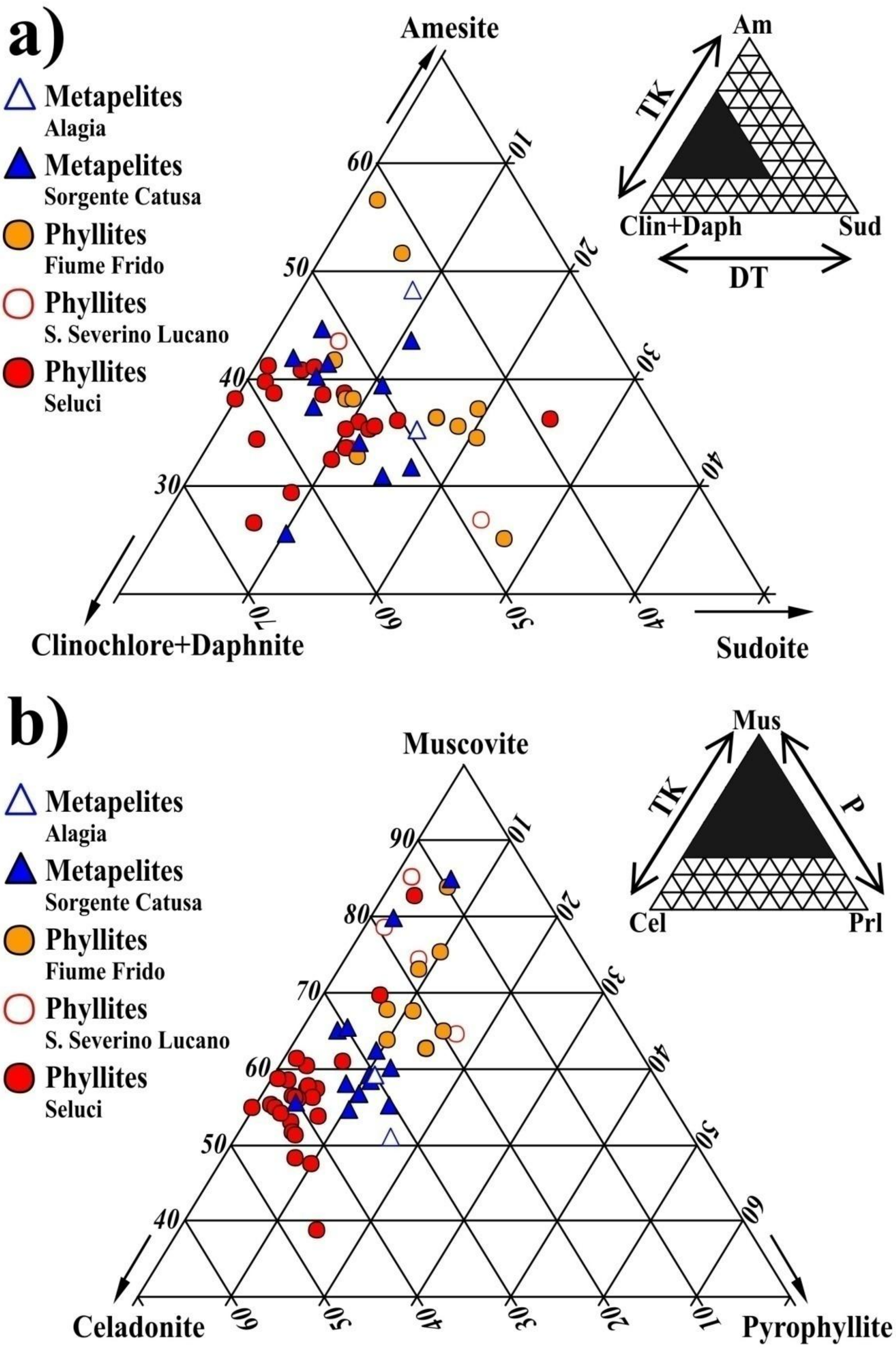
a)
Metapelites Alagia
Metapelites Sorgente Catusa
Phyllites Fiume Frido
Phyllites S. Severino Lucano
Phyllites Seluci
Amesite
Clinochlore+Daphnite
Sudoite
Am
TK
Clin+Daph
Sud
DT
b)
Metapelites Alagia
Metapelites Sorgente Catusa
Phyllites Fiume Frido
Phyllites S. Severino Lucano
Phyllites Seluci
Muscovite
Celadonite
Pyrophyllite
Mus
TK
P
Cel
Prl

Fig. 11- (a) Amesite-(clinochlore + daphnite)-sudoite ternary diagram and (b) celadonite-muscovite-pyrophillite ternary diagram for chlorite and mica from the *Frido* Unit. The insets in the upper left and upper right corners indicate the position of the magnified portion of the diagram where analyzed individuals plot (black area) and the effects of the Tschermack (TK), di/trioctahedral (DT) and pyrophyllitic (P) substitutions.

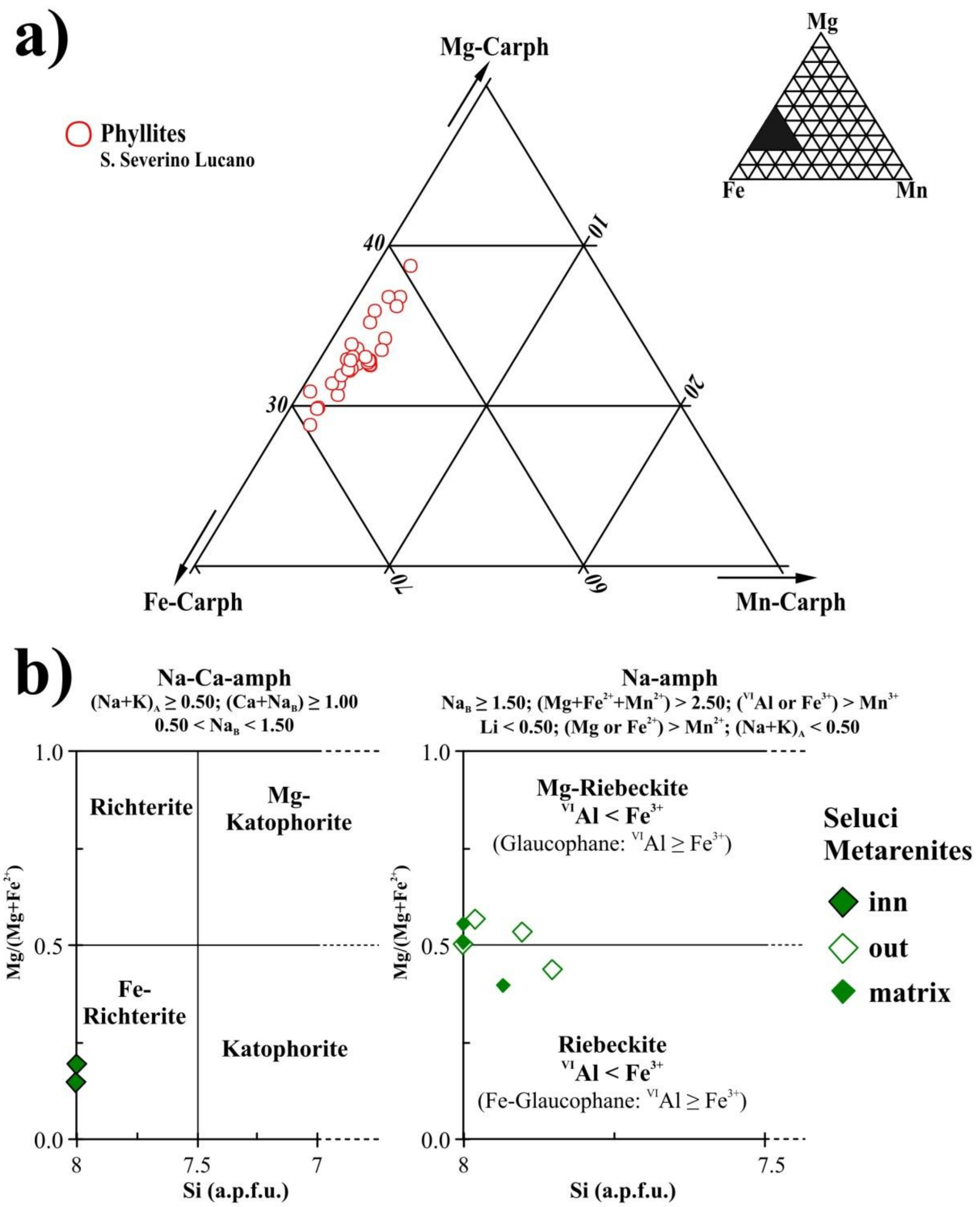

Fig. 12- (a) Composition of Fe-Mg carpholite from the *Frido* Unit. The inset in the upper left corner indicates the position of the magnified portion of the diagram where analyzed individuals plot (black area). (b) Composition of amphiboles from the *Frido* Unit according to the scheme proposed by Leake et al. (1997). inn = inner portions of the sheaf-like aggregates green cores; out = outer portions of the sheaf-like aggregates blue rims; matrix = microcrystals of the surrounding matrix.

2.4. *Nord Calabrese* Unit

2.4.1. Stratigraphic setting

The *Nord-Calabrese* Unit is formed by *Crete Nere* and *Saraceno* Formations (Fig. 4; Bonardi et al., 1988a). The *Crete Nere* succession, in the lower part, is made of oceanic (ophiolites) and continental crust masses (Spadea, 1982), the former preserved in a coherent succession in the *Timpa delle Murgie* locality (Fig. 5; Bonardi et al., 1988a), including gabbros, dolerites, pillow lavas, pillow breccias, and a deep basin cover (Fig. 13a, b) formed by argillites, quartz-arenites, jaspers and allodapic limestones, known in literature as "*Calcari di Mezzana*" (Bousquet, 1973). The latter correspond to "*scaglia*-type" deposits, directly covering pillow lavas and pillow breccias (Fig. 13c). Continental crust-derived bodies consist of gneisses and amphibolites cropping out only in the "*Timpa di Pietrasasso*" locality (Fig. 5). The age of this part could reach the Upper Cretaceous as suggested by Bonardi et al. (1988a). The middle-upper part of *Crete Nere* succession, Middle Eocene in age, is formed by dark-brownish argillites alternated to gray-greenish quartz-arenites, followed by a thick succession of black shales (Fig. 13d) with intercalations, in the upper part, of arenites and calcareous beds. The *Crete Nere* Fm. gradually passes to the upper *Saraceno* Fm., which is made of four members (Ciarcia et al., 2012): (i) *Punta Telegrafo* member (Fig. 13e), made of calciclastic, locally silicified, arenitic turbidites with dark chert lenses and rare lithic sandstones; (ii) *Terranova di Pollino* member (Fig. 13f), characterized by thin layers of calciclastic, pelitic and arenitic turbidites with lenses and nodules of dark chert and subordinately arkosic-lithic sandstones; (iii) *Carpineta* member, consisting of an alternance of marly, silty and arenitic beds, occasionally with dark chert nodules and layers of microbreccia at the top; and finally by (iv) *Sovereto* Member (Fig. 4; Bonardi et al., 2009), comprising thinly layered immature sandstones. The age of the *Saraceno* Fm. is Upper Eocene-lowermost Burdigalian (?) (Di Staso and Giardino, 2002; Bonardi et al., 2009). The thickness of the whole succession is more than 1200 meters (Bonardi et al., 1988a).

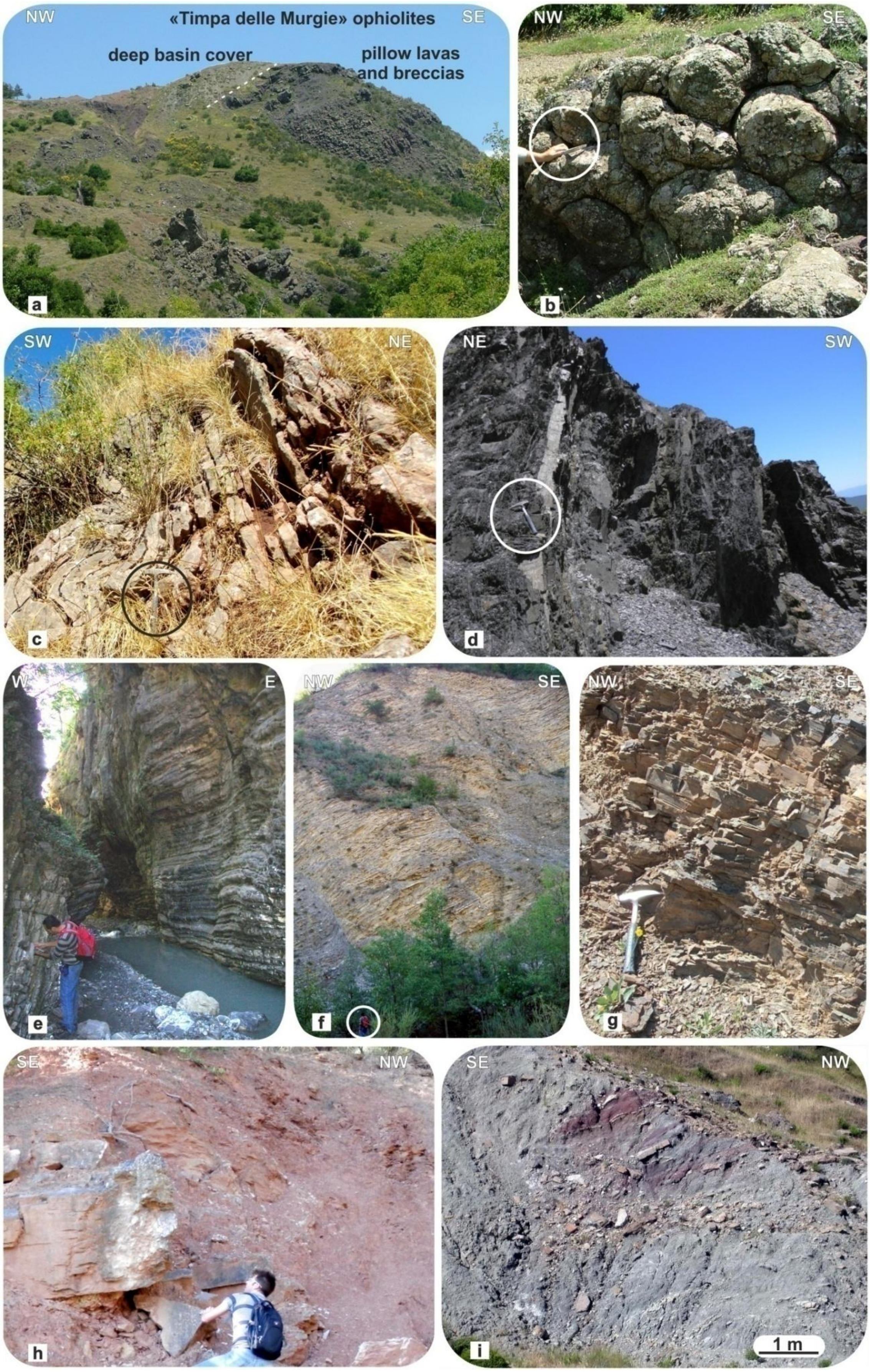
«Timpa delle Murgie» ophiolites
deep basin cover
pillow lavas and breccias
NW
SE
a
b
SW
NE
c
NE
SW
d
W
E
e
NW
SE
f
NW
SE
g
SE
NW
h
SE
NW
i
1 m

Fig. 13- Examples of stratigraphic features. *Nord-Calabrese* Unit: (a) *Timpa delle Murgie* hill view showing the stratigraphic boundary between pillow lavas and breccias, and deep basin sedimentary cover; (b) pillow lavas of *Timpa delle Murgie*; (c) slumping in the *scaglia*-type deposits ("*Calcari di Mezzana*", *Mezzana*); (d) black shales in *Crete Nere* Fm. (road between *Terranova di Pollino* and *S. Lorenzo Bellizzi*); (e) *Punta Telegrafo* Member of *Saraceno*Fm. (*Sarmento* River Valley); (f) *Terranova* Member of *Saraceno* Fm. (*Sarmento* River Valley). *Sicilide* Unit: (g) Silicified marly clays and slates of *Argille Scagliose* Fm. (*Roseto Capo Spulico*); (h) *Argille Varicolori* Fm. (*RosetoCapoSpulico*). (i) *Argille Varicolori* Fm. (*Oriolo*).

2.4.2. Structural analysis

The deformation of *Nord Calabrese* Unit was studied since the early 70's by several author (e.g. Guzzetta and Ietto, 1971; Mauro and Schiattarella, 1988; Zuppetta and Mazzoli, 1997; Mazzoli, 1998), which recognized that this succession was affected by a poly-phased deformation evolution highlighted by the superposition of structures of different generations. In order to provide a coherent structural analysis, the *Crete Nere* and *Saraceno* Fms. will be analyzed separately.

The overprinting relationships suggest that all observed structures are associated to three main folding stages (D_1-D_2-D_3). A further folding event (D_4) is related to deeply rooted thrusts and back thrusts involving the buried Apulian Platform carbonates and deforming the whole thrust sheet pile, especially in the outer sector of the Apennine Chain (e.g. Piedilato and Prosser, 2005; Ciarcia and Vitale, 2013). The first three stages are characterized by different grades of coaxiality in every analyzed part and the third deformation phase is normally recorded as macro-scale folds. Early tectonic structures (D_1), hosted in *Crete Nere* Fm., are tight to isoclinal and intrafolial F_1^{CN} folds (Fig. 14a, b). In the argillitic layers an axial plane slaty cleavage (S_1^{CN}) occurs, whereas in the arenitic and calcareous beds a spaced disjunctive convergent fan cleavage is observed. The D_2 folding stage produces close to tight folds (F_2^{CN}), usually showing a kink shape, verging to SE and NW (Fig. 14c, d), and locally associated with meso-scale thrust fault (Fig. 14d). In the argillitic levels this deformation stage is associated with a well developed crenulation cleavage (S_2^{CN}) and a crenulation lineation (CL_2^{CN}). The interference pattern produced by F_1^{CN} and F_2^{CN} fold sets (Fig. 14c) ranges between the types 2 and types 3 of the Ramsay's classification (Ramsay, 1967). The overprinting between these two tectonic foliations generates a characteristic pencil cleavage especially in the argillitic layers (Fig. 14e).

Poles to bedding (S_0^{CN}) are scattered (Fig. 15a); F_1^{CN} fold hinges (A_1^{CN}) and crenulation lineations (CL_1^{CN}) show a NW-SE main direction (Fig. 15b), whereas related axial plane poles (AP_1^{CN}) spread out around a NE-SW directed roughly vertical cyclograph (Fig. 15c). S_1^{CN} cleavage poles indicate NW-SE about vertical planes (Fig. 15d). F_2^{CN}fold hinges (A_2^{CN}) and crenulation lineations (CL_2^{CN}) are scattered, though a mean NE-SW trend results (Fig. 15e). Related axial plane poles (AP_2^{CN}) indicate a mean SW gently dipping plane (Fig. 15f).

The calcareous turbidites of *Punta Telegrafo* member (lower part of *Saraceno* Fm.) host early structures as tight to isoclinal folds (Fig. 14f). To D_1 deformation stage is associated also a boudinage affecting the long limbs of F_1^{SA} folds, with stretching direction orthogonal to fold axes, where competent layers may locally form asymmetric boudins (Fig. 14g). Often a further synchronous extension, orthogonal to the previous, forms a chocolate tablet boudinage. Meso-scale thrust faults occasionally developed duplex structures in pelitic inter-layers (Fig. 14h), whereas the calcareous beds, embedded in pelitic layers, locally host pre-buckle thrusts. D_1 structures are deformed by the second folding phase, producing open to tight folds, normally verging to SE (F_2^{SA}). In argillitic layers, crenulation cleavage (S_2^{SA}) and crenulation lineation (CL_2^{SA}) are well developed. As described previously for *Crete Nere* Fm., the interference pattern between the two fold-sets ranges between types 2 and 3. Rare meso-scale folds associated to the third deformation stage (D_3) superpose onto the previous tectonic structures. The middle-upper part of the *Saraceno* Fm. (*Terranova*, *Carpineta* and *Sovereto* members) is less deformed with respect to the lower part. The first deformation stage (D_1) is recorded by chevron to rounded, tight to isoclinal folds F_1^{SA} (Fig. 16a-d), with an associated slaty cleavage S_1^{SA} which is particularly well-developed in the pelitic inter-layers. The previous structures are deformed by open to tight folds showing a kink geometry (F_2^{SA}), often overturned both to SE and NW (Fig. 16c, d), with the development of crenulation cleavage and crenulation lineation. Pre-buckle thrusts are normally hosted in arenitic layers embedded in pelitic interlayers. Fold axes of the two superposed deformation stages vary between almost orthogonal, generating an interference pattern of type 2 (Fig. 16d), to parallel, with patterns of type 3 (Fig. 16c). The third deformation is recorded only as macro-scale folds, often overturned, affecting also the wedge-top basin deposits of the *Albidona* Fm. Poles to bedding (S_0^{SA}) for the whole *Saraceno* Fm. are scattered, although they lie around an almost vertical N10 striking great circle (Fig. 15g). F_1^{SA} fold hinges are random (Fig. 15h), whereas poles to axial planes spread out around a sub-vertical NNE-SSW great circle with a maximum frequency peak given by southeast dipping planes (Fig. 15i). Also F_2^{SA} fold hinges (A_2^{SA}) are dispersed; however showing main W/SW-trending sub-horizontal clusters (Fig. 15j). Poles to axial planes (AP_2^{SA}) lie along an ENE moderately dipping cyclograph (Fig. 15k). Rare F_3^{SA}fold hinges (A_3^{SA}) show a mean NNW-SSE trend (Fig. 15l), whereas related axial plane poles (AP_3^{SA}) spread out around a NNE-SSW great circle (Fig. 15m).


NE
SW
F1
1 m
a
NE
SW
F1
10 cm
b
NE
SW
AP2
AP1
10 cm
c
NE
SW
10 cm
d
e
NE
SW
AP1
AP1
20 cm
f
NE
SW
10 cm
g
NE
SW
10 cm
h

Fig. 14- Examples of tectonic structures in the *Nord-Calabrese* Unit.*Crete Nere* Fm.: (a) F_1 recumbent isoclinal fold (*Destra delle Donne*, *Terranova di Pollino*); (b) F_1 tight fold (*Terranova di Pollino*); (c) interference pattern of type 2 between F_1 isoclinal and F_2 close folds (*Terranova di Pollino*); (d) meso-scale thrust fault (*San Lorenzo Bellizzi*); (e) pencil cleavage (*Terranova di Pollino*). *Punta Telegrafo* member (*Saraceno* Fm.): (f) F_1 tight chevron folds (*Sarmento* River); (g) asymmetric boudin (*Sarmento* River); (h) duplex structure in argillitic layers embedded in calcareous strata (*Sarmento* River).

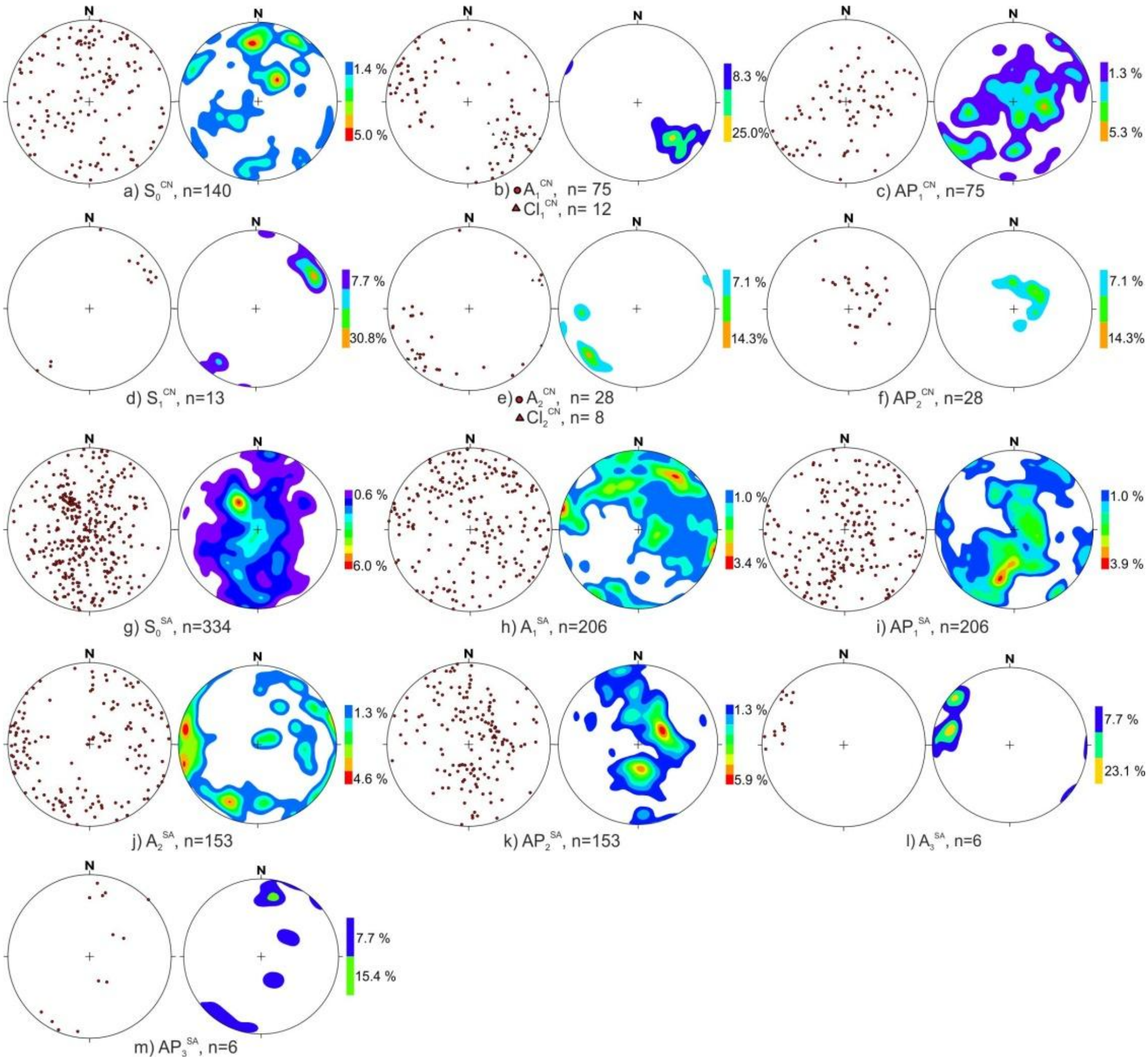

Fig. 15- Stereographic projections and contour plot of analyzed structures in *Nord-Calabrese* Unit (lower hemisphere, Schmidt net). CN: *Crete Nere* Fm.; SA: *Saraceno* Fm.


NW
SE
a
NW
SE
b
NW
SE
F1
F1
AP1
AP2
10 cm
c
NW
SE
AP1
AP2
10 cm
d
NE
SW
AP1
AP2
20 cm
e
NE
SW
AP2
AP2
AP1
1 m
f
NE
SW
10 cm
g
NE
SW
1 m
h

Fig. 16- Examples of tectonic features. *Terranova* Mb. (*Saraceno* Fm.): (a) F_1 isoclinal fold (*Ferro* River Valley). (b) F_1 chevron fold (*Ferro* River Valley). (c) Interference pattern of type 3 between F_1 tight and F_2 open folds (*San Lorenzo Bellizzi*). *Carpineta* Mb. (d) Interference pattern of type 2 (*Sapri*). *Parasicilide* and *Sicilide* Units: (e) Interference pattern of type 2 between F_1 isoclinal and F_2 open folds (*Torraca*). (f) Interference pattern of type 3 (*Farneta*); (g-h) F_3 meso-scale folds associated to thrust faults (*Farneta*).

2.5. *Parasicilide-Sicilide* Units.

2.5.1. Stratigraphic setting

The *Parasicilide* and *Sicilide* Units (Fig. 4) are characterized by two analogous sedimentary successions, often disrupted and showing the typical features of a broken formation (Mattioni et. al 2006). The former is characterized by four formations (Ciarcia et al., 2009). At the bottom, the *Postiglione* Fm. is made of clays and slates, followed by *Monte Sant'Arcangelo* Fm. made of marls and limestones. The succession continues with the *Contursi* Fm., characterized by whitish marls and marly limestones, and closes with the foredeep deposits of the *Arenarie di Albanella* Fm. (Donzelli and Crescenti, 1962). The thickness of the whole succession exceeds 800 meters and the age ranges from Middle Eocene to Burdigalian, although it is not excluded that the lower undated deposits could reach the Upper Cretaceous, in analogy to the *Crete Nere* Fm. (Bonardi et al., 1988a; Guerrera et al., 2005).

The *Sicilide* Unit (Fig. 4) is similarly divided into four formations (Guerrera et al., 2005), from bottom to top: (i) clays and slates of *Argille Scagliose* Fm. (Fig. 13g); (ii) marls and limestones of *Monte Sant'Arcangelo* Fm.; (iii) clays and marls (locally including calcarenites rich in foraminifera), of *Argille Varicolori* Fm. (Fig. 13h, i); and (iv) foredeep deposits of the *Arenarie di Corleto* or *Tufiti di Tusa* Fms. (Fig. 3). The thickness is about 1000 meters (APAT, 2005). The age of these deposits ranges between the Upper Cretaceous(?) and Burdigalian.

2.5.2. Structural analysis

The *Parasicilide* Unit shows a heterogeneous deformation especially localized in the argillitic layers, where more competent beds are completely dismembered giving to the rocks an appearance of a broken formation (e.g. Mattioni et al., 2006). As well as the *Nord Calabrese* Unit, the *Parasicilide* succession is affected by three main folding stages. The first fold set (F_1^{PS}) shows different shapes, from chevron to rounded and from tight to isoclinal folds (Fig. 16e), locally related to meso-scale thrust faults. In argillitic layers an axial plane cleavage occurs, whereas in the more competent rocks it is disjunctive convergent fan cleavage. Previous structures are deformed by open to tight folds (F_2^{PS}; Fig. 16e), usually with a kink conjugate geometry. The interference pattern is intermediate between 2 and 3 types of the Ramsay's classification (Fig. 16e). F_1^{PS} fold hinges are very scattered (Fig. 17a) such as the poles to axial planes (Fig. 17b). F_2^{PS} fold hinges (Fig. 17c) indicate a large dispersion with two main clusters, E-W and N-S directed. Poles to axial planes (Fig. 17d) indicate a main gently N dipping plane. F_3^{PS} fold hinges (Fig. 17e) show a mean NNE-SSW trend with axial planes mainly dipping to N (Fig. 17f).

Like the previous units, the *Sicilide* succession is characterized by the superposition of three meso-scale fold sets. The rare early generally isoclinal folds F_1^{SI} (Fig. 16f) are deformed by a more frequent second fold set (F_2^{SI}) characterized by open to close geometries (Fig. 16f). The third fold set (F_3^{SI}) consists of open to close folds often associated with thrust faults both verging to NE and SW (Fig. 16g, h). Poles to bedding (S_0^{SI}) spread out around an almost vertical NNE-SSW cyclograph (Fig. 17g). F_1^{SI} fold hinges are scattered (Fig. 17h), whereas the poles to axial planes lie along a NNE-SSW almost vertical great circle (Fig. 17i). F_2^{SI} fold hinges show a mean E-W trend (Fig. 17j), whereas the poles to axial planes are scattered (Fig. 17k). Finally, F_3^{SI} fold hinges (Fig. 17l) indicate a mean NW-SE trend and the poles to axial planes (Fig. 17m) are located around a NE-SW vertical cyclograph.

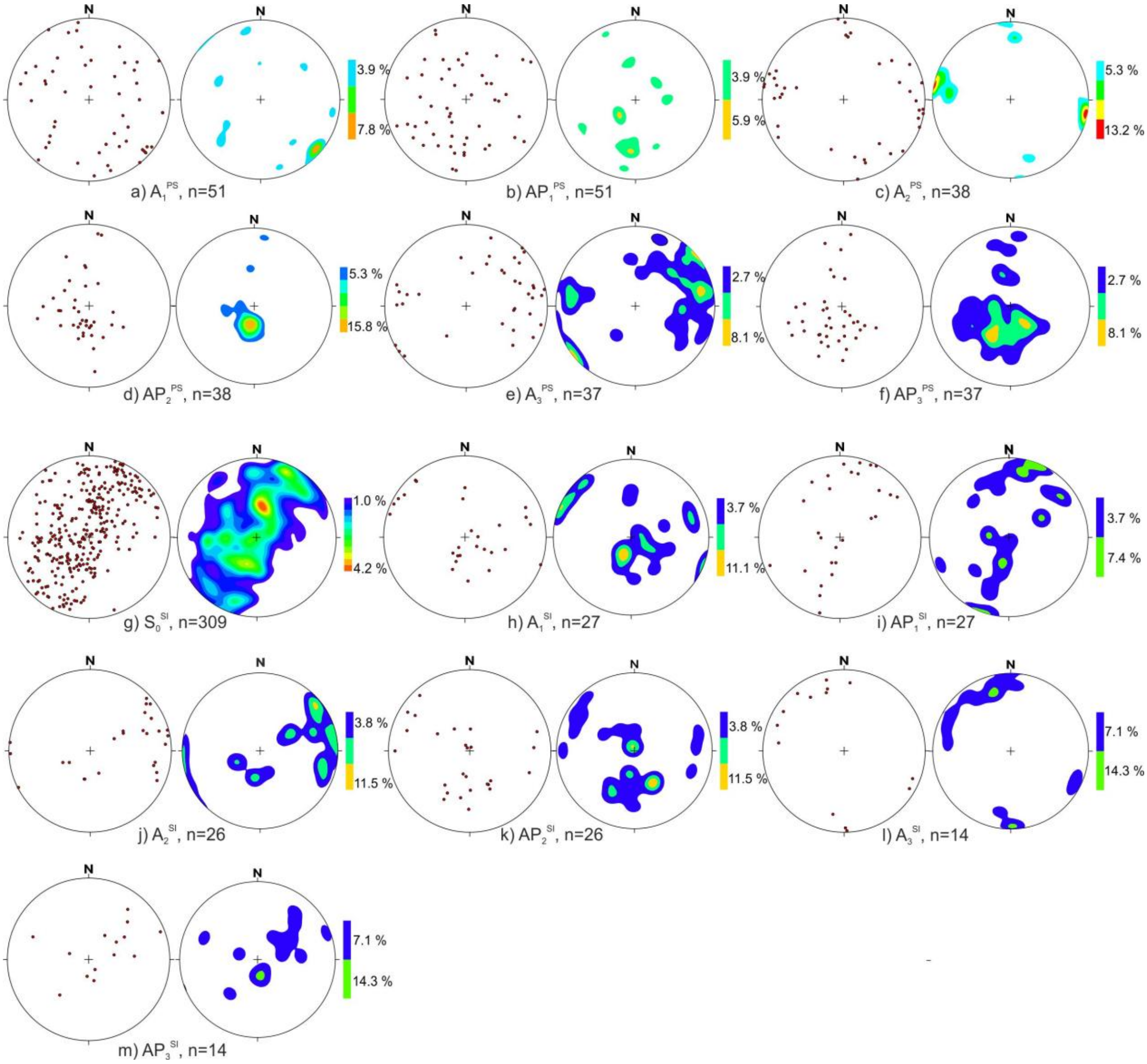

Fig. 17- Stereographic projections and contour plot of analyzed structures of *Parasicilide* and *Sicilide* Units (lower hemisphere, Schmidt net). PA: *Parasicilide*U.; SI: *Sicilide* U.

Chapter 3-LAC in northern Calabria

3.1. Introduction

The LAC Units cropping out in the northern *Calabria* (Fig. 18) are all characterized by HP/LT metamorphic ophiolitic sequences (e.g. Liberi and Piluso, 2009), ranging in age from Jurassic to Early Cretaceous age (Lanzafame and Zuffa, 1976). These include *Diamante-Terranova*, *Malvito* and *Gimigliano* Units, commonly interpreted as slices of oceanic lithosphere belonging to the Jurassic Tethys realm, consisting of metabasites and metasedimentary covers. These tectonic units are located between the overlying Paleozoic rocks and relative cover of Calabrides and the underlying carbonatic Apennine Units. In this work, as explained in the successive paragraphs, the study focused on the *Diamante-Terranova* Unit and shed lights on the complex metamorphic and deformative pattern affecting both metabasites and metasedimentary cover of this ophiolitic unit. By means of a geological and structural survey were collected a good number of data, and several samples in the different localities where this unit crop out. The results of the petrological and micro- and meso-scale structural analysis, together with the discussion of the tectono-metamorphic evolution, are explained below.

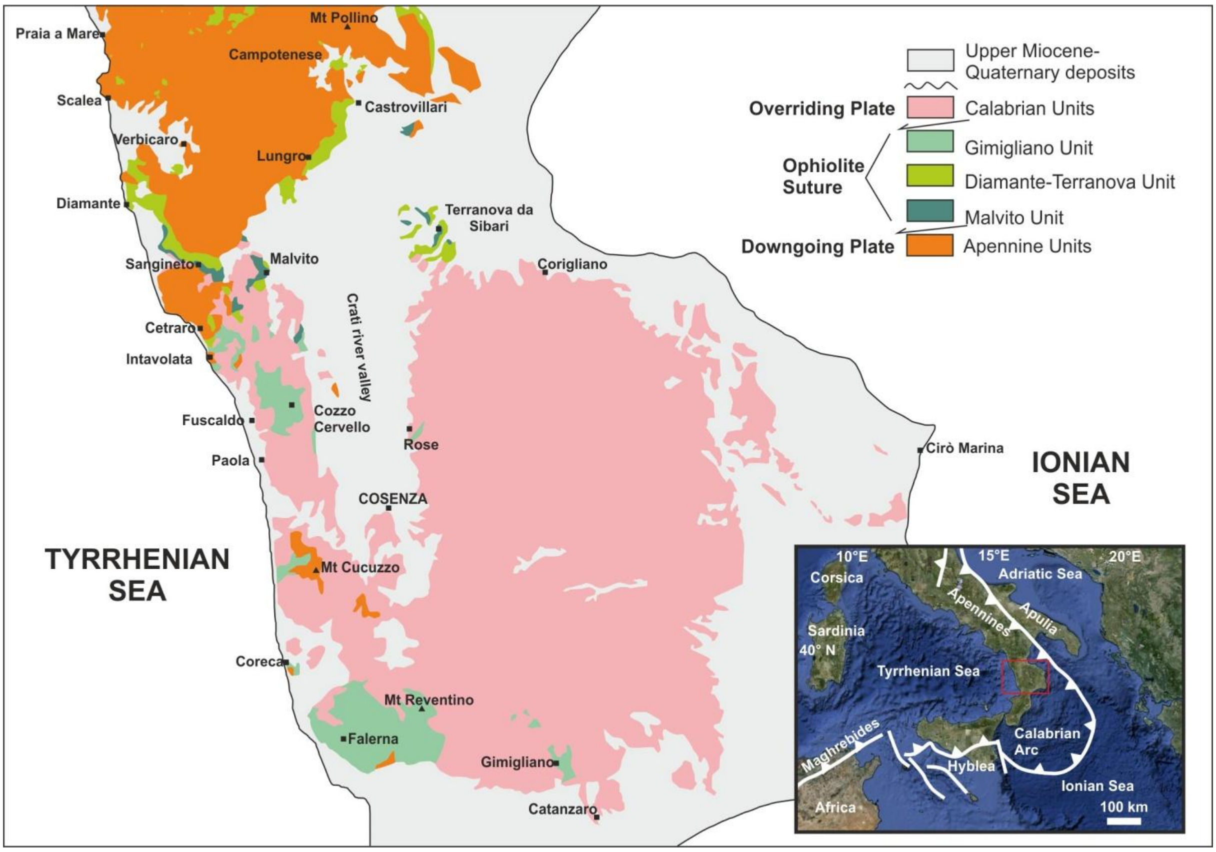

Fig. 18- Geological sketch map of *Calabria* (modified after Amodio-Morelli et al., 1976; Spadea 1976; Iannace et al., 2007).

3.2. Geological setting of LAC in northern Calabria

In northern *Calabria* (Fig. 18), several ophiolitic successions, known in literature as *Diamante-Terranova*, *Malvito* and *Gimigliano* Units (*Ofioliti Calabresi*; De Roever, 1972; Dietrich and Scandone, 1972; Spadea, 1976; Lanzafame et al. 1979, Beccaluva et al. 1982; Guerrera et al., 1993; Cello et al., 1996; Rossetti et al., 2001, 2004; Liberi et al. 2006; Liberi and Piluso, 2009) crop out. These tectonic elements are interposed between: (i) Apennine Units, in the lower part of thrust sheet pile, characterized by Middle Triassic-Lower Miocene carbonate and siliciclastic deposits (Ietto e Barillaro, 1993; Iannace et al. 1995; Iannace et al., 2007; Vitale et al., 2007; Vitale and Mazzoli, 2008); and (ii) the *Calabride* Complex on the top (Ogniben, 1960; Amodio-Morelli et al., 1976; Bonardi et al., 2001), formed by crystalline basement rocks of continental crust comprising three major units: (i) the *Bagni* Unit, made of Paleozoic phyllites with Triassic-Lower Cretaceous cover showing a green schist facies metamorphism; (ii) the *Castagna* Unit characterized by Paleozoic micashists, gneiss and granites, which locally shows an HP\LT metamorphysm and a metamorphic overprinting in greenschist facies (Rossetti et al., 2001, 2004). (iii) Finally, the *Sila* Unit includes biotite and garnet gneisses, diorites, tonalites, metabasites and, subordinately, peridotites showing a retrograde metamorphism in greenschist facies (Rossetti et al., 2001).

The whole ophiolitic suite (*Diamante-Terranova*, *Malvito* and *Gimigliano* Units) includes (Liberi and Piluso, 2009): (i) serpentinized ultramaphic mantle rocks, cropping out only in *Gimigliano-Reventino* Mt. area, associated with the upper metabasites; (ii) massive and foliated metabasaltic pillows, both porphyric and aphyric, and subordinately metaradiolarites; (iii) a metasedimentary cover, including pelagic sediments and Calpionella limestones, Titonian-Neocomian in age (Lanzafame and Zuffa, 1976; Spadea, 1976), and an alternance of metapelites, metalimestones and metarenites.

The *Diamante-Terranova* Unit is characterized by foliated metabasites with fine-grained blue and greenish bands, blue glaucophanites and subordinately medium to coarse grained rocks. The metasedimentary cover includes a ten meters-thick succession of phyllites and calcshists (Spadea, 1976; Rossetti et al., 2001; Liberi et al., 2006; Liberi and Piluso, 2009). In the *Terranova di Sibari* town (Fig. 18), the outcrops are made of massive mafic rocks, occurring as pillow lavas and pillow breccias, which rarely display a weak foliation. The Calabrian ophiolites were the object of a detailed study focused on the stratigraphy, petrography, tectonic and structural evolution (Amodio-Morelli et al., 1976; Spadea, 1976; Spadea et al., 1980; Cello et al., 1996; Rossetti et al., 2001, 2004; Liberi et al. 2006; Liberi and Piluso, 2009). The tectonic evolution of the *Diamante-Terranova* Unit was generally interpreted as a poli-phased deformation consisting of three deformative events (Cello et al., 1996; Rossetti et al., 2001, 2004; Liberi et al. 2006; Liberi and Piluso, 2009). The first stage, associated with a metamorphic recrystallization in the blueschist facies, comprises structures such as intrafolial tight to isoclinal folds, a pervasive foliation and a stretching lineation dipping to SE, the latter recorded only in metabasites (Cello et al., 1996; Liberi et al. 2006; Liberi and Piluso, 2009). The structures of the second deformative stage are centimeter- to meter-sized open to tight folds, verging mainly to NW, and a crenulation foliation developed under greenshist facies conditions (Cello et., al. 1991; 1996). The last deformative stage is recorded only from normal faults, cataclastic zone and veins. In conclusion the metamorphic evolution of the *Diamante-Terranova* Unit consists of a first step in blueschist facies and a successive re-equilibration in greenschist facies (Cello et al., 1996; Liberi et., al., 2006; Liberi and Piluso, 2009; Rossetti et al., 2001, 2004).

3.3. Structural analysis

The micro- and meso-structural analysis carried out in this work for the *Diamante-Terranova* Unit sheds light on a complex deformative pattern recorded in the whole succession by means of a lot of structures (Figs. 19-21-22-23). In order to better analyze the whole tectono-metamorphic evolution, micro- and meso-scale structures are separately analyzed and the results illustrated in the following paragraphs.

3.3.1. Meso-scale structures

At meso-scale the glaucophanites, cropping out close to the *Diamante* town, show a foliation marked by bluish (glaucophane + lawsonite) and greenish (chlorite + epidote + lawsonite) bands (Fig. 19a). The S_1 appears as the main foliation also in metapelites, and rare relicts of bedding planes (S_0) are preserved only in the metarenites of *Diamante-Terranova* metasedimentary corver (Fig. 21a). This deformation stage does not produce micro- and meso-scale folds in metabasites, whereas rare F_1 tight to isoclinal folds are preserved in the cover rocks (Fig. 21a). In the metabasaltic rocks, several veins occur, at places forming orthogonal sets, producing a table-chocolate boudinage (Fig. 19d). Also a severe boudinage of lawsonite-epidote-chlorite-rich layer in Na-amphibol-rich matrix occur (Fig. 20a). S_1 foliation and early veins are deformed by isoclinal to tight folds (F_2) both in basement and cover rocks (Figs. 19c, f; 21b), often with kink geometry in metapelites. Both in metabasites and meta-sedimentary cover, a crenulation cleavage (S_2) (Fig. 19g) with associated crenulation lineation (CL_2) (Fig. 19e) developed, related to F_2 folds (Fig. 19b). A mineral/stretching lineation (SL_1), in epidote, is well evident, especially in metabasites (Fig. 19b) along the S_1 foliation, generally orthogonal to the F_2 fold axes. D_3 deformation stage produces, in glaucophanites, close to open folds (F_3) (Fig. 19 f, h), locally associated with thrust faults with centimetric to metric displacements; whereas in metasedimentary cover rocks F_3 folds occur with kink geometry (Fig. 21d). A crenulation cleavage (S_3) and a crenulation lineation (CL_3), occur both in metabasites (Fig. 19a) and in metapelites. F_2 and F_3 folds, in metabasites generally show an axial trend ranging from parallel to orthogonal and forming interference pattern from type 2 to type 3 (Fig. 19h) according to Ramsay's classification (Ramsay, 1967). As well as in the metabasites, also in metasedimentary cover rocks an interference pattern, formed by F_2 and F_3 folds and ranging between type 2 and 3, occur (Fig. 21c). A fourth deformation stage (D_4) is recorded mainly in metabasites by high-angle normal faults, sometimes characterized by cataclasites and fault breccias rich in chlorite and epidote (Fig. 20b, c). Finally a D_5 stage includes normal (Fig. 20d) and strike-slip faults (Fig. 20e).

Poles to S_1 show a cluster distribution both in basement (Fig. 22a) and cover (Fig. 23d) rocks with mean values of 333/64 and 339/57, respectively. The S_0 poles preserved only in metasedimentary cover, show a cluster distribution with 280/59 mean value (Fig. 23a). As well as stratification, also rare early isoclinal to tight folds (F_1), occurring only in the cover rocks, are characterized by a scattered distribution of A_1 (Fig. 23b), whereas poles to axial planes (Fig. 23c) show a broad cluster distribution with 277/69 mean value. The stretching lineation (SL_1), measured both in metabasites and in cover rocks, are characterized by an orientation ranging from E/W to NE/SW (Figs. 22b; 23e). F_2 fold axes (A_2) and crenulation lineation (CL_2), of metabasites (Fig. 22c, e), show scattered distribution but, a main NNW-SSE trend can be observed; also poles to axial planes (AP_2) of these folds show a scattered distribution but a main cluster to NE can be detected (Fig. 22d). F_2 fold axes (A_2), recognized in the cover rocks, are characterized by a NE/SW main trend (Fig. 23f), whereas poles to axial planes are scattered (Fig. 23g). Poles to S_2 foliation show a cluster distribution both in metabasites and cover rocks, furnishing a mean value of 332/51 and 048/62, respectively (Figs. 22f; 23h). F_3 fold axes (A_3) and crenulation lineation (CL_3) show a NW/SE direction, both in the metabasites (Fig. 22g, i) and in metasedimentary cover rocks (Fig. 23i, k) whereas poles to AP_3 show a scattered distribution (Figs. 22h; 23j).

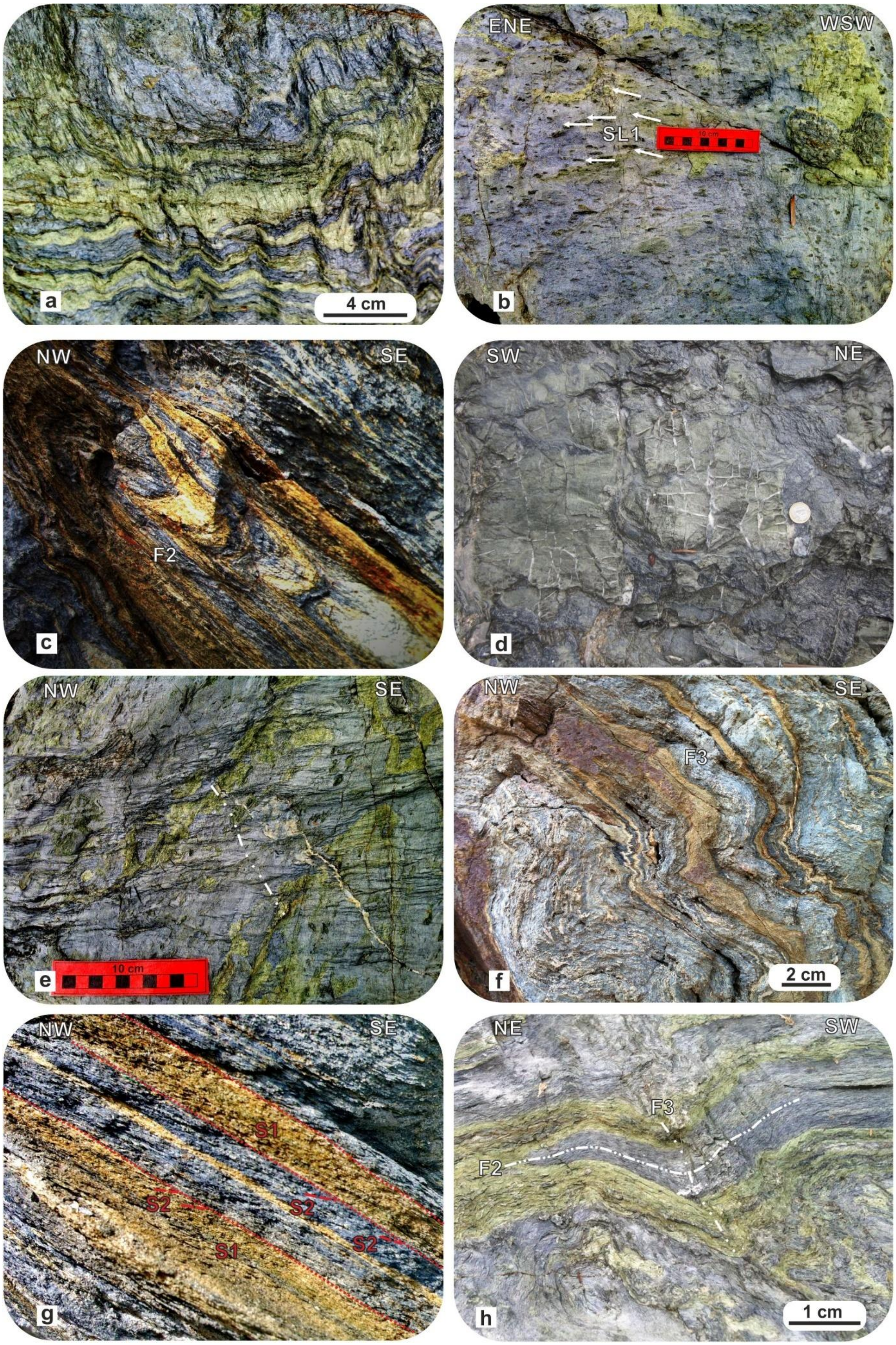
a
4 cm
ENE
WSW
SL1
10 cm
b
NW
SE
F2
c
SW
NE
d
NW
SE
10 cm
e
NW
SE
F3
2 cm
f
NW
SE
S1
S2
S2
S2
S1
g
NE
SW
F3
F2
1 cm
h

Fig. 19- Examples meso-structures of *Diamante-Terranova* Unit: (a) S_1 metamorphic foliation well-marked by bluish (Na-amphibole + lawsonite) and greenish (epidote-chlorite-lawsonite) bands deformed by F_2 isoclinal folds and D_3 crenulation. (b) Stretching lineation (SL_1) marked by isoriented epidote minerals along the S_1 foliation. (c) F_2 meso-scale tight to open folds. (d) Two orthogonal vein sets forming a tablet-chocolate boudinage. (e) Crenulation lineation (CL_2) related to S_2 crenulation cleavage. (f) F_3 tight to open meso-scale folds overprinting F_2 isoclinal folds. (g) Overprinting between S_1 and S_2 foliations. (h) Type-3 interference pattern between F_2 and F_3 folds.

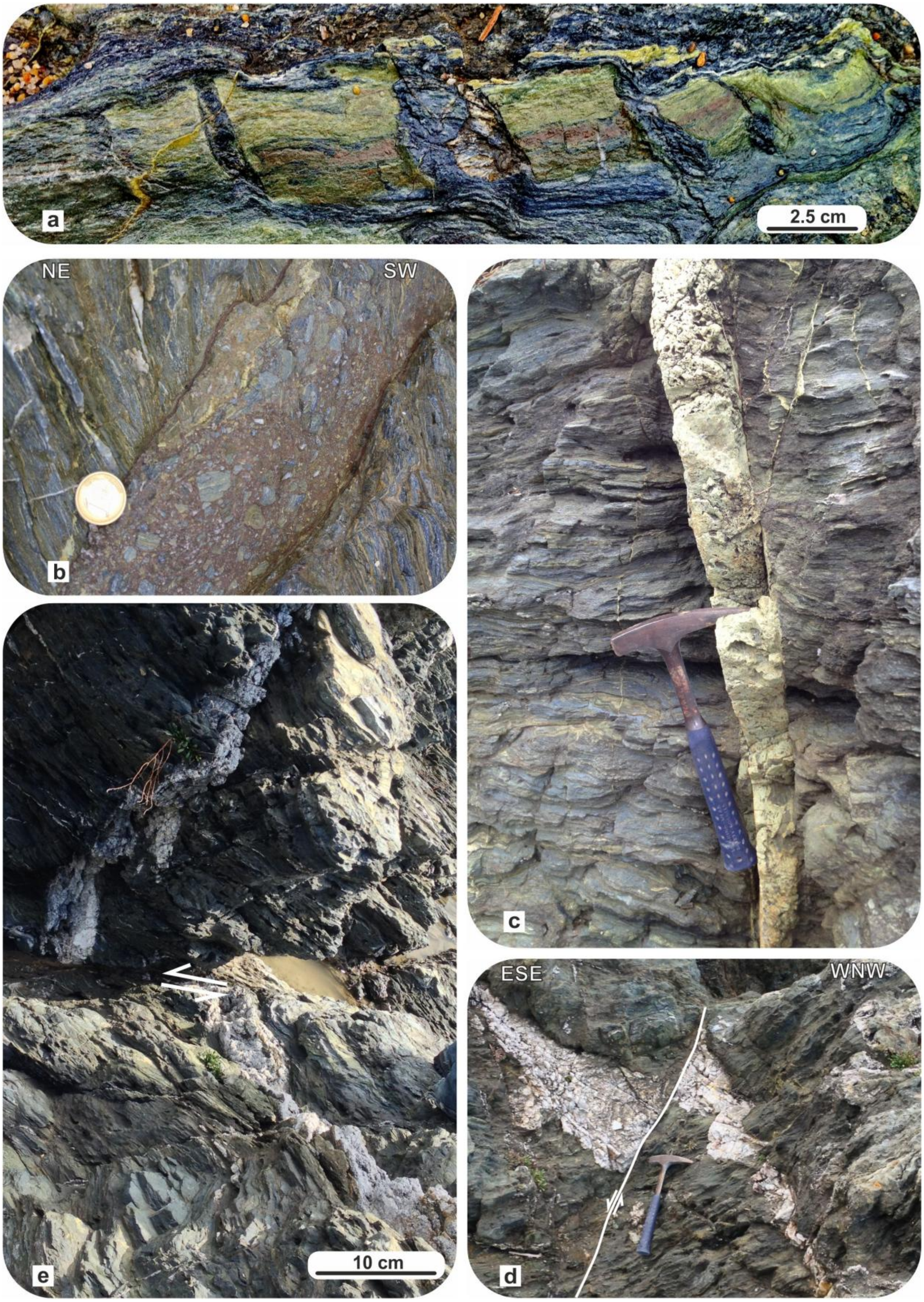
a
2.5 cm
NE
SW
b
c
ESE
WNW
d
e
10 cm

Fig. 20- Examples meso-structures of *Diamante-Terranova* Unit: (a) Boudinated lawsonite-epidote-chlorite-rich layer in Na-amphibol-rich matrix. (b) D_4 normal fault producing cataclasites rich in epidote and chlorite. (c) D_4 normal faultwith a aplitic dyke. (d) D_5 high-angle normal fault (e) D_5 left-lateral strike-slip fault.

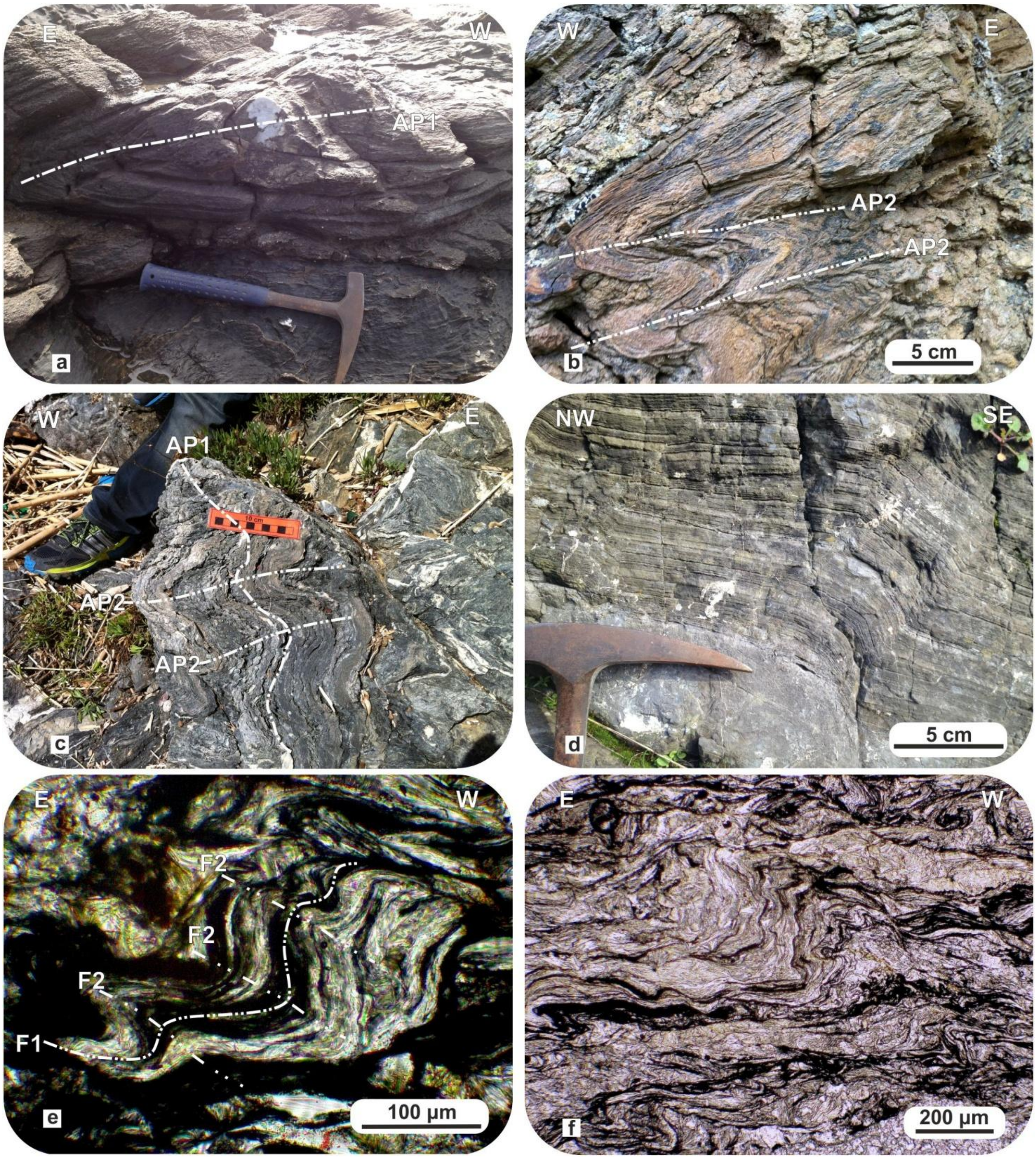

Fig. 21- Examples of micro- and meso-structures of the *Diamante-Terranova* Unit metasedimentary cover: (a) S_0 relicts deformed by F_1 isoclinal fold in metarenites. (b) F_2 tight to isoclinal folds. (c) 3-type interference pattern between F_1 and F_2 folds. (d) Kink shape F_3 fold. (e) Thin section microphotographs showing a 3-type interference pattern between F_1 and F_2 folds (DIA-6). (f) Thin section microphotographs showing a D_2 crenulation cleavage (DIA-6).

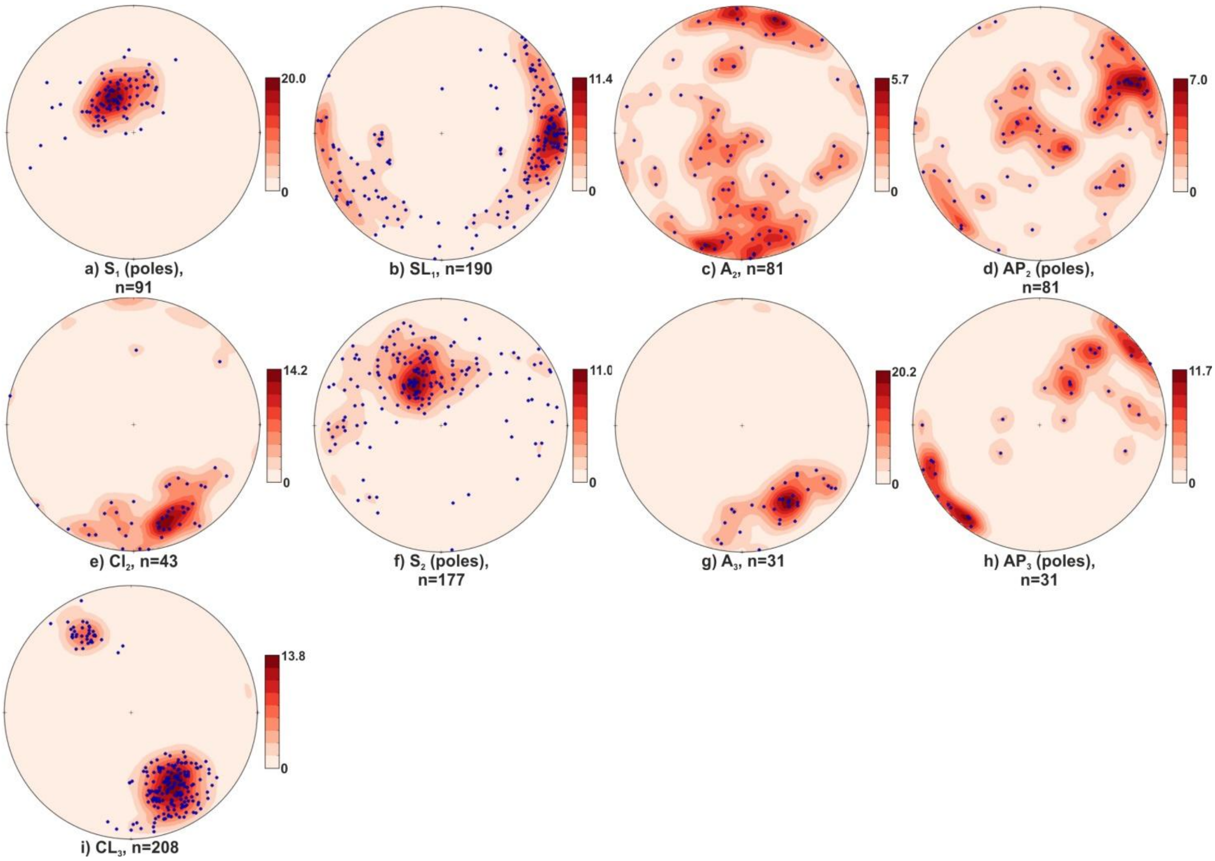

Fig. 22- Stereographic projections and contour plot of analyzed structures of metabasites of *Diamante-Terranova* Unit (lower hemisphere, Schmidt net).

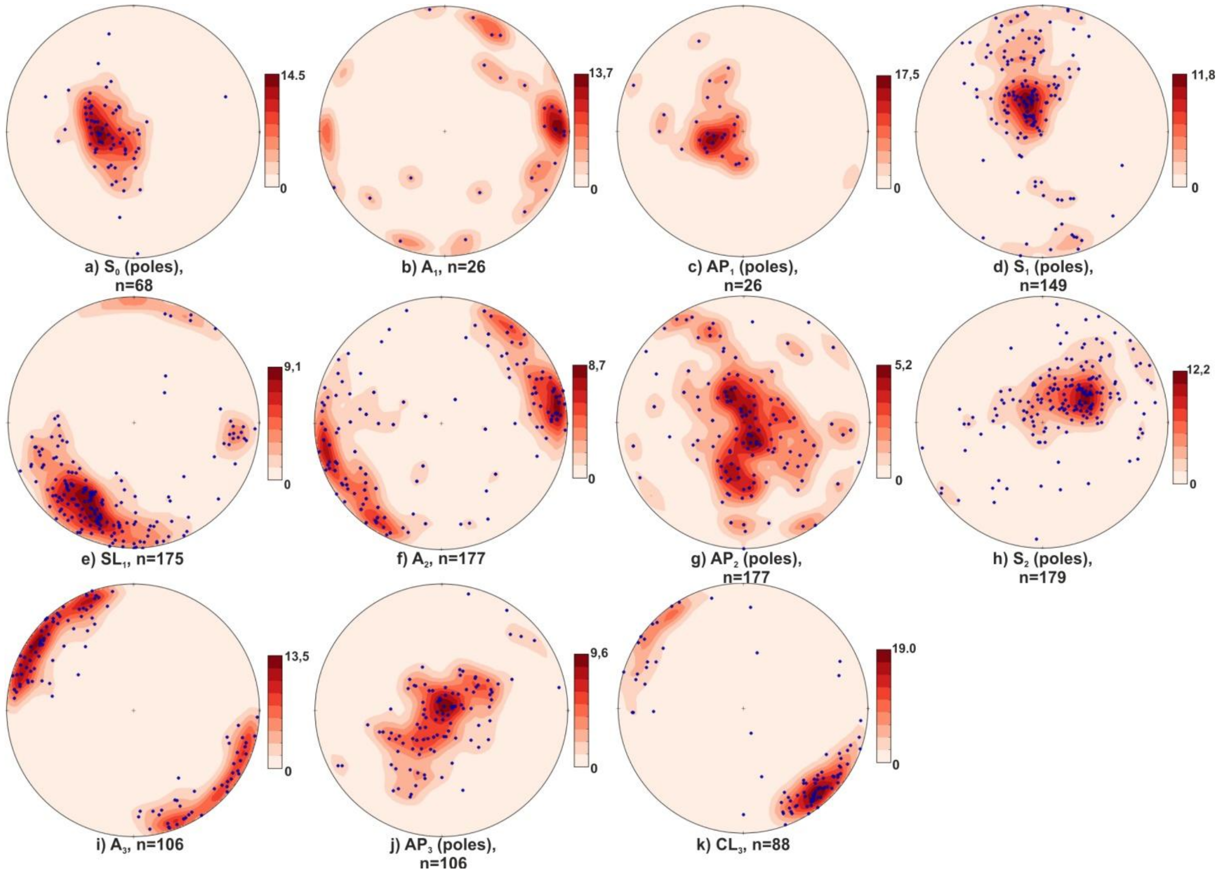

Fig. 23- Stereographic projections and contour plot of analyzed structures of metasedimentary cover rocks of *Diamante-Terranova* Unit (lower hemisphere, Schmidt net).

3.3.2. Micro-scale structures

The thin section analysis carried out on metabasites of the *Diamante-Terranova* Unit revealed the occurrence of several metamorphic features. An early deformation was recorded by means of a metamorphic foliation (S_1) highlighted by bluish and greenish band alternations (Fig. 24a), characterized by isorientation of lawsonite and white mica. To this deformation stage is associated the growth of syn- (Fig. 24b), inter- and post-D_1 lawsonite (Fig. 25) together with Na-amphibole, epidote and chlorite (Fig. 25). D_2 deformation stage is characterized by folds (Fig.24c) and related foliation (S_2) (Fig. 24d), deforming the previous structures. Also late D_2 veins (Fig. 24d, e), hosting Na-amphibole, epidote and chlorite, occur. The growth of lawsonite happens in the late stages of this deformation stage (Fig. 24e). However, although syn- and inter-D_2 lawsonite are not found in the analyzed samples, the recurrence of this mineral in the whole deformation allow us to assume a continued growth (Fig. 25). Late D_2 S-C' structures (Fig. 24h) are recorded in thin section. These latter, the only clear kinematic indicators, are orthogonal to the stretching lineation and indicate a S/SSE tectonic vergence. The structural constraint, giving the relative timing of these structures, is the D_3 crenulation cleavage, which deforms the S-C' structures.

The third deformation step (D_3) produces folds and a crenulation cleavage (S_3) (Fig. 24f). In this case the relationship between foliation (S_3) and lawsonite suggest a growth post D_3 (Fig. 24f). Even though there aren't clear evideces to link the occurrence of the Ca-amphibole to a precise deformative stage, its presence on the rim of Na-amphibole (Figs. 24g, 25), suggest a growth during the latest deformation stages, probably during the D_4.

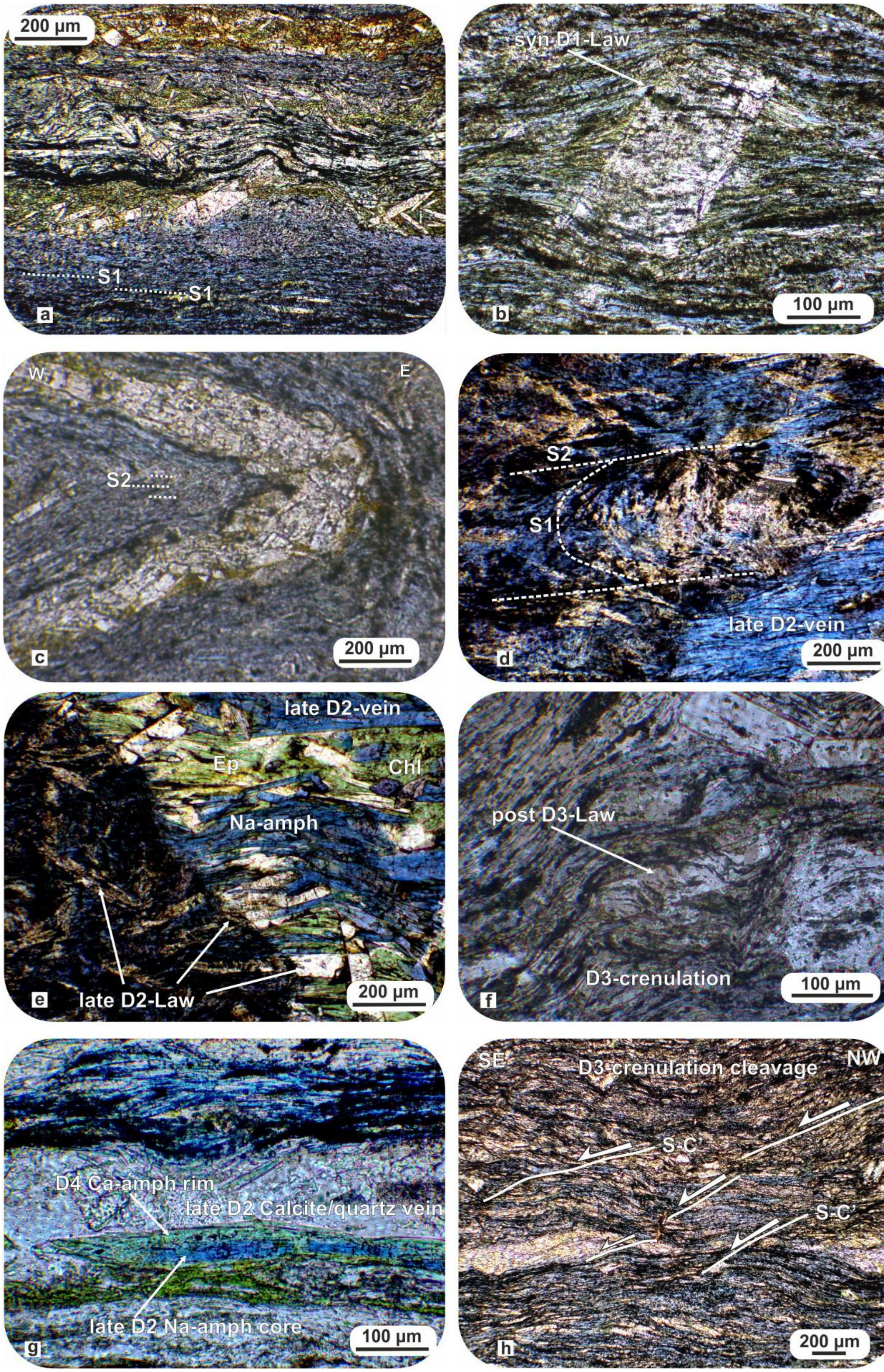
200 µm
S1
S1
a
syn D1-Law
100 µm
b
W
E
S2
200 µm
c
S2
S1
late D2-vein
200 µm
d
late D2-vein
Ep
Chl
Na-amph
late D2-Law
200 µm
e
post D3-Law
D3-crenulation
100 µm
f
D4 Ca-amph rim
late D2 Calcite/quartz vein
late D2 Na-amph core
100 µm
g
SE
D3-crenulation cleavage
NW
S-C'
S-C'
200 µm
h

Fig. 24- Thin sectionsmicrophotographs of some samples of *Diamante-Terranova* Unit: (a) S_1 metamorphic foliation in metabasites (DIA-1). (b) Syn-D_1 lawsonite (DIA-1). (c) F_2 fold with associated S_2 axial plane cleavage well-marked by a green layer formed by lawsonite and epidote (DIA-7). (d) Thin section microphotographs showing S_1 (disjuntive foliation relict in microlithons) and S_2 (crenulation foliation) in metabasites (FT-3). (e) Late-D_2 vein formed by Na-amphibole, epidote, chlorite and lawsonite, crosscutting a host rock formed by S_1-S_2 foliation and late-D_2 static lawsonite (DIA-5). (f) D_3 crenulation cleavage and post-D_3 static lawsonite including the crenulated S_2. (g) Zoned amphibole, in late-D_2 quarz/calcite vein, with Na-richcore (glaucophane) and Ca-rich rim (actinolite) (DIA-1). (h) Late D_2 S-C' structures deformed by D_3 crenulation cleavage (DIA-5).

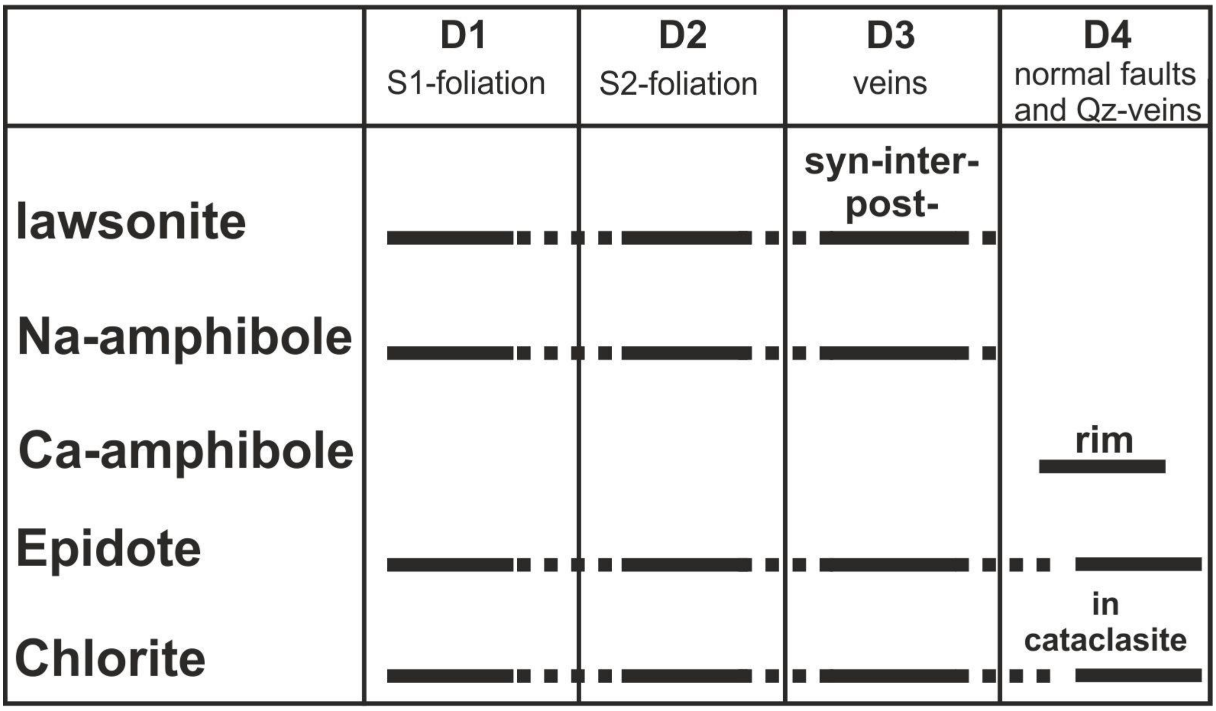

Fig. 25- Blastesis-deformation diagram.

3.4. Petrography of *Diamante-Terranova* Unit

The analyzed successions are made of metabasites covered by phyllites, metarenites and calcshists. Metabasites of *Diamante* occur as bluish-greenish, pervasively foliated blocks (Fig. 24a) in which the original layering was completely deleted and the original igneous structures obliterated. Metabasalt samples were recovered in two different localities, namely *Diamante* and *Terranova di Sibari* (Fig. 18). Mineral parageneses include mainly lawsonite, blue amphibole (glaucophane), chlorite epidote and green amphibole (tremolite), plus accessory quartz, albite, titanite and oxides. No significant differences have been observed between metabasaltic samples from different outcrop localities, although the *Terranova di Sibari* samples generally display a finer grain size. Lawsonite occurs as abundant, relatively well-developed and coarse-grained bladed crystals showing a wide range of textural relations with the surrounding matrix, suggesting a continuous growth (from pre- to inter- post-tectonic stages; Fig. 24b, e, f). Blue amphibole crystals (Fig. 24e, g) are represented by extremely abundant small, needle-like isoriented crystals outlining the main foliation of the rocks (Fig. 24a). Worth of note is the evident zonation shown by some individuals which display a clearly more Ca-rich greenish rim developed on the Na-rich blue core (Fig. 24g). The metabasites frequently host quartz and calcite veins (Fig. 24g), within which zoned amphibole aggregates are often observed, as well as epidote veins. The former structures are commonly folded (ptygmatic folds). Also the main foliation is sometimes deformed by F_2 micro-folds (Fig. 24c).

The thin-section analysis performed for the metapelites reveal a low crystallinity and a mineral assemblage characterized mainly by mica (in cleavage domains) and quartz microlithons. These rocks are affected by intrafolial folds (Fig. 21e), crenulation cleavage (Fig. 21f), and occasionally are cutted by large quartz veins.

Chapter 4-Disussion

4.1. *Frido* Unit

The structural and petrographic analysis on the *Frido* Unit sheds light on the complex evolution of this metamorphic succession. The *Frido* Unit recorded a single coherent tectonic evolution of both oceanic and continental crust rocks and experienced an HP/LT metamorphism for the various lithologies.

The whole succession recorded five deformation stages: (i) the first two deformative pulses (D_1-D_2) are characterized by a consistent orientation and metamorphic grade, suggesting a common genesis within a progressive deformation and producing main structures as foliations, folds, veins and faults. (ii) Extensional brittle-ductile shear zones (D_3), related to the tectonic exhumation of the Unit and deforming the previous structures, occur in all lithologies. (iii) The last two stages (D_4 and D_5), which affect the whole LAC, developed at shallower crustal conditions, are probably related to the post-Middle Miocene tectonic evolution of the Apennines fold and thrust belt. F_2 folds generally show fold hinges roughly parallel to the stretching lineation. These features may be interpreted as a result of intense, non-coaxial plastic strain that allowed the rotation of the early fold hinges towards the maximum lengthening axis (i.e. in the direction of the orogenic transport; e.g. Alsop and Holdsworth, 2004).

The geological map of Fig. 5 shows the tectonic vergence/transport direction associated with the D_2, D_4 and D_5 deformation events. For D_2, the direction of the tectonic transport was interpreted as being parallel to the mineral/stretching lineation (SL_2), which shows a mean NW-SE trend.

In analogy with those recorded in the *Lungro-Verbicaro* Unit, in northern *Calabria* (Vitale and Mazzoli, 2008) and in the *Nord Calabrese* and *Parasicilide* units in the *Cilento* area (Ciarcia et al., 2012; Vitale et al., 2011) a dominant top-to-the-SE kinematics may be envisaged for this deformation stage.

For D_4 and D_5, the structures vergence was established by means of asymmetric folds and meso-scale thrust faults. The former stage tectonic transport ranges from NE to E, whereas for D_5 it ranges between NW and NNE.

Stratigraphic and structural observations, illustrated in this work, allow to constraint the age of progressive deformation (D_1, D_2 and D_3 stages) from the Late Oligocene (age of the upper part of the *Frido* succession) to the middle Tortonian (age of the first unconformable deposits on top of the exhumed *Frido* Unit). The D_4 structures are very similar to the Tortonian features hosted in the Langhian-lowermost Tortonian wedge-top-deposits of *Albidona* Fm., indeed show similar deformative style, geometry and are also characterized by a main NE vergences (e.g. Cesarano et al., 2002; Ciarcia et al., 2012).

According to Mattei et al. (2007), a ~60° counterclockwise rotation was experienced for the pre-Upper Miocene successions of the Apennine wedge; this means that for the observed NE to E vergences, a general SE-directed original tectonic transport may be inferred. Finally, D_5 is likely to postdate the deposition of the younger wedge-top basin deposits of the *Perosa* Fm. (middle-upper Tortonian).

The petrographic analyses carried out on selected metapelite and phyllite samples allowed rough estimates of the geothermobarometric conditions experienced during metamorphism, as thoroughly discussed in Vitale et al. (2013). The most interesting petrographic feature is surely the occurrence of carpholite, a typical HP/LT phase in

Alpine-Himalayan metapelitic complexes. Textural and chemical evidences suggest its formation at P > 0.6 GPa and T < 350 °C. This is consistent with the relatively Fe-rich character of the *Frido* carpholite when compared with the carpholite crystals from other units of the Western Alps and Apennines.

Another important petrographic feature of the *Frido* Unit parageneses is the presence of strongly zoned Na-Ca to Na-amphibole, which shows a decrease of Al_2O_3 from core to rim, interpreted as an indicator of switching conditions, from high to low pressures. Finally, geothermobarometric indications resulting from the composition of chlorite and white mica indicate T values of ~350-360 °C for the phyllites and of ~330-340 °C for the metapelites, coupled with P values of ~1.4 GPa and ~1.2 GPa, respectively.The reconstructed P-T-t path of *Frido* Unit (Fig. 26) provides some points for reflection. It's worth noting that respect to those carried out for *Lungro-Verbicaro* Unit (Iannace et al., 2007) and for Calabrian ophiolite Units (Liberi and Piluso, 2009; Rossetti et al., 2002), the *Frido* Unit experienced lower temperatures during burial and subsequent exhumation. However it must be underlined that only for the *Frido*, the *Lungro-Verbicaro* (Iannace et al., 2007) and the *Gimigliano* (Rossetti et al., 2002) Units, the P-T metamorphic peak conditions were calculated by means of carpholite-chlorite-mica assemblages (Fig. 26). The lack of evidences of greenschist facies re-equilibration for all the ophiolite-bearing units can be taken as indicative of a fast exhumation, possibly occurring within the subduction channel and associated with the development of an extrusion wedge similarly to the exhumation process envisaged for relatively high pressure (HP) and ultra-high pressure (UHP) units in various mountain belts of the Alpine-Mediterranean area (e.g. Searle et al., 2004). Such extruded wedges are bounded by a reverse shear zone at their base and by a 'normal-sense' shear zone at the top, the latter representing a geometric requirement for extrusion rather than a true extensional structure (e.g., Mazzoli and Martín-Algarra, 2011; Ring and Glodny, 2010). When the P-T-t paths reconstructed for the Tuscan Archipelago and Alpine Corsica (e.g., Brogi and Giorgetti, 2012; Jolivet et al., 1998) are compared with those estimated in the southern Apennines and northern *Calabria* (Iannace et al., 2007; Liberiand Piluso, 2009; Rossetti et al., 2002), including the results of this study (Fig. 27), it appears that the P-T-t evolution of the *Frido* Unit is similar to that recorded by the rocks of the *Schistes Lustrés* and Ligurian ophiolites cropping out in *Gorgona* and *Giglio* Islands, respectively (Jolivet et al., 1998). Summarizing, subduction of the *Frido* succession to depths of ~40 km can be envisaged, accompanied by high pressure/very low temperature (HP/VLT) metamorphism (T ~330-360 °C; P ~1.2-1.4 GPa) and the development of two generations of superposed structures (D_1 and D_2 stages described in this study). Subsequently, fast exhumation occurred, testified by the lack of higher temperature metamorphic overprints and by the growth of lower pressure minerals along extensional shear planes (D_3). Finally, the last two deformation phases (D_4 and D_5) postdate substantial exhumation of the *Frido* Unit.

4.2. *Nord Calabrese, Parasicilide* and *Sicilide* Units

The structural analyses, carried out for sedimentary succession of LAC (*Nord Calabrese*, *Parasicilide* and *Sicilide*), reveal a poly-phased tectonic evolution characterized by the superposition of three main folding stages. The *Nord Calabrese* Unit show intense deformation principally focused in the upper part of *Crete Nere* Fm. and in the lower part of *Saraceno* Fm. (i.e. *Punta Telegrafo* Mb.). The middle-upper part of *Saraceno* Fm. and the lower part of *Crete Nere* Fm. host, respectively, sporadic folds and thrust faults and a pervasive cleavage in the black shales and argillites. As these latter portions of *Nord Calabrese* Unit, also the *Parasicilide* and *Sicilide* Units are less deformed, however locally the deformation, localized in argillitic levels, produced a complete bedding disruption, giving to this unit the aspect of a broken formation (Mattioni et al. 2006). The analyzed successions on the *Calabria-Lucania* boundary, in analogy with remnants of LAC cropping out in the *Cilento* and *Sele* river valley (Ciarcia et al., 2009, 2012; Vitale et al., 2010, 2011), show a tectonic evolution consisting of: (i) two progressive folding stages, D_1 showing E-W, NW-SE and D_2 characterized by N-S, NE-SW fold trends (Fig. 4). These latter are related to the building of thrust sheet pile in the Burdigalian time, i.e. following the foredeep deposition (*Tufiti di Tusa* Fm.) and before the Langhian sedimentation of the wedge-top basin deposits (*Albidona* Fm.). A third folding and thrusting stage (D_3) show a dominant NW-SE fold trend (Fig. 4) and affect also the wedge-top basin deposits of the *Albidona* Fm. and the underlying carbonates of the *Pollino-Ciagola* Unit. The successive folding phase (D_4) probably occurred before the deposition of the unconformable upper Tortonian-lower Messinian wedge-top basin deposits of *Oriolo* Fm., and synchronous with the *Lagonegro* Units early deformation, as consequence of the accretion of these units within the Apennine thrust sheet pile (Vitale and Ciarcia, 2013). In the *Monte Alpi, Ferro* River Valley, *Farneta*, *Valsinni* Ridge and *Rotondella* areas (Fig. 4), the whole thrust sheet pile and the Miocene wedge-top deposits are deformed by deeply rooted thrusts and back-thrusts characterized by a constant NE-SW shortening (e.g. Piedilato and Prosser, 2005). A further deformation stage is described by several authors (e.g. Catalano et al., 1993; Bonini and Sani, 2000;

Ferranti et al., 2009) at the *Lucania-Calabria* border and the external sector of the Lucanian Apennines. Such a Pleistocene deformation is expressed as a strike-slip faulting with a mean NW-SE compression that may locally have distorted the orientation of pre-existing folds and to be the cause of the dispersion of fold hinges as shown in the map of Fig. 4. Though distinct also in this work, as suggested by Bonardi et al. (1988), *Parasicilide* and *Sicilide* Units show more similarities than differences, hence taking into account (i) the stratigraphic and deformation evolution described in this work and in Ciarcia et al. (2009, 2012) and Vitale et al. (2013b); (ii) the structural position both below the *Nord Calabrese* Unit and (iii) the lacking of a clear tectonic feature between them, these deposits can be considered as a single succession although characterized by significant lateral facies heteropies. Another most important aspect consist also in the similarities existing between *Sicilide* Unit and the Paleogene-Lower Miocene succession of *Lagonegro-Molise* Basin Units (*Flysch Rosso*; Scandone, 1967), which led notable ambiguity in the literature comprising also the new Italian geological cartography (CARG project). The comparable deposition of *Parasicilide* and *Sicilide* successions could be interpreted as the consequence of the connection between the W-located MFB and the *Lagonegro-Molise* and *Imerese* Basins to the E (Fig. 28) which divided Apennine and Apulian Platform, located to north and the African margin located to south. As concerning the meaning of oceanic and continental crust bodies at base of the *Nord Calabrese* succession, recently Shimabukuro et al. (2012) provided a ^{40}Ar-^{39}Ar dating of 193±2 Ma for the lower continental crust rocks (amphibolites) sampled in the *Timpa di Pietrasasso* (Fig. 5). The authors suggest that this post-Hercinian age is related to the exhumation of the lower continental crust during a Jurassic early rifting stage, as previously proposed by Piccardo (2009) for the corresponding Ligurian Units cropping out in the northern Apennines.

4.3. *Diamante-Terranova* Unit

The structural survey on the *Diamante-Terranova* Unit (Fig. 29) revealed a complex deformation pattern coherently recorded both in the metabasites and in the cover rocks; furthermore the thin section analysis allowed several considerations on the microstructures and on the main mineral parageneses occurring in metabasites of this tectonic unit.

The whole succession recorded five deformation stages including several structures such as foliations, folds and veins related to three main steps (D_1, D_2 and D_3) suggesting a common tectonic evolution within a progressive deformation; extensional brittle-ductile shear zones and normal faults (D_4), the latter characterized by epidote and chlorite bearing cataclasites, related to the tectonic exhumation and finally (D_5) normal and strike-slip faults crosscutting all previous structures. Stretching lineations hosted in the metabasites show a main cluster distribution indicating a main E-W direction (Fig. 22b), whereas those located in the metasedimentary cover (Fig. 23e) show an about orthogonal direction. It worth to note that the only clear kinematic indicators in the metabasites are S-C' structures orthogonal to the SL indicating a S/SSE tectonic vergence for the *Diamante-Terranova* Unit, then completely different from those suggested for the metamorphic deformation stage by Rossetti et al. (2004) (NE/E), Liberi and Piluso (2006) (WNW) and Cello and Mazzoli (1998) (NW). It follows that the E-W directed SL in the metabasites indicate an extension related to a pure shear component orthogonal to the shear sense (e.g. lateral extrusion; Jones et al.,

1997) such as the *Lungro-Verbicaro* Unit (Vitale and Mazzoli, 2009), whereas the SSW-trending main cluster of the SL in the cover is about parallel to the tectonic transport. F_2 fold hinges range from parallel to orthogonal to the SL both in metabasites and in the cover rocks. This variability may be interpreted as result of different grades of rotation towards the maximum lengthening axis (e.g. Alsop and Holdsworth, 2004). On the contrary, the F_3 fold axes are always orthogonal to the sense of shear, indicating a SW vergence.

The P-T-t path of the *Diamante-Terranova* Unit (Liberi and Piluso, 2009), (Fig. 26-27) provides, for the metamorphic peak, pressure value from 0.9 to 1.1 GPa and temperature of 380 °C. Comparing these values with that calculated for the *Frido* Unit, higher temperature of pressure peak is evident. The microstructure analysis on thin section provides at least two foods for thought: (i) the occurrence of pre- to inter- and post-tectonic lawsonite during the D_1-D_3 deformation, indicates HP/LT metamorphic conditions for these stages; (ii) the zoning shown by some amphiboles displaying Ca-rich greenish rim developed on the Na-rich blue core (Fig. 24g) suggests that the D_4 deformation stage occurred at lower pressure conditions. Finally, the D_5 deformation stage, recorded by normal and strike-slip faults, occurred at very shallow crustal level.

4.4. Geodynamic implications

The results of this work, together with available geological evidences (Handy et al.,2010;Carminati et al., 2012; Turco et al., 2012; Vitale and Ciarcia, 2013), suggest that the Calabrian and *Frido* ophiolites were originated from a single oceanic domain, starting subduction from the Eocene (Vignaroli et al., 2012) and Late Oligocene

(Bonardi et al., 1988a), respectively, and record a similar geodynamic evolution. The best evidences are:

1) LAC and Calabrian ophiolites are located between the Calabrian Complex (CPT), on the top, and the Apennine Platform carbonates, at the bottom. In other words, they form an oceanic suture between the overriding and downgoing plates.
2) The timing of subduction and closure of the eastern branch of the Ligurian Ocean ranges between the Eocene and Upper Oligocene. These ages result from:
   a) stratigraphic ages of the uppermost meta-sedimentary cover of the Calabrian and *Frido* ophiolites, respectively (Bouillin, 1984; Bonardi et al., 1988a);
   b) the ~30/33 Ma (Rupelian) and 46.7±0-4 Ma (Lutetian) on HP phengites $^{40}Ar/^{39}Ar$ ages for HP/LT metamorphism of the Calabrian ophiolites (Rossetti et al., 2004; Shimabukuro et al., 2012);
   c) the Late Oligocene-early Tortonian syn-convergence exhumation recorded by apatite fission track cooling ages (Thomson, 1998) for the CPT (*Bagni* Unit, 11-15 Ma; *Castagna* Unit, 12-17 Ma; *Sila* Unit, 21-15 Ma; and *Aspromonte* Unit, 18-33 Ma), presently located in the hanging wall to the Calabrian ophiolites (Amodio-Morelli et al., 1976);
   d) the Eocene (Lutetian-Bartonian) age of the first subduction-related volcanism in the present-day Genoa Gulf (Réhault et al., 2012) and northern Sardinia (Lustrino et al., 2009).
3) The P-T-t paths (Fig. 26) reconstructed for the *Frido* Unit and for the Calabrian ophiolites are comparable and suggest a similar tectonic evolution characterized by HP/LT metamorphism and subsequent fast exhumation (possibly occurring, for the *Frido* Unit, along a cooler path).

Following recent studies (e.g. Carminati et al., 2012; Handy et al., 2010; Turco et al., 2012; Vitale and Ciarcia, 2013), we envisage a Eocene paleogeography for the proto-Central-Western Mediterranean area (Fig. 28) involving the CPT overriding a NW-ward downgoing lithosphere formed by the Calabrian ophiolites and an OCT hosting the *Frido* and the *Nord Calabrese* successions, and a large sector of thinned continental crust hosting the *Parasicilide* and *Sicilide* successions. A thinned continental crust was probably also the substratum to the *Lungro-Verbicaro* succession, which was cut by basaltic dykes in Jurassic times (Iannace et al., 2007).

Therefore, here it is proposed a geodynamic evolution since the Eocene when the subduction had not yet begun (Fig. 30a). Calabrian ophiolites, actually forming part of a strip of oceanic crust, were subducted in the Eocene (Rossetti et al., 2004). During the Late Oligocene the *Frido* succession subsided in the foredeep (Fig. 30b) and was subsequently subducted. In the late Aquitanian (Fig. 30c) the *Nord Calabrese* succession subsided in the foredeep, where deposition of the *Sovereto* sandstones occurred (Bonardi et al., 2009). Subsequently (Fig. 30d) the succession was detached from its substratum and frontally accreted in the embryonic LAC with a mean SE-vergence as a consequence of the coeval counter-clockwise rotation of the Sardinia-Corsica block (Gattacceca et al., 2007). The *Parasicilide* and *Sicilide* successions entered the foredeep during Burdigalian time, as recorded by the sandstones of the *Arenarie di Albanella* Fm. (Donzelli and Crescenti, 1962) on top of the *Parasicilide* Unit, and by the *Corleto* sandstones (Lentini, 1979) and the *Tufiti di Tusa* (Zuppetta et al., 1984) volcaniclastic deposits on top of the *Sicilide* Unit. The latter deposits testify the coeval andesitic volcanism recorded in the Sardinia Island (e.g., Lustrino et al., 2009, 2011) associated with the NW-directed subduction of the Ligurian lithosphere.

These units were then frontally accreted in the tectonic wedge, as the ocean-ward margin of the Apennine Platform (*Lungro-Verbicaro* Unit) reached the foredeep (as recorded by the deposition of the terrigenous deposits of the *Scisti del Fiume Lao* Fm.; Iannace et al., 2007). The *Lungro-Verbicaro* Unit was then subducted to depths of ~45 km, experienced HP/LT metamorphism (P = 1.2-1.4 GPa; T = ~380 °C) and was eventually exhumed as an extrusion wedge (Iannace et al., 2007). In the latest Burdigalian-Langhian (Fig. 30e), the Apennine Platform carbonates of the *Pollino-Ciagola* Unit were uncorformably covered by the foredeep deposits of the *Bifurto* Fm. (Selli, 1957). The Burdigalian-Langhian tectonic accretion, one of the most significant Apennine orogenic pulses, corresponds to the fastest rotation stage of the Sardinia-Corsica block (Gattacceca et al., 2007) and consequently to the fastest phase of thrust front migration (e.g., Vitale and Ciarcia, 2013). Overthickening of the LAC resulting from buttressing against the crustal ramp of the Adria continental margin was followed by subsequent extensional collapse, leading to the formation of wedge-top basins filled by the Langhian to lower Tortonian *Albidona* Fm. deposits (Ciarcia et al., 2012; Fig. 30e-g). This period of apparent stasis in the subduction process was interpreted by Faccenna et al. (2001) as a consequence of the subducted oceanic slab reaching the mantle transition zone (660 km depth), stopping its further sinking. Alternatively, the Langhian stasis in Apennine subduction was associated with the arrival at the trench of the hardly subductable Apennine carbonate platforms. This period correlates also with the end of the Sardinia-Corsica block rotation and the end of back-arc opening in the Ligurian-Provençal Basin (Carminati et al., 2012; Faccenna et al., 2001; Gattacceca et al., 2007; Lustrino et al., 2009). Subsequently, in the early Tortonian (Fig. 30g), when the Tyrrhenian Sea started to open, a new tectonic pulse allowed overthrusting of the

Lungro-Verbicaro and *Frido* Units onto the *Pollino-Ciagola* succession. The whole tectonic prism, then, overthrust the *Lagonegro-Molise* Basin succession, where the *Serra Palazzo* Fm. (Selli, 1962) was deposited during the foredeep stage. Finally, in the late Tortonian (Fig. 30h) syn-tectonic exhumation produced a new emersion and erosion of the CPT and part of the LAC, and the deposition of the *Perosa* (Vezzani, 1966) and *Oriolo* (Selli, 1962) wedge-top basin deposits onto the *Frido*, *Nord Calabrese*, *Parasicilide* and *Sicilide* successions. At the same time, several extensional basins formed in the overriding plate (e.g., *Belvedere* and *Amantea* Basins, Mattei et al., 1999; Cifelli et al., 2007). The late exhumation stages of the *Lungro-Verbicaro* Unit are recorded by ~11-9 Ma apatite fission track cooling ages (Iannace et al., 2007), whereas final arrival at surface of the *Lungro-Verbicaro* and *Frido* Units is attested by unconformable middle-upper Tortonian deposits (Cifelli et al., 2007; Perrone et al., 1973) fed by the Calabrian continental crust of the overriding plate (Critelli, 1999).

Grouping all tectonic vergences, such as result from the kinematic analysis of brittle and ductile structures related to tectonic wedge accretion, for (i) LAC Units (from Ciarcia et al., 2012; Vitale et al., 2013a, b); (ii) *Lungro-Verbicaro* Unit (Iannace et al., 2007; Vitale and Mazzoli, 2009) and (iii) *Lagonegro-Molise* Basin Units in three temporal stages (Early-Middle Miocene, Late Miocene and Plio-Quaternary) from the *Sele* River Valley and *Cilento* up to study area (Fig. 31), a complex kinematic pattern appears: (i) Early-Middle Miocene vergences indicate a mean SE tectonic transport; (ii) Late Miocene vergences are scattered between NW to NE forming an arcuate belt; (iii) Plio-Quaternary vergences indicate a constant NE tectonic transport.

According to the reconstructed P-T-paths for the Calabrian ophiolites, *Frido* and *Lungro-Verbicaro* Units (Fig.26), with a metamorphic grade decreasing from *Lungro-*

Verbicaro to *Malvito* Units, and taking into account their presently tectonic setting (Fig. 2), i.e. from the bottom to the top: *Lungro-Verbicaro, Diamante, Gimigliano, Frido* and *Malvito* Units, all sandwiched between the two non-(Alpine) metamorphic successions of *Sila* Unit in the top and *Pollino-Ciagola* Unit to the bottom, we infer that the presently tectonic contacts between these units are of extensional type unless the basal contact between *Lungro-Verbicaro* and *Pollino-Ciagola* Units that is a thrust (Vitale and Mazzoli, 2009).

The tectonic exhumation of these HP/LT units occurred in a subduction channel as suggested by several authors (Chemenda et al., 1996; Searle et al., 2004; Iannace et al., 2007; Brun and Faccenna, 2008).

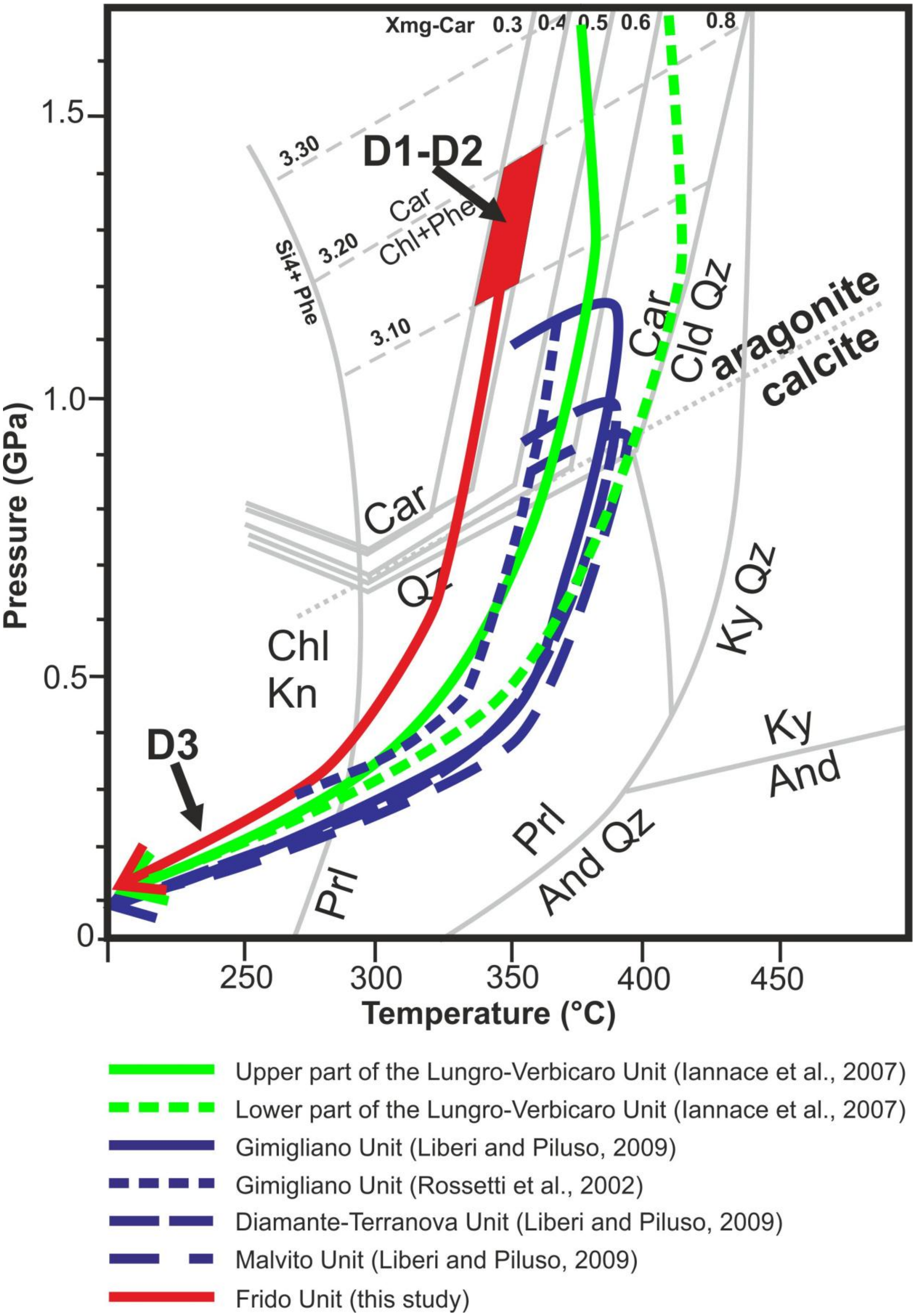

Fig. 26- P-T-t paths for the *Frido, Lungro-Verbicaro* and Calabrian ophiolite Units.

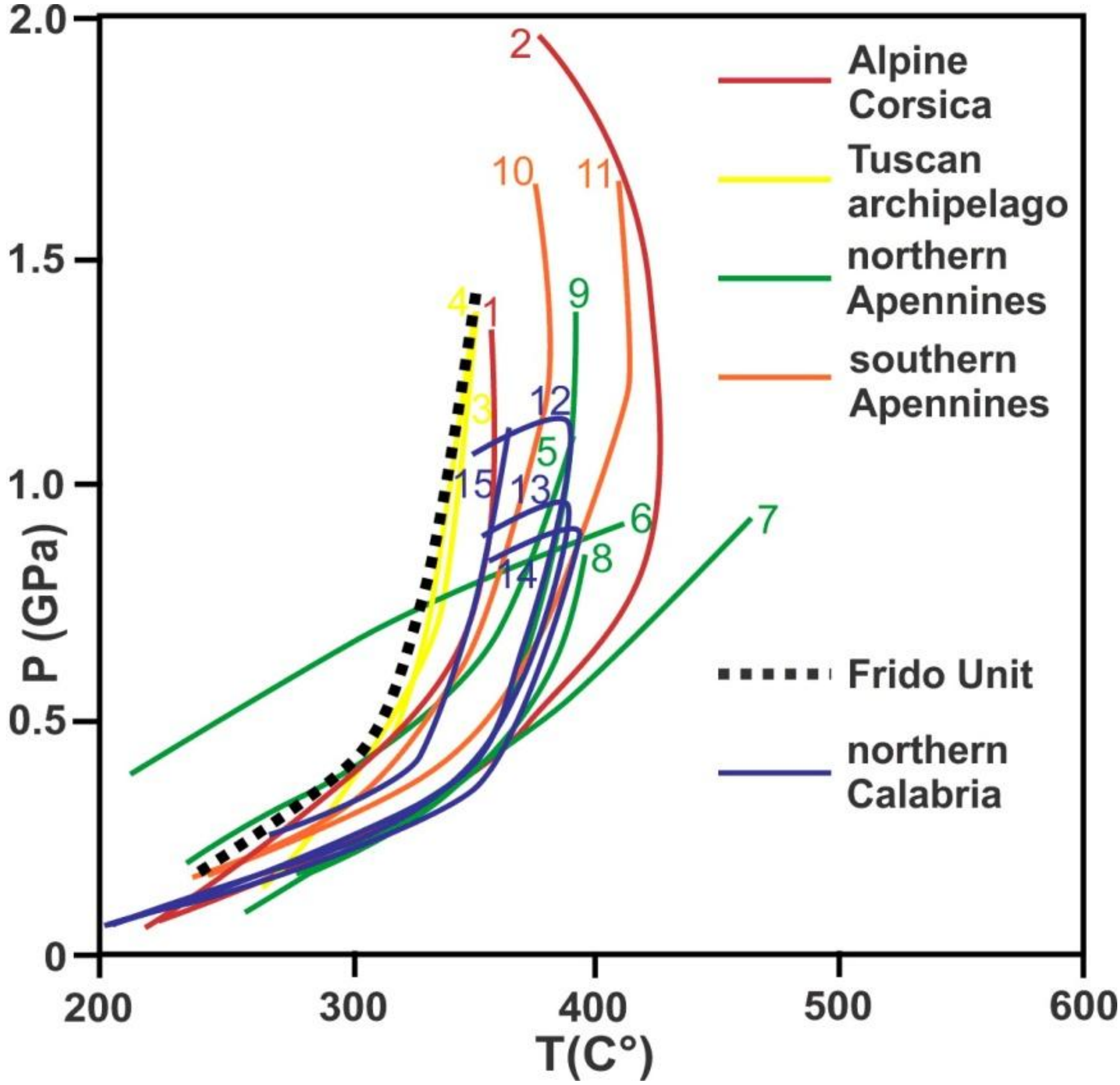

Fig. 27- P-T-t paths for some metamorphic units cropping out in Alpine Corsica (1: *Schistes Lustrés*; 2: eclogites); Tuscan archipelago (3: *Gorgona* Island; 4: *Giglio* Island; 5: Mt. *Argentario*); northern Apennines (6: Apuan Unit; 7: *Massa* Unit; 8: Mt. *Leone*; 9: *Monticiano*); southern Apennines (*Lungro-Verbicaro* Unit, 10: upper part; 11: lower part); Calabria (12-15: *Gimigliano* Unit; 13: *Malvito* Unit; 14: *Diamante-Terranova* Unit). See text for references.

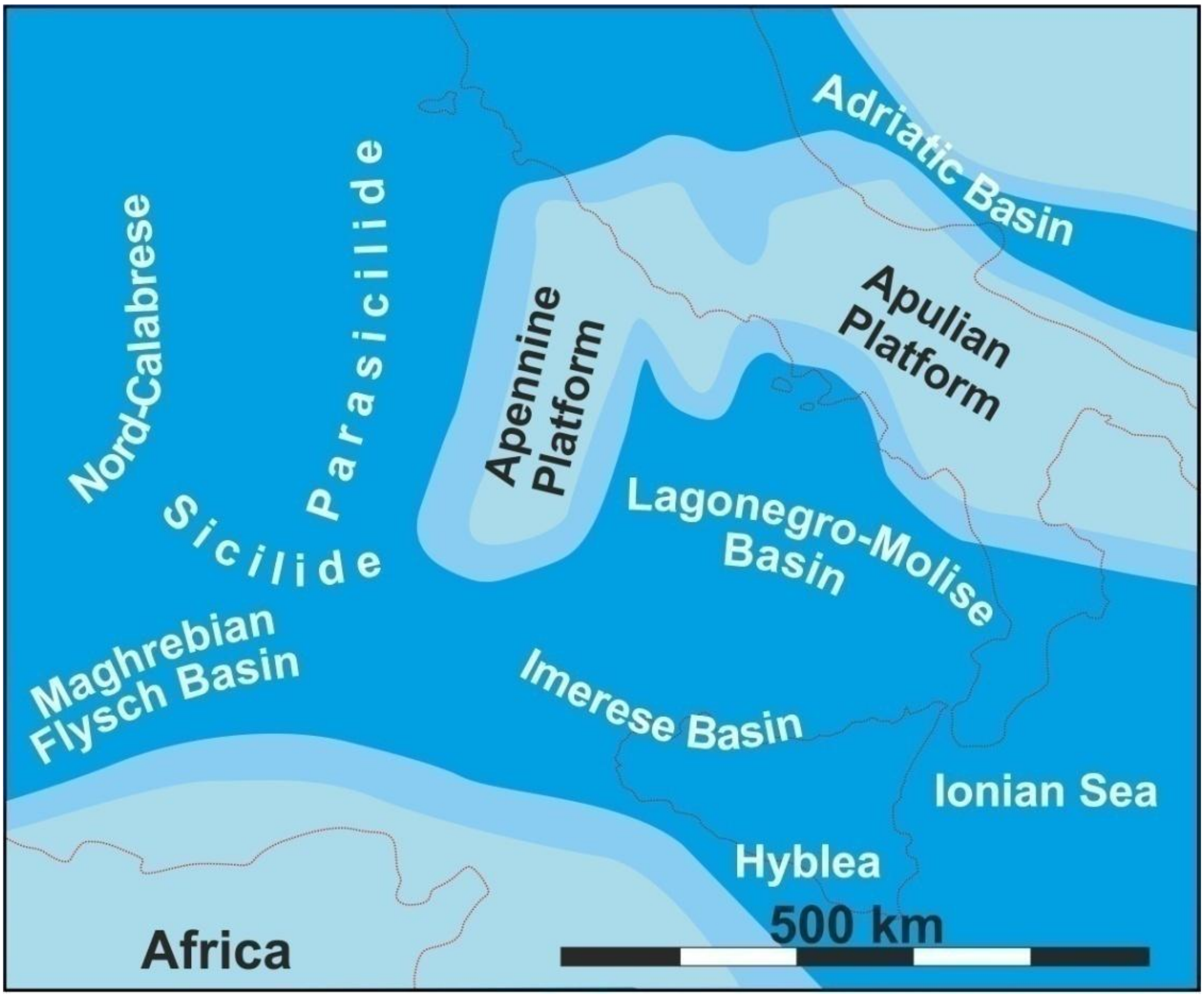

Fig. 28- Late Oligocene paleogeography (modified after Vitale and Ciarcia, 2013).

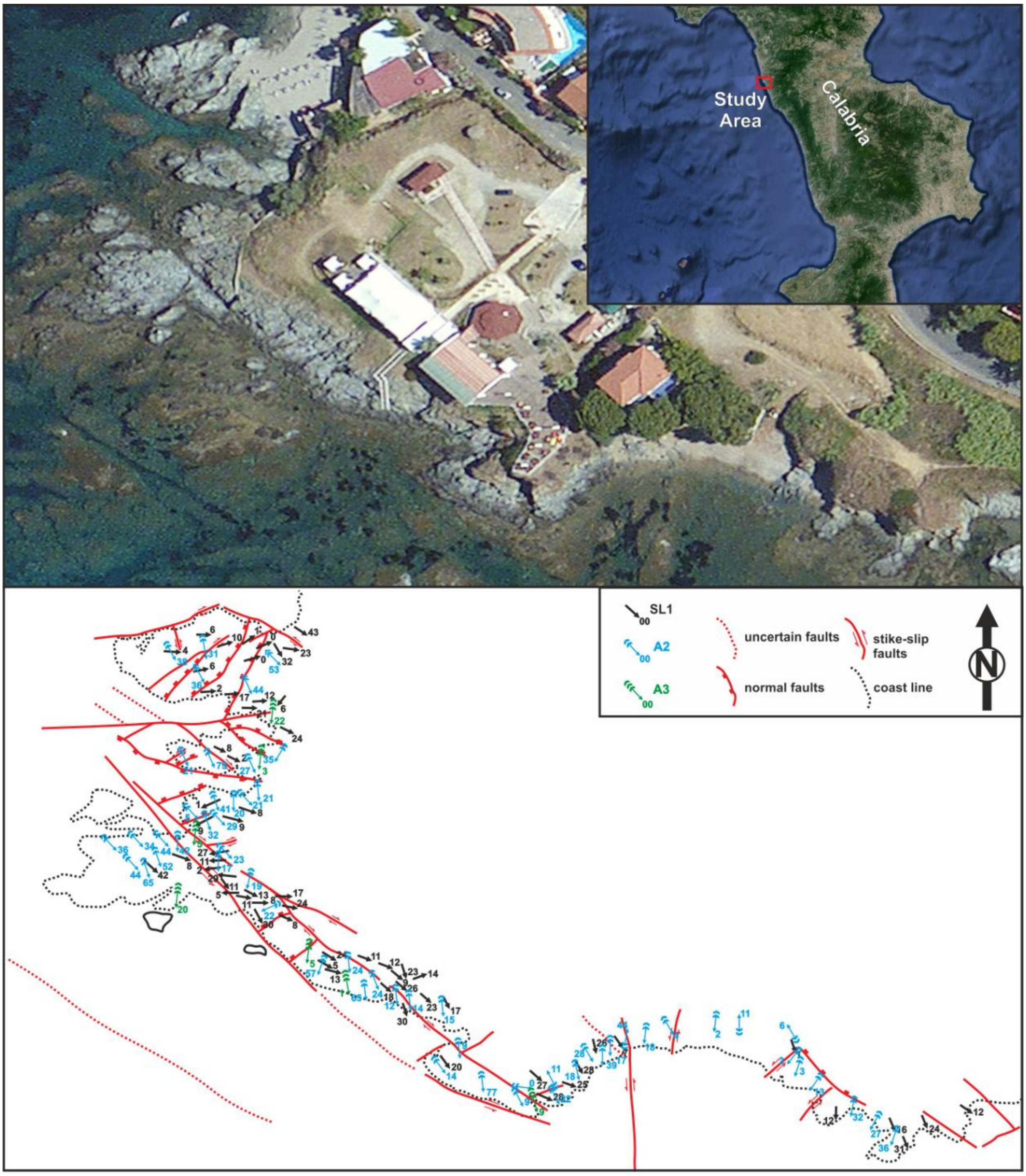

Fig. 29- (a) Satellite image of the *Diamante* outcrop (northern *Calabria*) (from Bing map). (b) Structural map of the analyzed area.

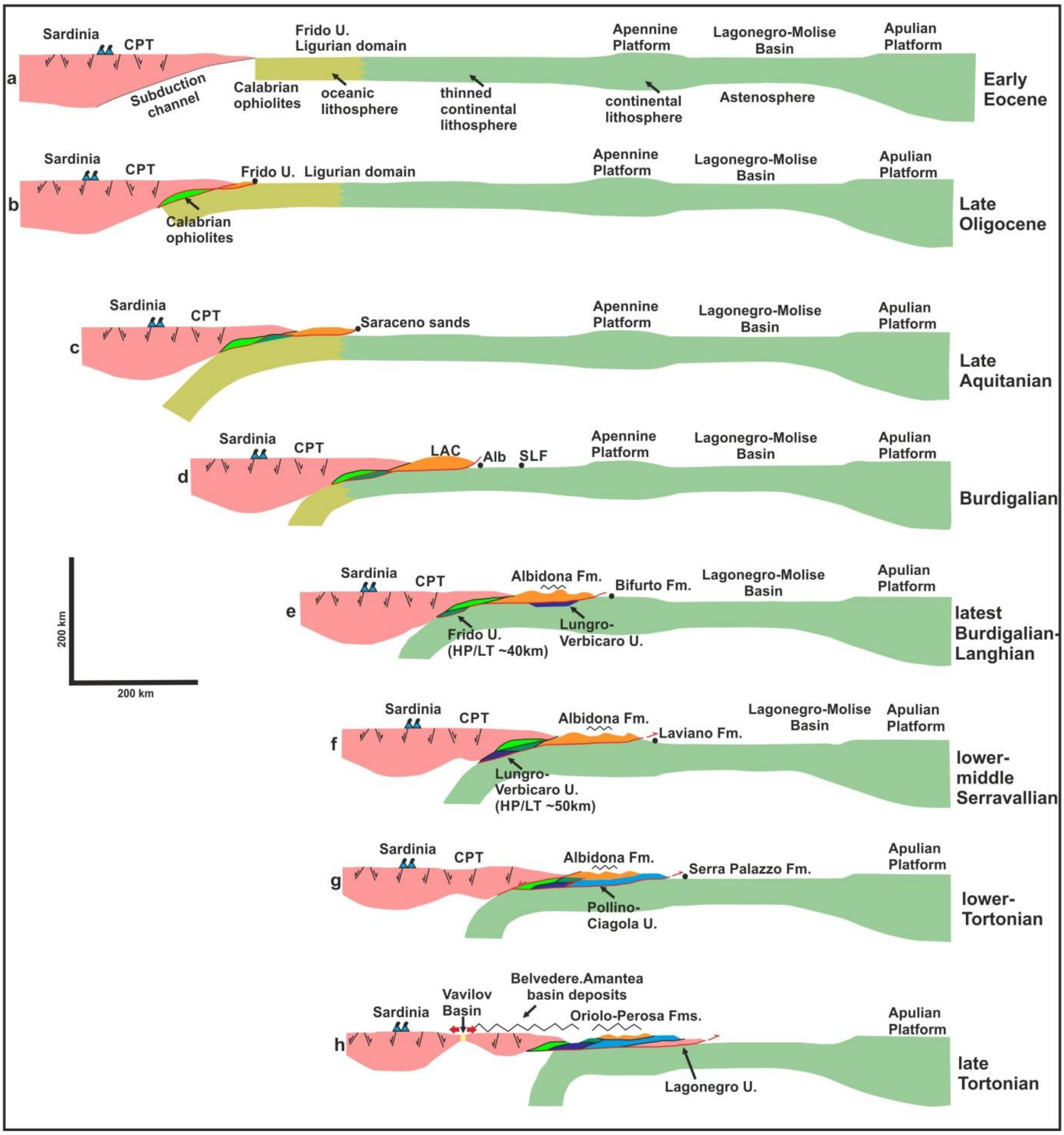

Fig. 30- Cartoons showing the reconstructed geodynamic evolution of the studied segment of the Apennine orogen between Early Eocene and late Tortonian (after Carminati et al., 2012 and Vitale and Ciarcia, 2013, modified). Note exhumation process dominated by the development of extrusion wedges within the subduction channel. Alb: *Arenarie di Albanella* Fm.; SFL: *Scisti del Fiume Lao* Fm.

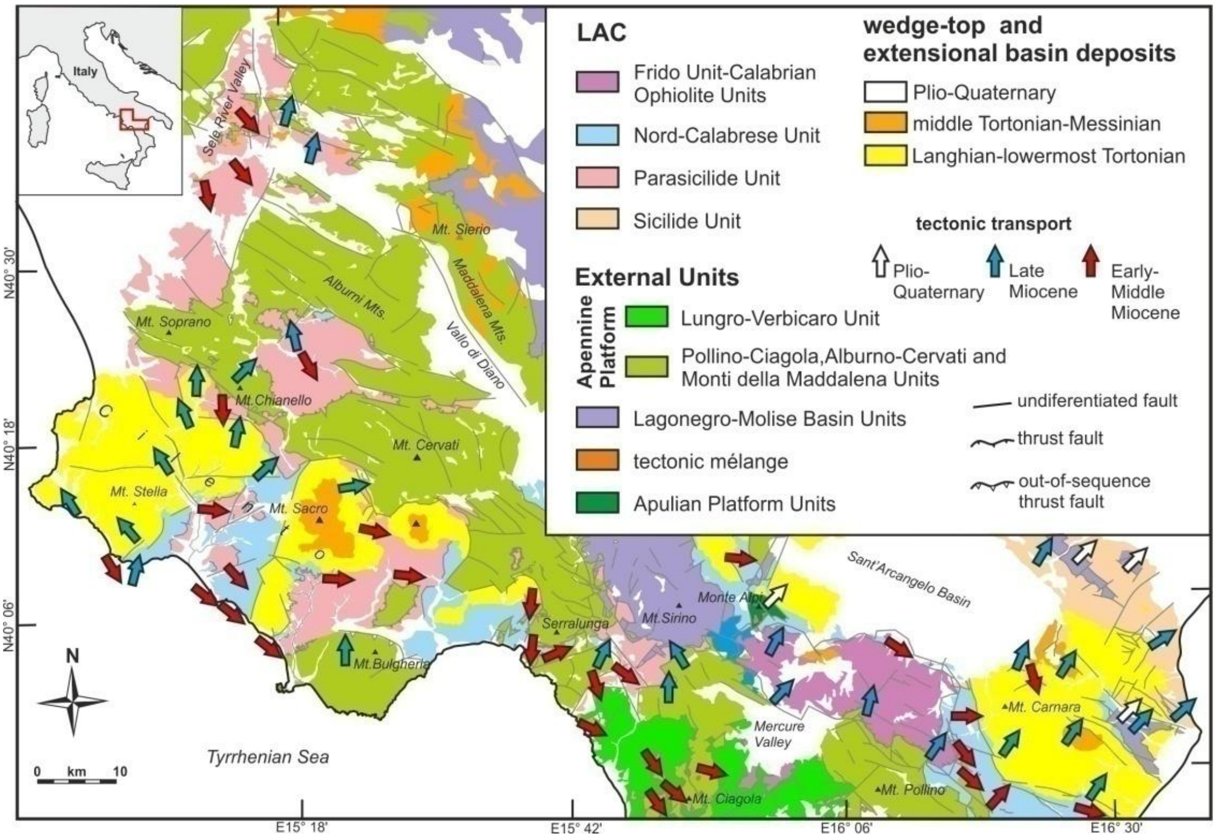

Fig. 31- Tectonic scheme of the area comprised between *Sele* River Valley, *Cilento* and *Calabria-Lucania* boundary showing tectonic transport vectors (the NW sector modified after Vitale et al., 2011).

Chapter 5 - Rif Chain: Stratigraphy, tectonic and structural setting

5.1. Introduction

The Rif chain and Betic Cordillera (Fig. 1), form an arcuate belt surrounding the Alboran Sea. These chains are characterized, as the other circum-Mediterranean belt, by the superposition of three main tectonic domains: (i) Internal Units (the so-called “Alboran Domain”; García-Dueñas et al., 1992); (ii) Maghrebian Flysch Basin Units (Bouillin, 1986; Guerrera et al., 1993; 2005) and (iii) External Units. The former domain includes the Sebtide, Ghomaride and *Dorsale Calcaire* Complexes (e.g. Michard and Chalouan, 1991; Michard et al., 1997; Chalouan and Michard, 2004; Chalouan et al., 2008; Fig. 32); the Sebtide Complex consists of sub-continentalmantle peridotites (Beni Bousera Unit; Kornprobst, 1974; Saddiqi et al., 1995; Afiri et al. 2011); granulites, gneisses and micaschists affected by HP/HT to MP/HT metamorphism (Lower Sebtide; Durand-Delga and Kornprobst, 1963; Kornprobst, 1974; Saddiqi et al., 1995); and from blue-schist to eclogitic facies re-equilibrated under lower pressure (Upper Sebtides Units or Federico Units, Permo-Triassic in age; Michard et al.,1997, 2006; Zaghloul, 1994).

These latter successions are covered by Ghomaride Complex, which encompasses Paleozoic rocks as slates, phyllites, metarenites and metalimestones, Ordovician-Late Carboniferous in age (Durand-Delga and Kornprobst 1963; Kornprobst 1974; Chalouan, 1986), affected by low-grade Eo-Variscan and Variscan metamorphism (Chalouan and Michard, 1990). These rocks are sealed by an unconformable Middle Triassic-Eocene sedimentary cover (Chalouan et al., 2008 and references therein).

The *Dorsale Calcaire* Complex (Fallot, 1937; Mattauer, 1960; Wildi et al., 1977; Kadiri et al., 1992; El Kadiri and Faouzi, 1996; Lallam et al., 1997; El Hlila, 2005; Zaghloul et al., 2005; Chalouan et al., 2008) is formed by Triassic to the Early Miocene successions, deposited on a Paleozoic basement, probably corresponding to the Sebtide or Ghomaride Complexes (Wildi 1983; Balanyá and García-Dueñas, 1988; Chalouan and Michard, 2004). The *Dorsale Calcaire* complex, which forms the backbone of the Rif internal sector, is classically subdivided in (i) Internal, (ii) Intermediate and (iii) External. Generally, these carbonates overthrust the Maghrebian Flysch Basin Units and in turn are covered by Sebtide and Ghomaride Units, however, in some sectors; back-thrust led the *Dorsale Calcaire* onto the Internal Units (Hlila and Sanz de Galdeano, 1995; Hlila, 2005).

The Maghrebian Flysch Basin domain includes Predorsalian Unit (Olivier, 1984) in turn tectonically covering the Mauritanian and Massylian Units (Guerrera et al., 1993, 2005). These three latter units were deposited in a basin floored by oceanic or thinned continental crust, the Maghrebian Flysch Basin Domain, which passes eastward to Ligurian Domain (Bouillin 1986; Durand Delga et al. 2000; Guerrera et al., 2005; Vitale et al., 2013a, b; 2014a, b). The age of these sedimentary successions, span in time from Early Cretaceous to Early Miocene.

Finally the External Rif Units (Prerif, Mesorif and Intrarif) consist of some Mesozoic-Miocene basin successions (e.g. Durand-Delga et al. 1960-1962; Suter, 1965, 1980; Andrieux, 1971; Didon et al. 1973) covered by upper Tortonian-Messinian wedge-top basin conglomerates and sandy marls (Di Staso et al., 2010 and references therein). Presently the Rif chain is segmented by some transfer regional structures, probably acting during the migration of the thrust-front allowing different displacements between different segments of the orogenic chain. Amongst them the left-lateral Jebha-Chrafate Fault cutting through Internal and External Units in the Central Rif belt (Benmakhlouf et al., 2012) and the left-lateral Nekor Fault in the eastern Rif belt (Leblanc, 1980; Frizon de Lamotte, 1985).

The work area, located near *Chefchaouen* city (Fig. 32), represent a good field to study the superposition of Internal onto the Maghrebian Flysch Basin Units due to the excellent outcrop expositions. Here, the carbonates of External *Dorsale Calcaire,* tectonically cover the Predorsalian Unit by means of a gently E-dipping thrust plane, forming a regional anticline NW verging. The latter succession in turn overlies the Massylian Unit (Fig. 32). The whole thrust sheet pile was cut by high-angle normal and strike-slip faults.

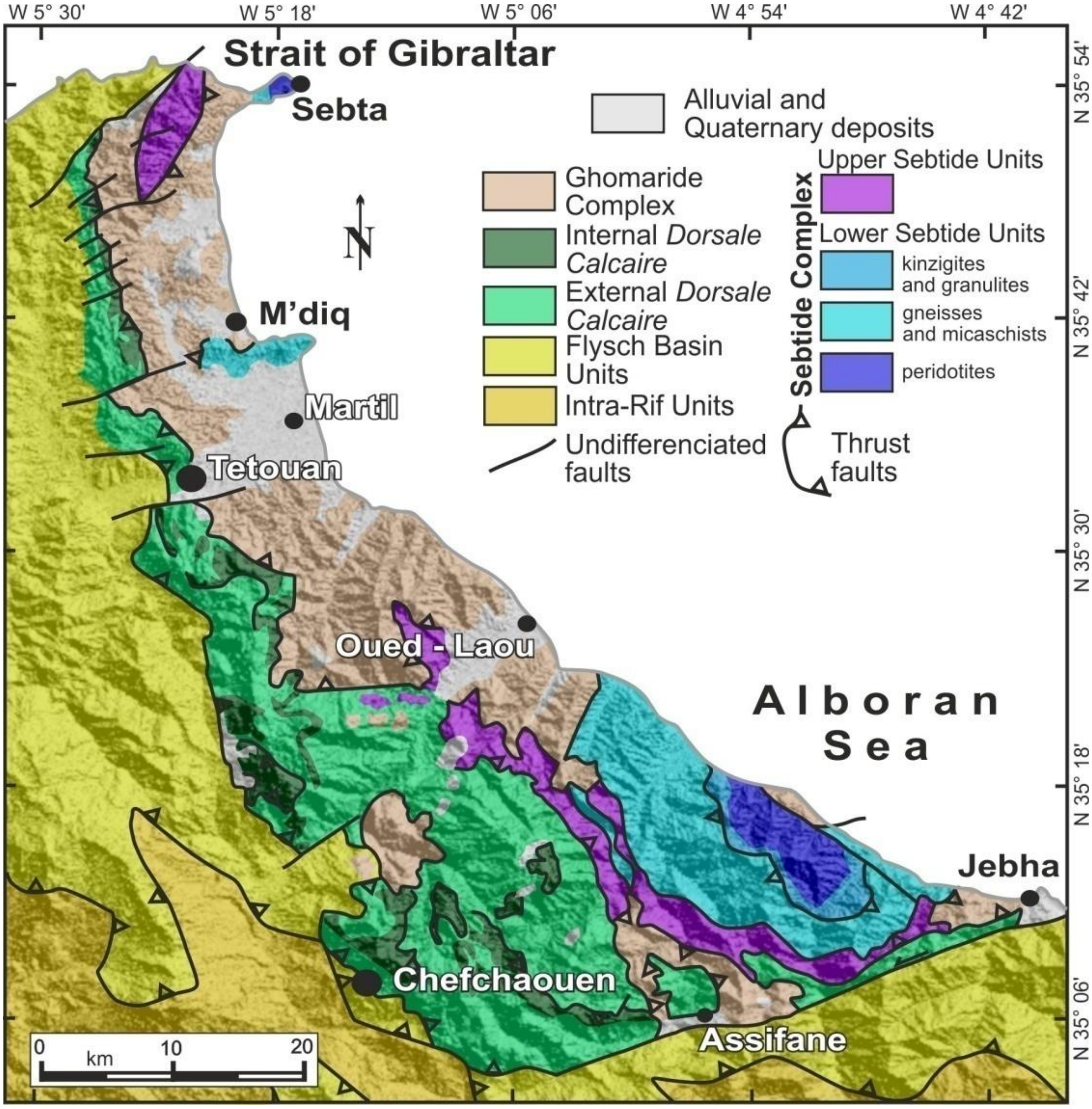

Fig. 32- Schematic geological map of northern Rif (from Chalouan et al., 2008, modified).

5.2. Stratigraphy of Predorsalian and Massylian Units

The Predorsalian Unit, corresponding to the Jbel Moussa Group (El Kadiri et al., 1990; and references therein), consists of a siliciclastic slope to basin sedimentary sequence characterized by carbonate debris, macro-breccias and olistoliths indicating an inner paleogeographic location in the Maghrebian Flysch Basin close to the *Dorsale Calcaire* domain (Olivier, 1984; Guerrera et al., 1993). The sedimentary succession, characterizing Predorsalian Unit (Fig. 33), span in age from Upper Cretaceous to Burdigalian time. From bottom to the top, it begins with green and black shales, hemipelagic mudstones, Maastrichtian in age; followed by Paleocene shales and calciturbidites; Eocene-lowermost Oligocene shales, calciturbidites and clayey limestones. The succession passes to Lower/Upper Oligocene boundary marls and hemipelagites, uppermost Oligocene-Aquitanian Numidian-like sandstones (an African sourced deposit, widespread in the most of circum-Mediterranean chains, e.g. Thomas et al., 2010). Finally, Burdigalian varicolored marls, jaspers, cherty limestones and calcareous conglomerates cap the succession. The whole sedimentary pile is strongly disrupted, containing a lot of olistostromes (Chalouan et al., 2008) and slumping, showing in some place the characters of broken formation (Mattioni et al., 2006).

The Massylian sequence (Fig. 33), corresponding to the Melloussa-Chouamat succession (Andrieux and Mattauer, 1963; Durand-Delga, 1965), is a sedimentary succession deposited in a basin floored by thinned continental or oceanic crust eastward passing to the Ligurian Domain (Maghrebian Flysch Basin Domain; Bouillin, 1986; Durand-Delga et al., 2000; Guerrera et al., 2005; Vitale and Ciarcia, 2013; Vitale et al., 2013a; 2013b; 2014a).

The whole succession, span in age from Lower Cretaceous to lower Burdigalian time and it consists, at the base, of some olistoliths of Malm dolerites and pillow-lavas, Dogger limestones embedded within a Cretaceous pelitic matrix (Andrieux and Mattauer, 1963; Durand-Delga et al., 2000); the succession continues with Aptian-Upper Cretaceous marls with phtanite beds, sandstones, pelites and marly limestones, followed by Paleocene-Oligocene marls, breccias and nummulitic-bearing limestones. The sequence is topped by Aquitanian-Burdigalian Numidian-like sandstones.

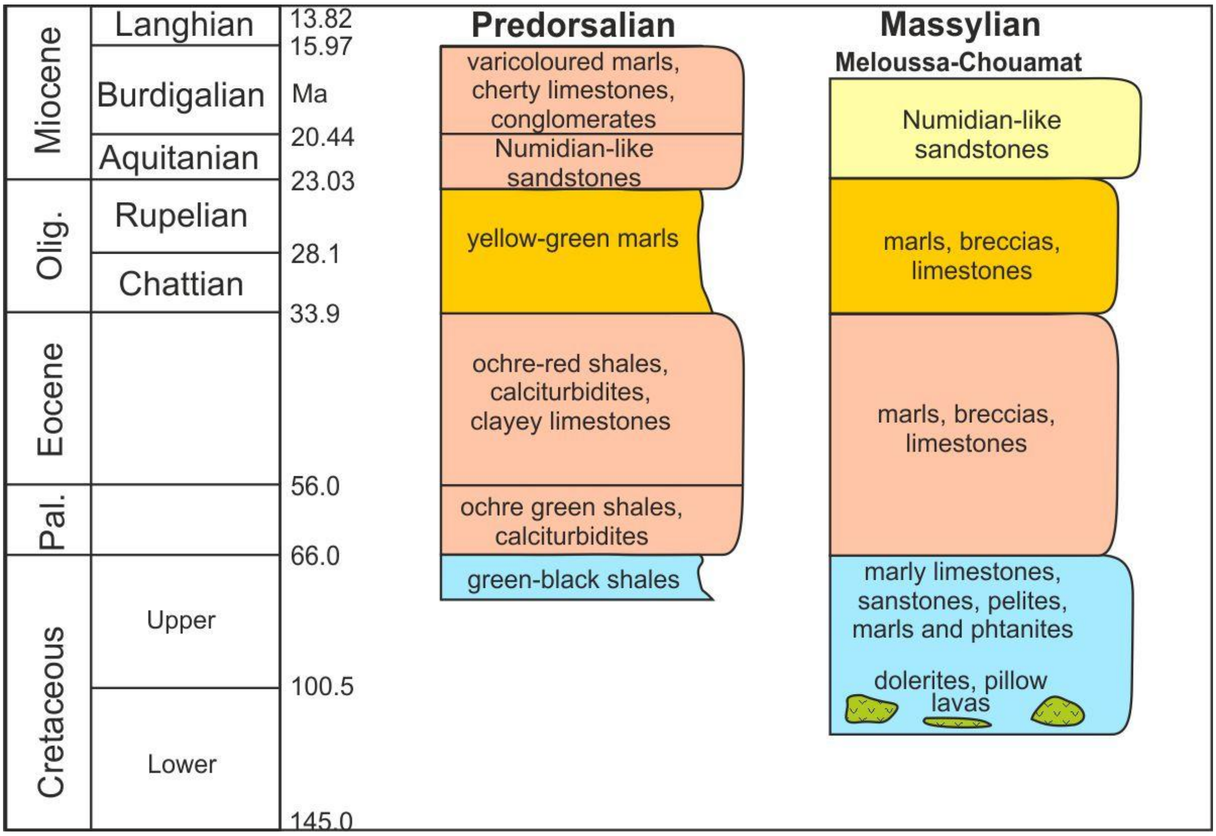

Fig. 33- Simplified stratigraphic logs of Predorsalian and Massylian Units.

5.3. Stratigraphy of External *Dorsale Calcaire*

The *Dorsale Calcaire* Complex (Fallot, 1937; Mattauer, 1960; Wildi et al., 1977; El Kadiri et al., 1992; El Kadiri and Faouzi, 1996; Lallam et al., 1997; Hlila, 2005; Zaghloul et al., 2005; Chalouan et al., 2008) is formed by ca. 30 tectonic thrust sheet and presently forms the backbone of the Rif internal sector. It was classically subdivided, according to Mesozoic paleogeography, in Internal and External sectors, both successions ranging in age from the Triassic to Lower Miocene. It was probably deposited on a basement corresponding to the Sebtide or Ghomaride Units. The *Dorsale Calcaire* generally, tectonically covers the Maghrebian Flysch Basin Units and in turn is overthrusted by Sebtide and Ghomaride Complexes, however in some sectors it back-thrust onto Ghomaride Units (Hlila and Sanz de Galdeano, 1995; Hlila, 2005).

The External *Dorsale Calcaire* cropping out in the study area is a succession with important heteropic relationship, characterized by some stratigraphic gaps and condensed series (after Wildi et al., 1977; El Kadiri et al., 1992; El Kadiri and Faouzi, 1996; Lallam et al., 1997; Hlila, 2005; Zaghloul et al., 2005; Chalouan et al., 2008). In order to provide a complete reconstruction, an overall stratigraphic log is shown in Fig. 34a. The stratigraphic succession begins with shallow water deposits consisting of Upper Triassic laminated stromatolitic dolomites with marly-calcareous interbeds, followed by Rhaetian marl-dolomite-limestone alternations and black shales; Hettangian dolomites and massive limestones. The succession passes from slope to basin Sinemurian deposits including cherty limestones, cherty conglomerates, *Ammonitico rosso* facies and Pleinsbachian-Toarcian cherty, marly and nodular limestones.

The sedimentary pile (Fig. 34a) upward passes to Middle and Upper Jurassic green and red radiolarites, Titonian-Berriasian aptychus limestones, late Upper Cretaceous Globotruncana marls, condensed deposits made of Paleocene yellow marls, black shales and dark limestones, Lower-Middle Eocene variegated marls and calcarenites and finally to Upper Eocene-Upper Oligocene chaotic deposits of calcareous conglomerates. The succession is capped by Aquitanian-lower Burdigalian alternance of marls and calcareous sandstones**.**

The curve of sediment thickness versus time (Fig. 34b), calculated with no decompaction, palaeo-water-depths, eustatic corrections nor back-stripping, show a dramatic change in the sediment thickness in the Rhaetian-Liassic interval with respect the previous Triassic and successive Jurassic deposits. The Rhaetian-Liassic lithofacies testify a paleoenvironment evolution from (i) inner shelf (massive limestones) to (ii) slope (cherty limestones, organized breccias and slumped limestones); (iii) base of slope (disorganized and thick megabreccias, breccias and conglomerates, and associated debrite-turbidite deposits), and (iv) basin (micrite limestones and fine-bedded cherty limestones; Lallam et al., 1997). From (ii) to (iv) rocks, accumulated along carbonate slopes and in small basins on tilted blocks bounded by normal faults, are interpreted as syntectonic deposits related to the Liassic extension as consequence of the Neotethys rifting (Mouhssine et al., 1990; Blidi and Hervouet, 1991; El Hatimi et al., 1991; El Kadiri et al., 1992; Blidi, 1993; Lallam et al., 1997; El Kadiri, 2002; Schettino and Turco, 2011).

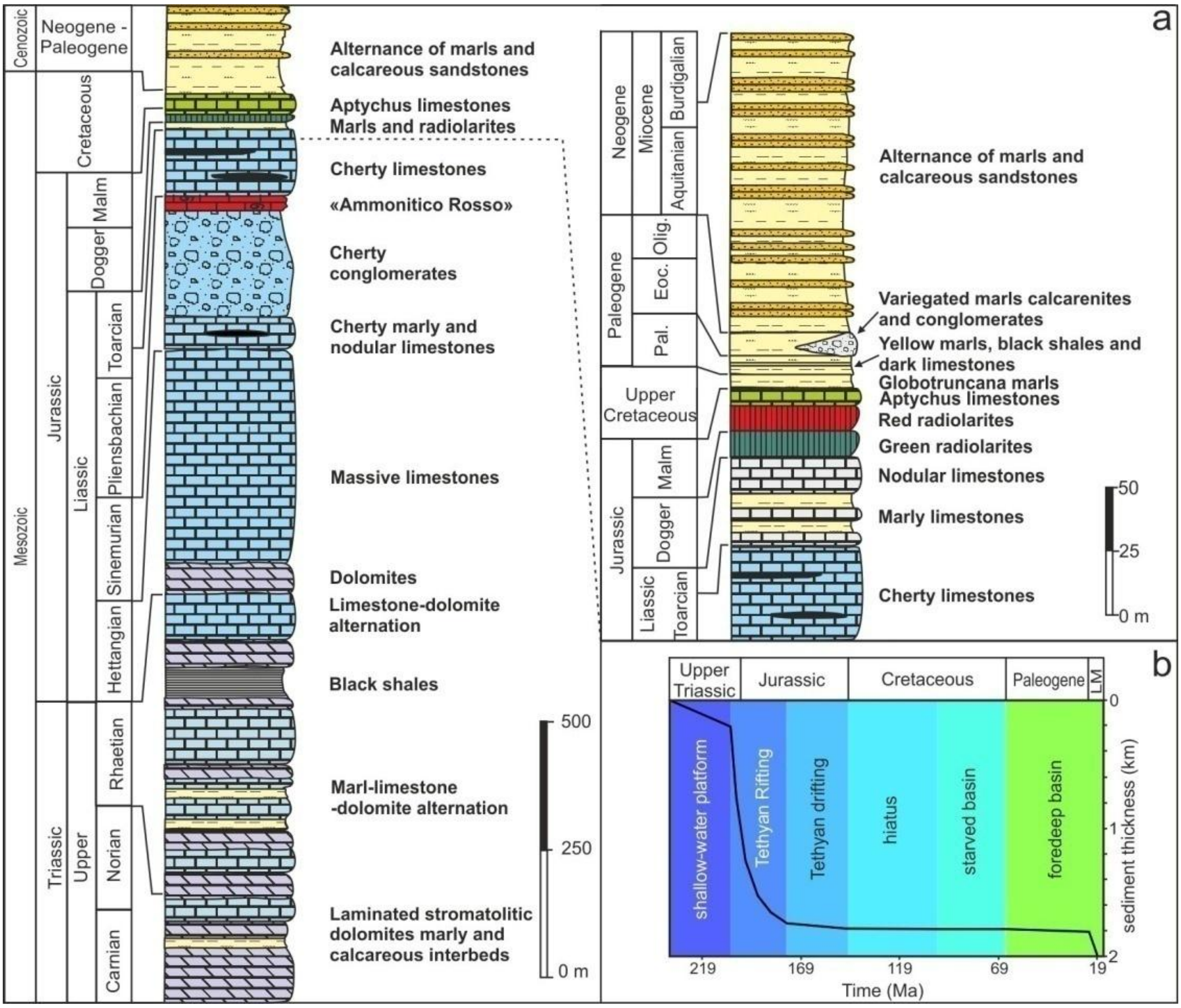

Fig. 34- (a) Schematic stratigraphic log of External *Dorsale Calcaire*. (b) Sediment thickness versus time diagram. LM: Lower Miocene.

5.4. Structural analysis

The analyzed area is located around the *Chefchaouen* city (Fig. 35). Here, a detailed geological survey has gathered several orientation data of main structures, and provided a geological map with two cross sections (Fig. 35). As shown in the geological map and related cross sections of Fig. 35, the whole area is characterized by the tectonic superposition of the External *Dorsale Calcaire* onto Predorsalian Unit, by means of low-angle thrust fault producing a hanging-wall anticline verging to SW and a strongly deformed zone in footwall. In turn the Predorsalian succession overlies, by means of a main flat-lying thrust fault, the Massylian Unit. The latter is characterized by several minor thrust faults causing the repetition of some succession portions. Finally, the whole structure was cut by late high-angle normal and strike-slip faults. The structural analysis, provided in the following paragraphs, was carried out separately on every tectonic unit. Analyzed structures, according to crosscutting relationships, were associated to different deformation stages ($D_{1,2...}$), as well as within each phase, progressive deformation stages ($(D_1)_{1,2...}$) were discriminated. Furthermore all stages and all structures were labeled with the unit acronyms (DC: *Dorsale Calcaire*; PD: Predorsalian; MA: Massylian).

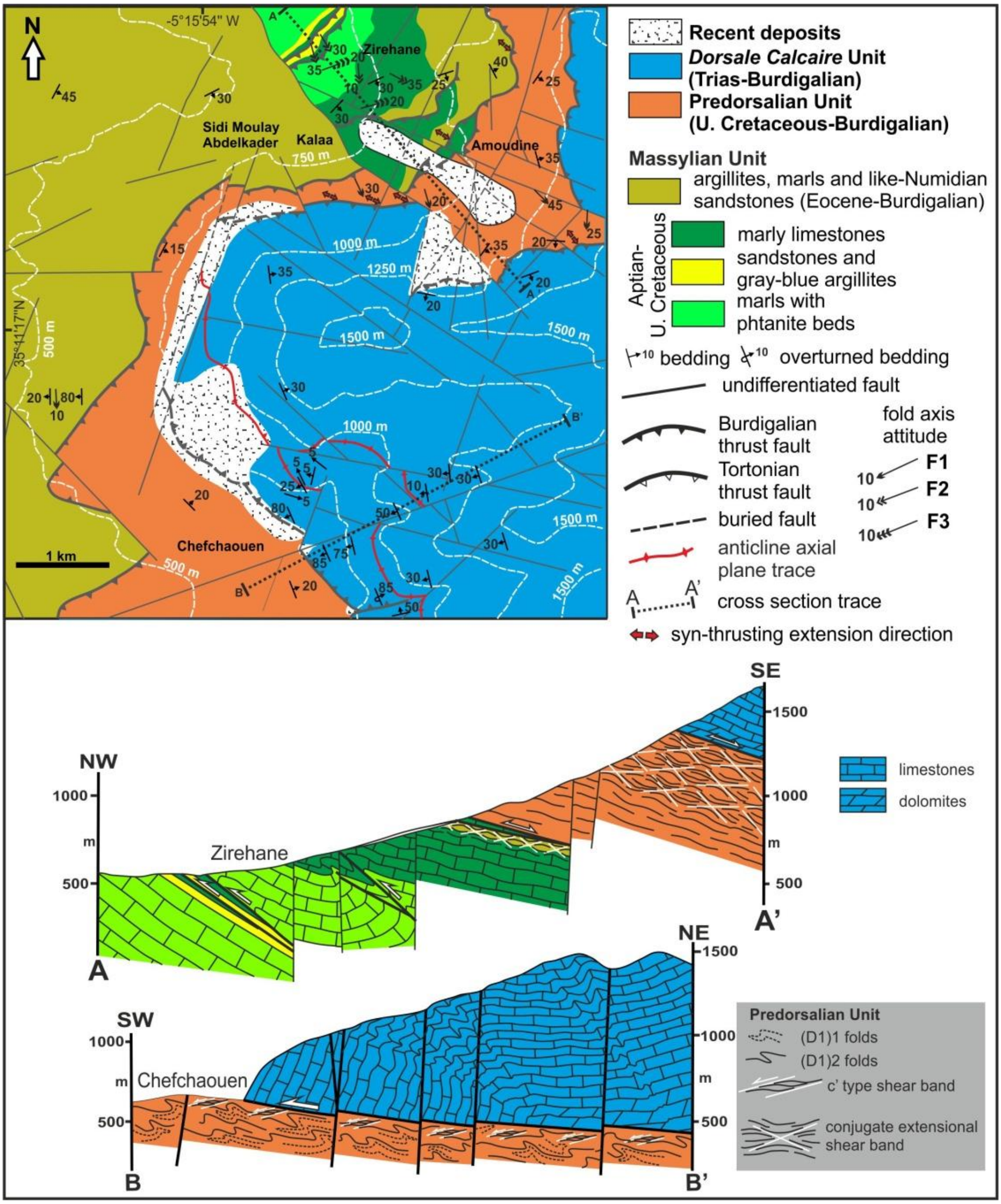

Fig. 35- Geological map and cross sections of the *Kalaa-Chefchaouen* area.

5.4.1. Massylian Unit

Tectonic structures and crosscutting relationships recorded in the Massylian Unit suggest a complex poly-phased deformation pattern showing a strain gradient from the base to the top, approaching to the tectonic contact with the overlying Predorsalian Unit. Early structures ($(D_1)_1$), includes isoclinal to tight folds ($(F_1)_1^{MA}$, Fig. 36a, b), which in pelitic intervals are rootless. Associated to the first folding stage, a pervasive axial plane cleavage ($(S_1)_1^{MA}$) occurs in pelitic levels and a spaced convergent foliation in more competent layers. Reverse faults and pre-buckle thrusts are hosted in sandstones and calcareous layers embedded in pelitic interstrata, hosting boudinated competent layers (Fig. 36c). Where pelitic layers are dominant, the rocks are most highly deformed, often causes the succession to appear as a broken formation (Fig. 36h). Rare C-type shear bands, associated to the main SW tectonic transport, are present, whereas more frequent conjugate extensional shear bands and normal faults, mainly dipping to NW and SE (Fig. 36f and g) and secondarily to NE and SW, affect the argillitic layers. Rare boudins are shortened by the $(D_1)_2^{MA}$ deformation (Fig. 36e), which produced open to close folds (Fig. 36i and j). The interference pattern between the $(F_1)_1^{MA}$ and $(F_1)_2^{MA}$ fold sets (Fig. 36i and j) is of type 3 (Ramsay, 1967). Associated to the $(F_1)_2^{MA}$ fold set, crenulation cleavage, crenulation lineation and reverse faults occur. A late shortening deformation (D_2^{MA}) is marked by pre-buckle thrusts (Fig. 36k), thrust and reverse faults (Fig. 36k) and related folds also to macro-scale (Fig. 36d). In places a spaced cleavage (S_2^{MA}) is associated to F_2^{MA} folds. This shortening is well recorded in the Massylian succession by the imbrication of several thrust sheets such as observed in the *Zirehane-Amoudine* area (Fig. 35). Finally strike-slip faults (D_3^{MA}) and normal faults (D_4^{MA}) cut this succession. Poles to bedding (Fig.

37a) are scattered, however the most of points lie along a NE-SW cyclograph indicating a theoretical fold axis of 148/13, consistent with the 120/44 attitude of the main cluster of meso-scale $(F_1)_1^{MA}$ fold hinges (Fig. 37b). Axial planes and related cleavage (Fig. 37c and d) are spread out, whereas $(D_1)_1^{MA}$ pre-buckle thrusts (Fig. 38a) indicate a compression (R=0.64) characterized by a sub-vertical σ_3 (283/77) and two sub-horizontal σ_2 (169/05) and σ_1 (078/12), providing an ENE-WSW shortening. Fold hinges $(A_1)_2^{MA}$ (Fig. 37e) and crenulation lineation $(CL_1)_2^{MA}$ (Fig. 37g) show a prevalence of data on the NW and SE sectors, whereas poles to axial planes $(AP_1)_2^{MA}$ and related cleavage $(S_1)_2^{MA}$ (Fig. 37f and h), show scattered attitudes with clusters indicating a main SE gently dipping plane. C-type shear bands (Fig. 37i) provide a WSW sense of shear. Normal faults and extensional shear zones, related to the $(D_1)_2^{MA}$ deformation, indicate a radial extensional regime (R=0) with a sub-vertical σ_1 (047/85) and two sub-horizontal σ_2 (208/04) and σ_3 (298/01) and NW-SE and NE-SW extensions (Fig. 38b). A_2^{MA} fold hinges show a mean NE-SW direction (Fig. 37j), whereas poles to AP_2^{MA} axial planes (Fig. 37k) and S_2^{MA} tectonic foliations (Fig. 37l) are spread out along mean 036/77 and 043/72 cyclographs, respectively. Thrust faults, related to the second phase D_2^{MA}, indicate a compression (R=0.61) characterized by a sub-vertical σ_3 (221/84) and two sub-horizontal σ_2 (056/06) and σ_1 (325/01), furnishing a NW-SE shortening (Fig. 38c). D_3^{MA} strike-slip faults indicate a wrench regime (R=0.5) (Fig. 38d) with a sub-vertical σ_2 (211/82) and two sub-horizontal σ_1 (108/02), σ_3 (018/08), and a WNW-ESE shortening. Finally late D_4^{MA} normal faults indicate a main W-E extension (Fig. 38e) and a secondary N-S extension (R=0.31), characterized by a vertical σ_1 (005/90) and two horizontal σ_2 (178/00) and σ_1 (268/00).

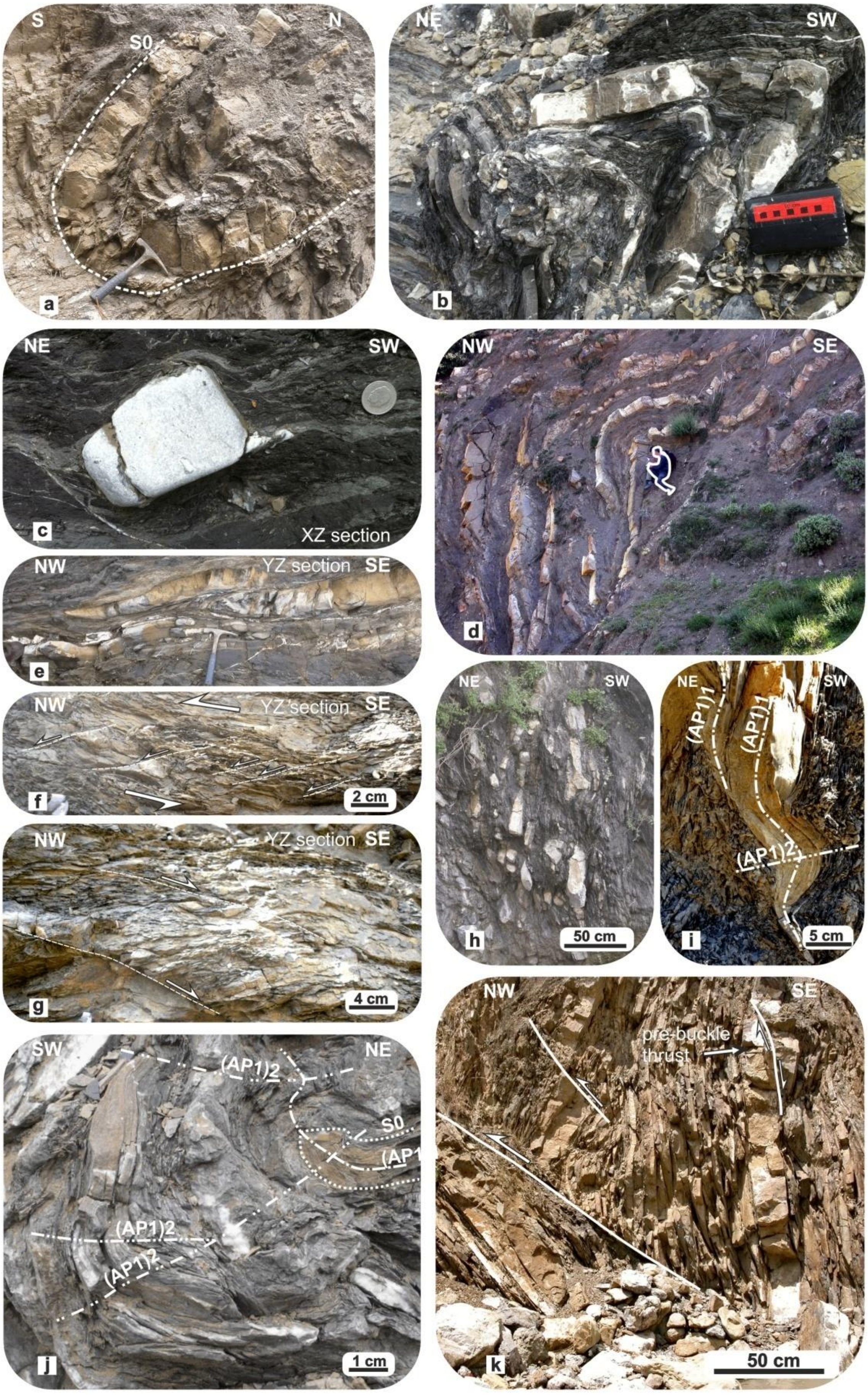
S
N
S0
a
NE
SW
b
NE
SW
c
XZ section
NW
SE
d
NW
YZ section
SE
e
NW
YZ section
SE
f
2 cm
NW
YZ section
SE
g
4 cm
NE
SW
h
50 cm
NE
SW
(AP1)1
(AP1)1
(AP1)2
i
5 cm
SW
NE
(AP1)2
S0
(AP1)2
(AP1)2
j
1 cm
NW
SE
pre-buckle thrust
k
50 cm

Fig. 36- Massylian Unit. (a and b) Tight to isoclinal $(F_1)_1^{MA}$ folds. (c) Asymmetric boudins. (d) Decimetric overturned F_2^{MA} fold. (e) Shortened boudins. (f and g) Extensional shear planes. (h) Boudinated competent layers in an argillite matrix. (i and j) 3 type fold interference pattern between $(F_1)_1^{MA}$ isoclinal fold and $(F_1)_2^{MA}$ close folds. (k) Pre-buckle thrust, thrust and reverse faults, and related F_2^{MA} drag folds.

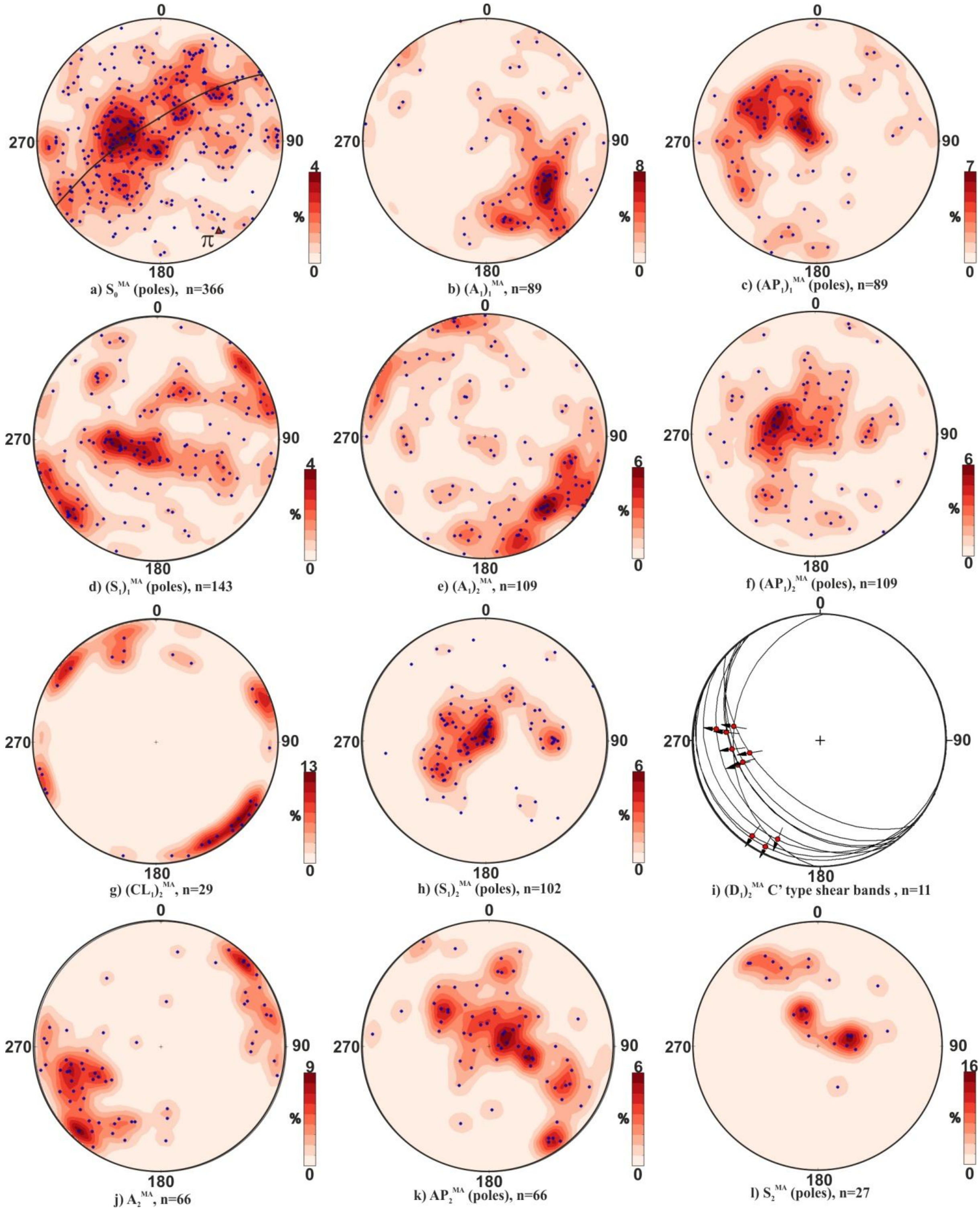

Fig. 37- Stereographic projections and contour plot of analyzed structures of Massylian Unit (lower hemisphere, Schmidt net).

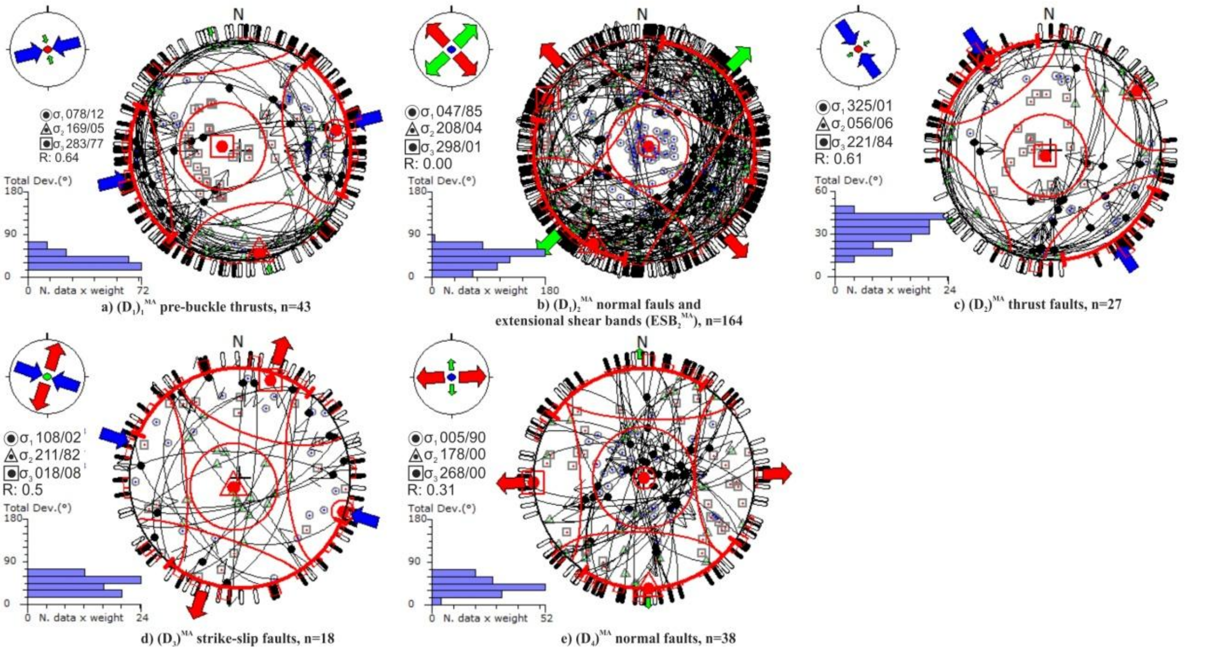

Fig. 38- Paleostress analysis plots (P–B–T method). (a) $(D_1)_1^{MA}$ pre-buckle thrusts. (b) $(D_1)_2^{MA}$ normal faults and extensional shear zones. (c) D_2^{MA} thrust faults. (d) D_3^{MA} strike-slip faults. (e) D_4^{MA} normal faults.

5.4.2. Predorsalian Unit

Predorsalian succession, located in the footwall of the *Dorsale Calcaire* Unit, is characterized by a highly deformed zone, 200 m thick, close to the overlying tectonic contact (Fig. 39a). As well as the previous described succession, early $(D_1)_1^{PD}$ structures are very rare isoclinal folds ($(F_1)_1^{PD}$; Fig. 39b). The latter are deformed by more frequent tight to close, $(F_1)_2^{PD}$ folds (Fig. 39b and c) with associated a crenulation cleavage ($(S_1)_2^{PD}$; Fig. 39b, c) and a crenulation lineation ($(CL_1)_2^{PD}$). Rare interference pattern between $(F_1)_1^{PD}$ and $(F_1)_2^{PD}$ folds (Fig. 39b) are of 3 type of Ramsay's classification (Ramsay, 1967). C-type shear bands (Passchier and Trouw, 2005) affect cherty limestones (Fig. 39d), marls and pelites (Fig. 39e) and calcareous conglomerates (Fig. 39f). This kind of structures occurs also in the thrust fault zone crosscutting both hanging wall carbonates (*DorsaleCalcaire*) and footwall argillites (Fig. 39a). Somewhere, these structures show WSW-ENE striations parallel to the tectonic transport. Conjugate extensional shear bands ($(ESB_1)_{1-2}^{PD}$) mainly dipping to NW and SE (Fig. 39g), indicate an extension both parallel and orthogonal to the mean WSW tectonic transport. Meso-scale $(D_1)_{1-2}^{PD}$, low and high-angle normal faults show a main E-W direction. Extension parallel to the tectonic transport produced also a strong boudinage, causing, in several zones, the total bedding disruption (Fig. 39h) and giving to these sectors the character of a broken formation (e.g. Mattioni et al., 2006). $(D_1)_3^{PD}$ reverse faults, verging between S and SW, occur. A subsequent mean NW-SE shortening is recorded by D_2^{PD} reverse and thrust faults with associated rare S-C structures. Finally, D_3^{PD} strike-slip faults and D_4^{PD} normal faults crosscut the whole succession. Poles to bedding (Fig. 40a) form an E-W girdle with a π-axis of 177/14. Fold hinges (Fig. 40b) are weakly scattered with a main cluster around the value of 177/17, whereas axial planes (Fig. 40c) are from sub-vertical to sub-horizontal mainly dipping to WSW, ENE and S. The crenulation lineations (Fig. 40b) are parallel to fold axes showing a mean N-S direction. $(D_1)_{1-2}^{PD}$ C-type shear bands (Fig. 40d) indicate a main W vergence. $(D_1)_{1-2}^{PD}$ conjugate extensional shear bands (Fig. 40e) and normal faults (Fig. 40f) indicate both a weakly radial extensional tectonic regime (R=0.37), characterized by an about vertical σ_1 (002/83 and 341/81, respectively) and two sub-horizontal σ_2 (215/06 and 088/03) and σ_3 (125/04 and 178/09), providing NW-SE and N-S extensions, respectively $(D_1)_3^{PD}$ moderately NE-dipping reverse faults (Fig. 40g) indicate a compression (R=0.5), providing a mean NNE-SSW shortening, characterized by a sub-vertical σ_3 (295/83) and two sub-horizontal σ_2 (118/07) and σ_1 (028/00). D_2^{PD} reverse faults, mainly dipping both to SE and WNW (Fig. 40h), furnish a compression (R=0.55) with a sub-vertical σ_3 (112/77) and two sub-horizontal σ_2 (213/02) and σ_1 (304/13), and a mean NW-SE shortening. D_3^{PD} strike-slip faults indicate a wrench regime (R=0.5; Fig. 40i) characterized bya sub-vertical σ_2 (289/73) and two sub-horizontal σ_1 (116/17) and σ_3 (025/02), and an ESE-WNW shortening. Finally, D_4^{PD} normal faults indicate a radial extension (R=0.27; Fig. 40j) with a sub-vertical σ_1 (311/72) and two sub-horizontal σ_2 (165/15) and σ_3 (072/10), and an ENE-WSW extension.

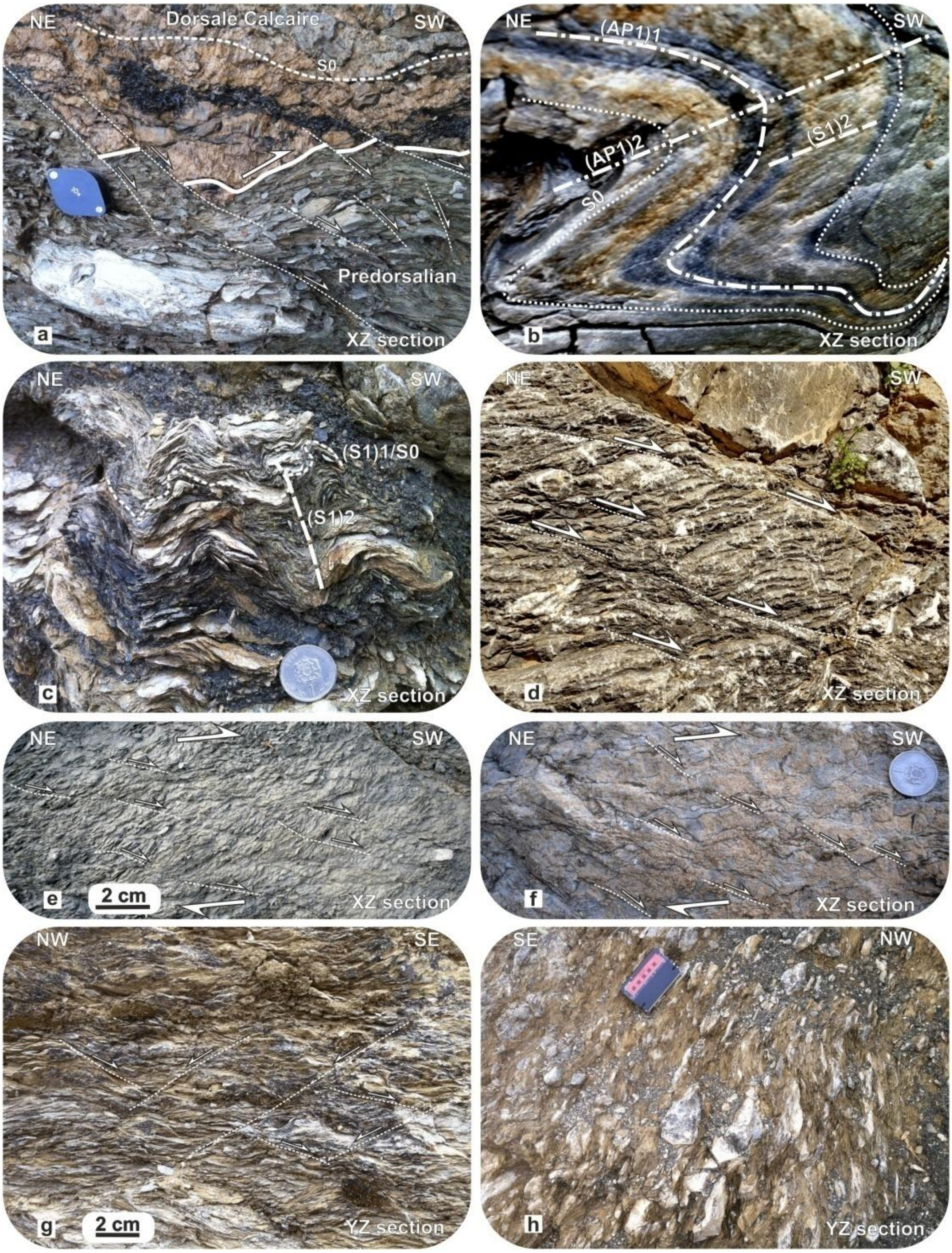
NE
Dorsale Calcaire
SW
S0
Predorsalian
a
XZ section
NE
(AP1)1
SW
(AP1)2
(S1)2
S0
b
XZ section
NE
SW
(S1)1/S0
(S1)2
c
XZ section
NE
SW
d
XZ section
NE
SW
e
2 cm
XZ section
NE
SW
f
XZ section
NW
SE
g
2 cm
YZ section
SE
NW
h
YZ section

Fig. 39- Predorsalian Unit. (a) Tectonic contact between Triassic dolomites of *Dorsale Calcaire* Unit (in the hanging wall) and argillites of the Predorsalian Unit (in the footwall) both cut by S-C' structures indicating a W/SW tectonic transport. (b) Isoclinal $(F_1)_1^{PD}$ fold deformed by SW-verging $(F_1)_2^{PD}$ fold with associated a $(S_1)_1^{PD}$ crenulation cleavage. (c) F_2^{PD} folds in argillites with related crenulation cleavage $(S_1)_2^{PD}$. (d) Extensional shear bands in cherty limestones. (e) Highly deformed argillites and (f) conglomerates hosting S–C' structures indicating a W/SW tectonic transport. (g) Conjugate extensional shear planes indicating a NW-SE extension orthogonal to the SW-verging tectonic transport. (h) Disrupted competent layers in an argillitic matrix.

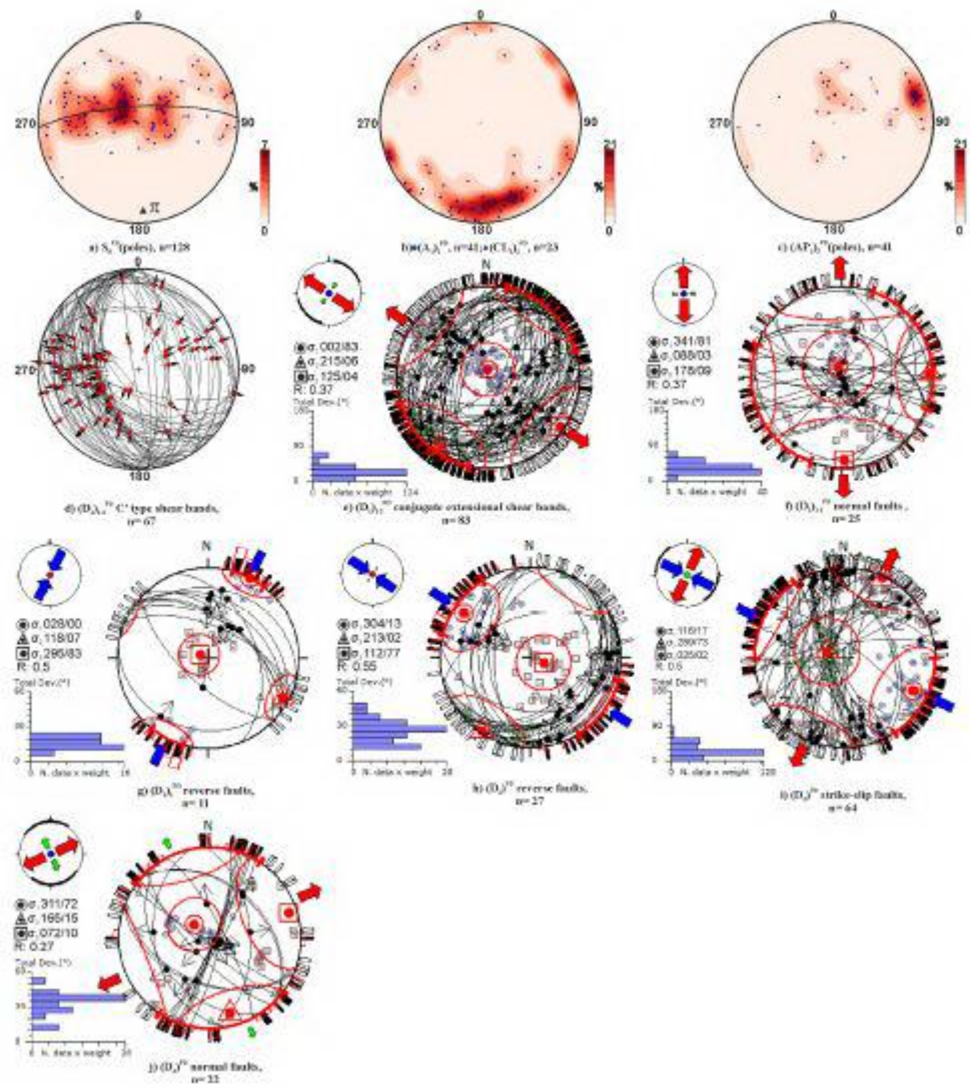

Fig. 40- Orientation data (lower hemisphere, equal-area projections), results of paleostress analysis (P-B-T method) for the analyzed structures. (e) $(D_1)_{1-2}^{PD}$ conjugate extensional shear bands. (f) $(D_1)_{1-2}^{PD}$ normal faults. (g) $(D_1)_3^{PD}$ thrust faults. (h) D_2^{PD} reverse faults. (i) D_3^{PD} strike-slip faults. (j) D_4^{PD} normal faults.

5.4.3. External *Dorsale Calcaire*

The Rhaetian-Liassic interval of External *Dorsale Calcaire*, cropping out in the study area, recorded the Liassic extension as consequence of the Neotethys rifting (Mouhssine et al., 1990; Blidi and Hervouet, 1991; El Hatimi et al., 1991; El Kadiri et al., 1992; Blidi, 1993; Lallam et al., 1997; El Kadiri, 2002; Schettino and Turco, 2011). Successively in Miocene time the latter structures were deformed by NE-SW shortening related to the tectonic stacking of *Dorsale Calcaire* onto Predorsalian Unit. In this section pre-orogenic and orogenic structures have been distinguished and separately analyzed.

3.4.3.1 Pre-orogenic structures

The Liassic limestones of External *Dorsale Calcaire* host widespread normal faults, generally occurring in conjugate sets, with rarely associated *en-echelon* veins (Figs. 41-42).

Due to successive shortening stage, these structures were deformed and presently are tilted showing a reverse kinematic, being located in the steep limb of the regional anticline (Vitale et al., 2014b).

Calcareous layers and cherty beds are deformed by synthetic normal faults often forming bookshelf structures (Fig. 41e, f) and sometimes showing deflections without a discrete plane of shear (Fig. 41a), or a brittle-ductile deformation (Figs. 41b, 42e, f, g) including *en-echelon* veins (Fig. 41g). Dip-separations are variable and usually centimeter-sized (Fig. 41c, d), expiring along short distances (Fig. 41c). The original dominant dip-slip kinematic is testified by slickenside structures, such as calcite fibers, occurring on the fault surfaces; inferred also by drag folds and deflexed layers (Fig.

41a, b). Diagenetic stylolites and veins are present, pre- and post-dating early extensional structures (Fig. 42b).

Meso-scale pre-orogenic normal faults, with metric displacements, commonly separate cherty limestones from overlying conglomerates (Fig. 42a). The latter sediments host, veins and stylolites and occasionally extensional structures such as conjugate normal faults with minor displacements (Fig. 42c) and associated drag folds. Conglomerates (Fig. 43a-c) are generally clast-supported with rounded to sub-rounded centimeter-sized calcareous and cherty clasts (Fig. 43a, b), commonly disorganized and only rarely showing coarsening or fining upward trends. Matrix-supported conglomerates usually occur with a calcareous-cherty matrix embedding the calcareous clasts (Fig. 43c). Being some of pre-orogenic structures, analyzed in this study, hosted in the steep limb of the regional fold (Fig. 43d), each datum was unfolded by rotating the corresponding bedding back to horizontal. Pre-orogenic normal faults (Fig. 44a), when restored (Fig. 44b), indicate a mean NW-SE direction (Fig. 44c). Normal fault planes usually form conjugate sets (Figs. 41c, d and 42c, e) providing restored sub-horizontal intersection lines and normal dip-slip kinematics (Anderson, 1951). Restored pre-orogenic veins show steeply dipping to vertical planes, with main NW-SE and subordinate NE-SW directions (Fig. 44d, e). Finally, restored pre-orogenic stylolites show gently dipping to sub-horizontal planes (Fig. 44f, g).

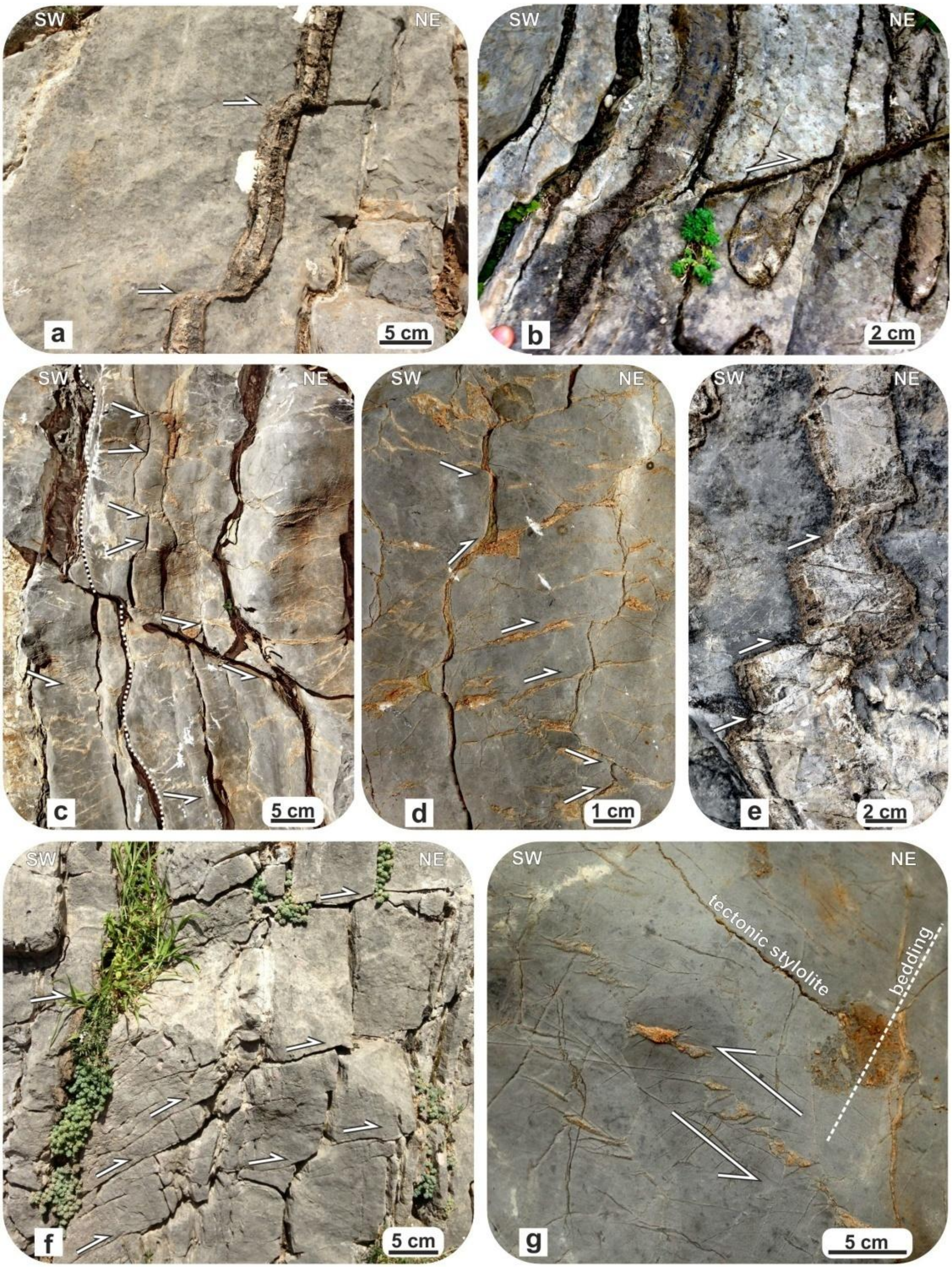
SW
NE
a
5 cm
b
2 cm
c
5 cm
d
1 cm
e
2 cm
f
5 cm
g
5 cm
tectonic stylolite
bedding

Fig. 41- Examples of pre-orogenic extensional structures. (a-b) Normal faults marked by plastically deflexed or faulted cherty layers presently with a reverse kinematics. (c-d) Conjugate normal faults with associated veins. Bookshelf structures presently with a reverse kinematics in (e) cherty layer and (f) cherty limestones. (g) Veins showing an *en-echelon* geometry.

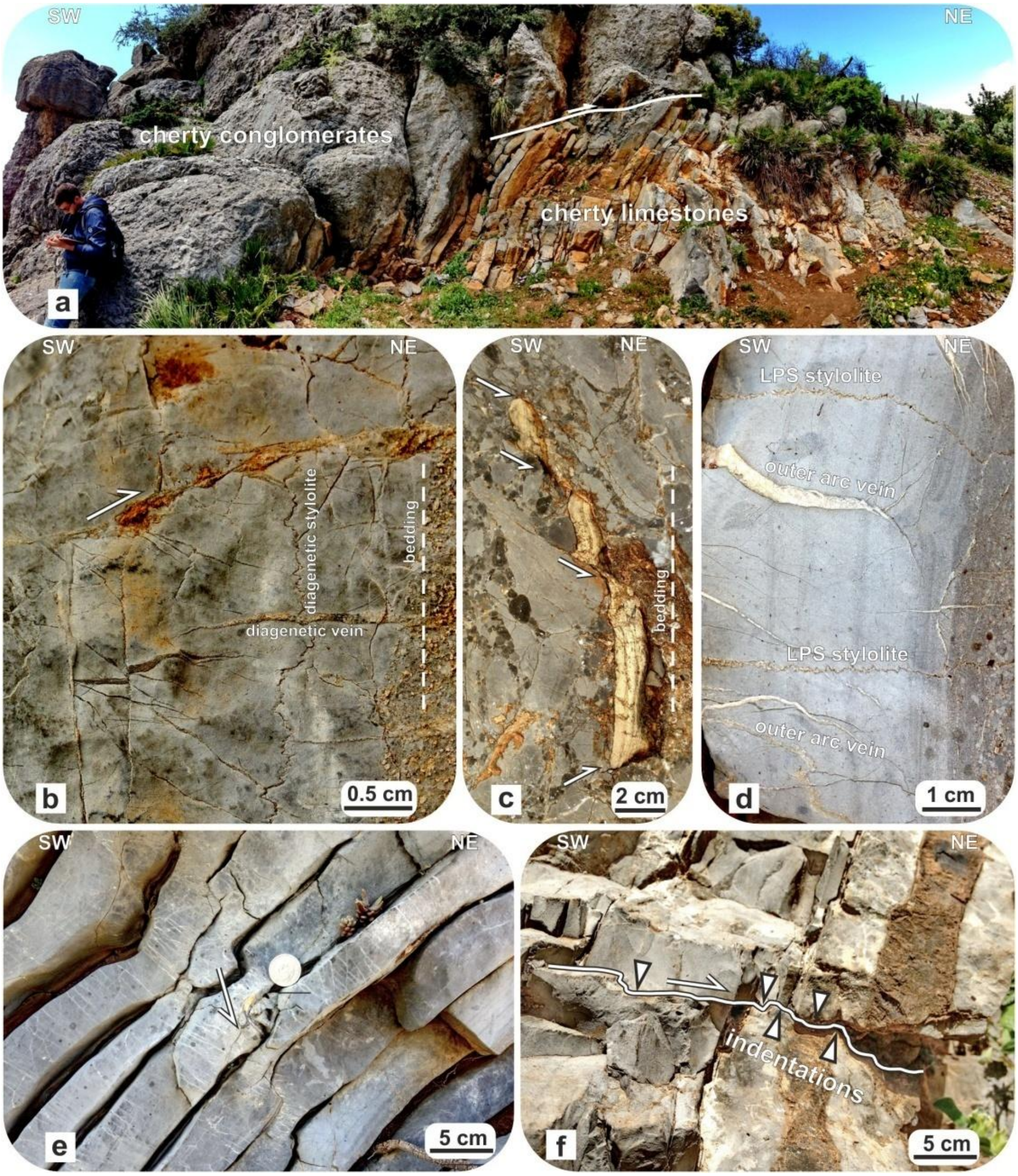
SW
NE
cherty conglomerates
cherty limestones
a
SW
NE
diagenetic stylolite
bedding
diagenetic vein
b
0.5 cm
SW
NE
bedding
c
2 cm
SW
NE
LPS stylolite
outer arc vein
LPS stylolite
outer arc vein
d
1 cm
SW
NE
e
5 cm
SW
NE
indentations
f
5 cm

Fig. 42- (a) Pre-orogenic normal fault, presently with a reverse kinematics, sealed by cherty conglomerates. (b) Calcareous bed hosting diagenetic veins and stylolites and a pre-orogenic normal fault. (c)Pre-orogenic conjugate normal faults in conglomerates. (d) LPS stylolites and outer arc veins. (e) Pre-orogenic conjugate normal faults in flat-lying cherty limestones and orogenic pre-buckle thrust. (f) Pre-orogenic normal fault with associated a brittle-ductile deformation. (g) Pre-orogenic normal faults crosscutting cherty layers. (h) Indentation of hanging wall and footwall blocks of a pre-orogenic normal fault.

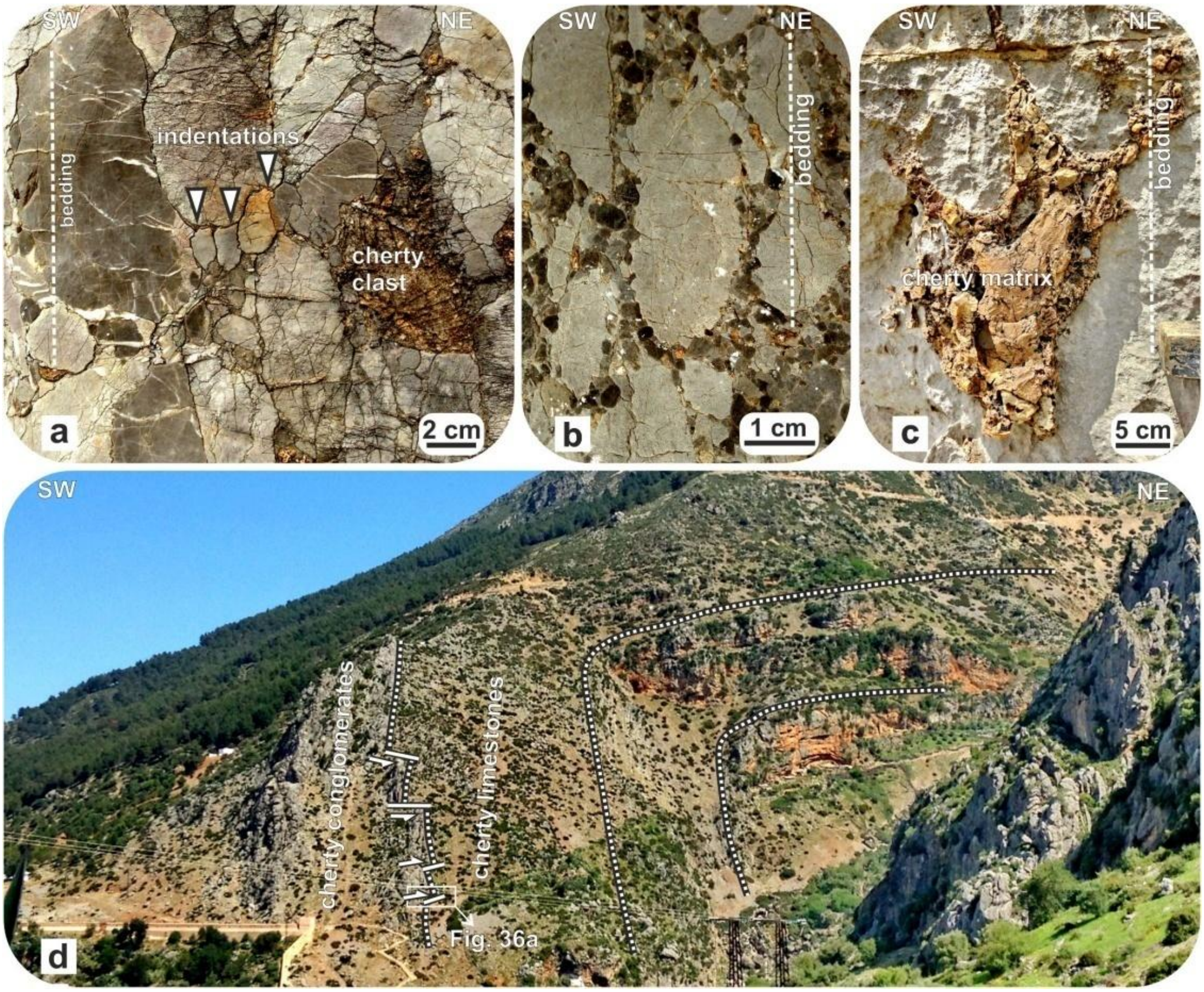

Fig. 43- (a-b) Indented clasts in cherty conglomerates. (c) Conglomerate with cherty matrix. (d) Panoramic view of the SW-verging anticline of Chefchaouen.

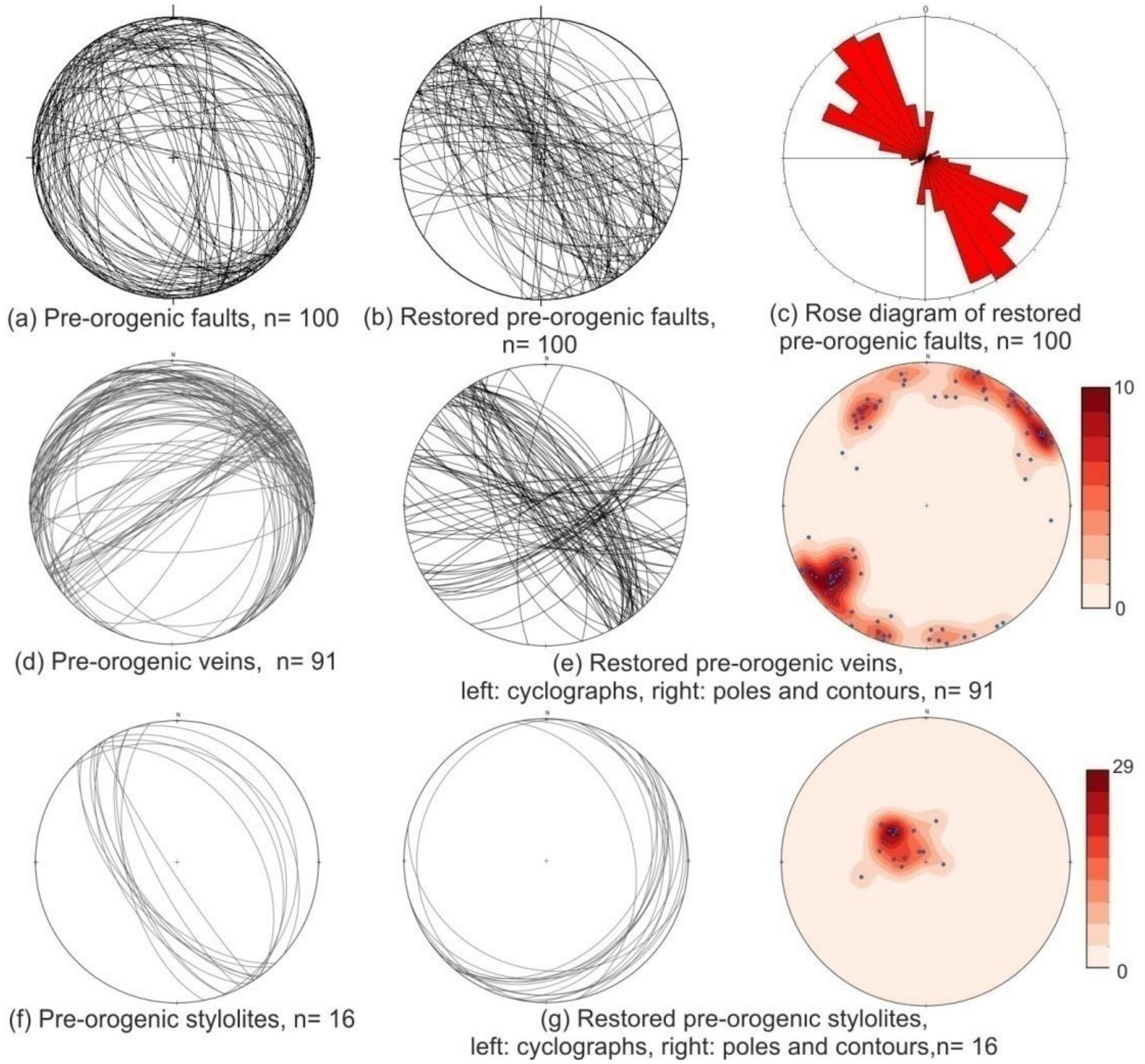

Fig. 44- Stereographic projections (equal-areal net, lower hemisphere), rose diagrams and contour plots of the analyzed pre-orogenic structures.

5.4.3.2. Orogenic structures

Some of pre-orogenic structures are deformed by meso- and macro-scales folds and thrust faults (Figs. 43, 45 and 46). The regional thrust, leading the carbonates of the External *Dorsale Calcaire* Unit onto argillites, marls and conglomerates of the Predorsalian Unit (Wildi et al., 1977; Olivier, 1984; Vitale et al., 2014a), forms a SW-verging anticline (Fig. 43d) characterized by several meso-scale structures such as minor folds, thrust and back-thrust faults indicating a main NE-SW shortening (Vitale et al., 2014a).

Early structures, related to layer parallel shortening (LPS) include stylolites orthogonal to the bedding, crosscutting the pre-orogenic veins (Fig. 42d), pre-buckle thrusts (Figs. 45e and 46b-d) characterized by minor displacement and hosted in cherty beds (Figs. 45e and 46c) or packages of cherty layers (Fig. 46b, d).

Parasitic F_1 folds, often located in the hinge zone of the regional fold (Fig. 41a), show open to isoclinal geometries (Fig. 45a, b, f) and are characterized by slickensides related to the flexural-slip mechanism on the bedding surfaces and also by veins hosted in the outer arc (Fig. 42d). Frequently meso-scale folds are accommodated, in the hinge zone, by fractures (Fig. 46e, f) or minor thrust faults, well-evidenced by dislocated cherty layers (Fig. 46e, g). A spaced cleavage convergent fan (S_1) is present in the inner arc of folded calcareous beds typically marked by pressure-solution surfaces. Late northeastward verging back-thrusts are regularly in association with S-C structures localized in the footwall (e.g. Vitale et al., 2014a). Another folding stage D_2 produce open to tight folds often related to thrust faults (Fig. 45c), which form an interference pattern of 3-type Ramsay's classification (Ramsay, 1967) such as shown in the Fig. 45f, and S-C structures (Fig. 45d).

The early layer parallel shortening causes the indentation of footwall and hanging wall of pre-orogenic normal faults, sometimes enhanced by pressure-solution mechanisms (Figs. 42f and 45e). This indentation is well evident also in conglomerates where pressure solution mechanism acts along calcareous clast boundary (Fig. 43a, b).

Only in a few cases it was possible to recognize pre-orogenic meso-scale normal faults reactivated as minor thrusts (Fig. 46a) or with the same kinematics in response to a push-up of the footwall (Fig. 46a). Poles to bedding (S_0) of the cherty limestones show a broad girdle distribution with a mean NE-SW direction (Fig. 47a). Poles to tectonic foliation (S_1) indicate weakly W-dipping to sub-vertical planes (Fig. 47b). F_1 fold hinges (A_1) are about sub-horizontal showing a mean NW-SE trend (Fig. 47c), whereas the axial plane poles (AP_1) spread out around a NE-SW cyclograph (Fig. 47d). Pre-buckle thrusts (Fig. 47e), when restored (Fig. 47f), indicate a prevalence of NE-SW and secondarily N-S planes. The corresponding rose diagram (Fig. 47g) points out a NW-SE main direction, providing a prevailing NE-SW shortening. Thrust faults (Fig. 47h), associated with the first orogenic deformation stage, provide a WSW-ENE shortening (Fig. 47i). F_2 fold hinges (A_2) are weakly to moderately plunging to NE and SW (Fig. 47j), whereas axial plane poles (AP_2) form a main cluster providing a mean 267/71 pole (Fig. 43k). Flexural-slip lineations show a mean NE-SW trend (Fig 47l). Finally orogenic stylolites (Fig. 47m), when restored (Fig. 47n), indicate moderately dipping to sub-vertical planes with a mean NW-SE direction.

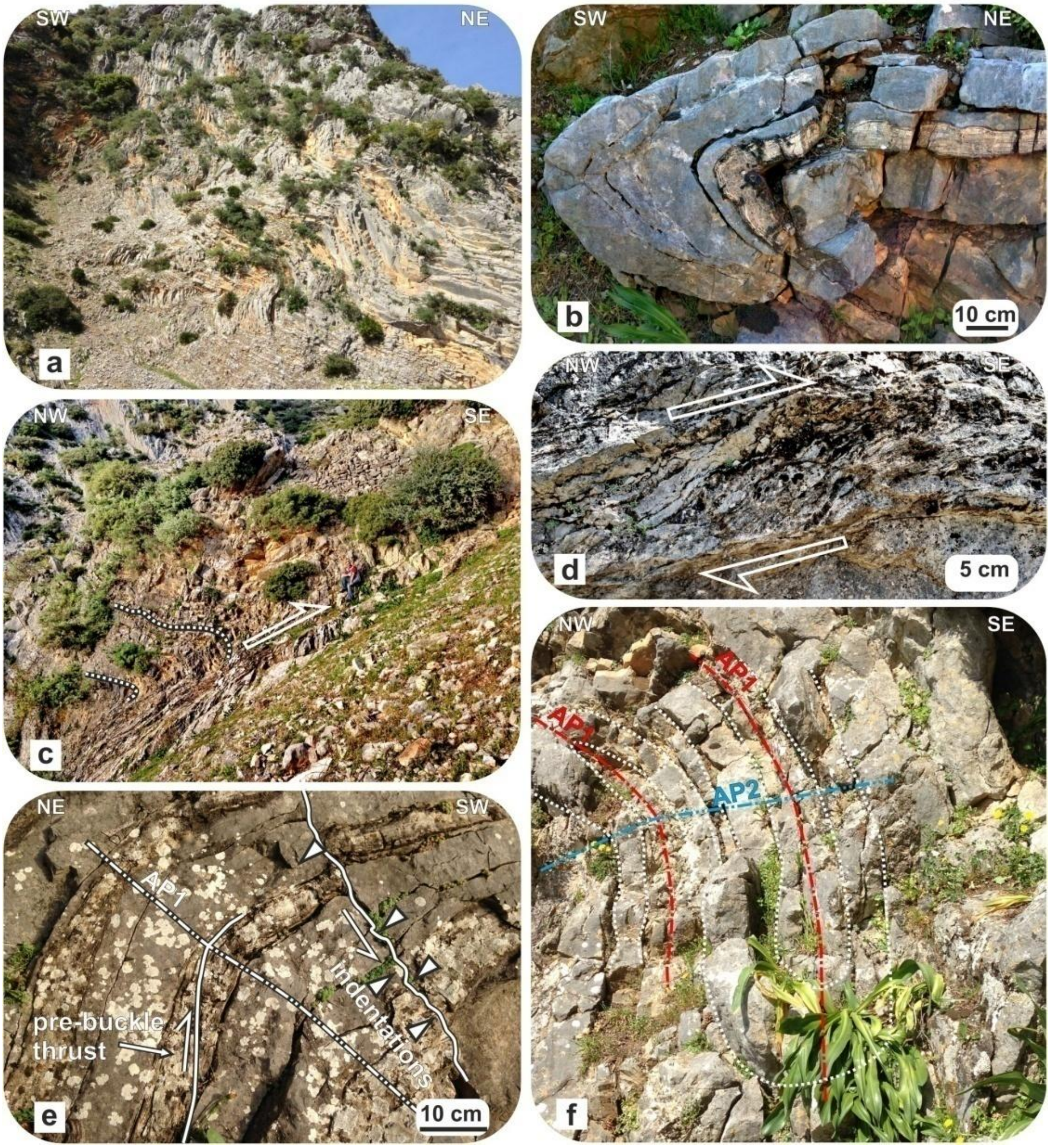

Fig. 45- (a) Parasitic F_1 folds in the hinge zone of the macro-scale anticline. (b) F_1 isoclinal fold. (c) SE-verging thrust fault and related F_2 fold. (d) S-C structures in the footwall block of a D_2 thrust fault. (e) A pre-orogenic normal fault deformed by the early LPS; pre-buckle thrust deformed by a late F_1 parasitic fold. (f) Interference pattern between F_1 and F_2 folds of 3-type Ramsay's classification.

Fig. 46- (a) Pre-orogenic normal faults reactivated as reverse or normal in the D_1 deformation stage. (b–d) D_1 pre-buckle thrusts affecting cherty layers. (e) F_1 fold deforming calcareous layers hosting pre-orogenic normal faults. (f) F_1 fold-related fractures. (g) Minor thrust faults in cherty layers accommodating deformation in the F_1 fold hinge.

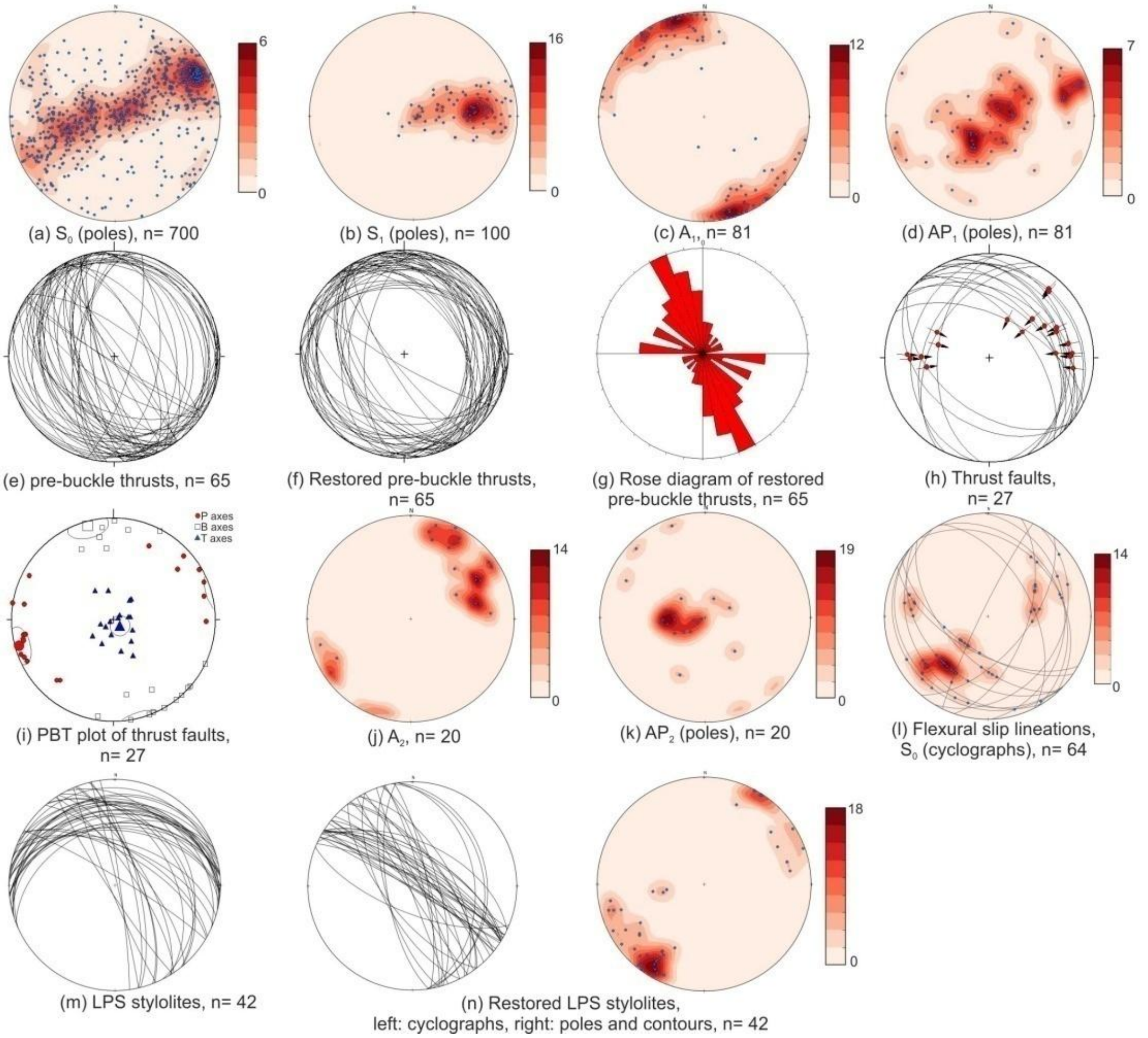

Fig. 47- Stereographic projections (equiareal net, lower hemisphere), rose diagram, contour and PBT plots (Angelier and Mechler, 1977; Reiter and Acs, 1996-2003) of the analyzed orogenic structures. PBT plot of thrust faults: P (254/05) R = 82%, B (345/06) R = 79%, T (133/83) R = 91%.

Chapter 6 - Discussion

6.1. Massylian and Predorsalian Units

Predorsalian and Massylian Units show deformations always heterogeneous often localized in levels where the pelitic component is dominant, however with similar characters, in terms of orientation, tectonic style and vergences. $(D_1)_{1\text{-}2}^{MA}$, $(D_1)_{1\text{-}2}^{PD}$ are characterized by almost coaxial folds (Fig. 48), indicating a progressive deformation associated to the overthrusting of the *Dorsale Calcaire* Unit onto Predorsalian Unit and together onto the Massylian succession. The most of structures indicate a ca. NE-SW shortening and SW tectonic vergence in line with previous studies about the Late Oligocene-Early Miocene tectonic evolution of the Internal and Maghrebian Flysch Basin Units in this sector of the northern Rif (e.g. Chalouan and Michard, 2004; Chalouan et al., 2006). Approaching the two main contacts, an increasing of strain gradient occurs and frequently, where the strain intensity is very high, the original bedding is completely disrupted. This is testified by the occurrence of pervasive C-type shear bands indicating consistently a mean WSW vergence, in the upper part of Predorsalian succession, and a very intense deformation producing the total disruption of bedding, in the upper part of Massylian Unit.

The occurrence of conjugate extensional shear bands, in the latter two successions, indicating extension both orthogonal and parallel to the main tectonic transport, suggests a pure shear component, synchronous with the dominant simple shear strain related to the regional thrusting. However the extensional structures, although dispersed, point out a prevalence of extension orthogonal to the shear direction, i.e. parallel to the axis of the orogenic belt. This is a frequent feature in arched mountains such as the Rif and Betic Chains (e.g. Balanyà et al., 2007, 2012) as well as the southern Apennines and Calabrian Arc (e.g. Ferranti et al., 1996), where the radial displacement caused a continuous arc spreading with divergent transport directions, extension parallel to the thrust front (Piedmont Glacier model of Hindle and Burkhard, 1999) and different rotations for adjacent arc sectors. The latter is testified in the Rif Chain and Betic Cordillera (e.g. Lonergan and White, 1997) by counterclockwise (Platzman et al., 1993; Saddiqi et al., 1995; Platt et al., 2003) and clockwise paleomagnetic rotations (Feinberg et al., 1996; Platzman et al., 2000; Calvo et al., 2001; Cifelli et al., 2008), respectively.

The successive deformation stage, well recorded in this two successions, includes reverse and thrust faults and associated folds mainly verging to NW, more or less orthogonal to the previous ($(D_1)_{1\text{-}2}^{MA}$, $(D_1)_{1\text{-}2}^{PD}$) shortening (Fig. 48). Two main almost orthogonal fold sets are described in the whole Rif Chain (e.g. Hlila, 2005) and a similar deformation evolution was recently described in tectonic equivalent successions of the Ligurian Accretionary Complex cropping out in the southern Apennines (Vitale et al., 2010, 2013; Ciarcia et al., 2012). An early shortening is recorded in Mauretanian, Massylian, Predorsalian and *Dorsale Calcaire* Units within the whole northern Rif, however with variable directions, as for the *Dorsale Calcaire* Unit where tectonic shortening ranges from E-W, SW-NE and N-S in the northern, southern and southernmost area, respectively, the latter bounding the Jebha-Chrafate Fault (Platzman et al., 1993; Hlila, 2005). Also the successive N-S/NW-SE shortening, expressed as folds and thrusts, is reported in the whole Rif Chain both in Maghrebian Flysch Basin and Internal Units (Hlila and Sanz de Galdeano, 1995; Hlila, 2005). Finally strike-slip and normal faults, affecting the whole thrust pile, indicate a NW-SE compression and an ENE-WSW/E-W extension, respectively (Fig. 48). For the former faults is not to exclude a close relationship with the last shortening stage having the similar NW-SE direction for the maximum stress.

6.2. Dorsale Calcaire

The Liassic succession of the External *Dorsale Calcaire* is affected by several structures, as *en-echelon* veins, normal faults, drag folds and deflexed cherty layers, suggesting a pre-orogenic, syn-sedimentary brittle-ductile deformation suggesting a not complete lithification of calcareous and cherty sediments. This deformation stage, according to several authors (Mouhssine et al., 1990; Blidi and Hervouet, 1991; El Kadiri et al., 1992; Blidi, 1993; Lallam et al., 1997; El Kadiri, 2002), was related to Liassic Neotethys rifting, synchronous with the deposition of cherty limestones and conglomerates (Fig. 49a). More in detail, the most of extensional deformation was probably recorded during the deposition of conglomerates, because they fill structural depressions, seal the graben-bounding normal faults and in turn host extensional structures.

The orientation of pre-orogenic normal faults, show a main NW-SE direction indicating a dominant NE-SW extension. Generally, associated to pre-orogenic normal faults, two orthogonal vein sets occur (Figs. 41c, d, g, 42b), with a main orientation NW-SE and a secondary NE-SW direction (Fig. 44e) probably related to a local exchange between the intermediate (σ_2) and the minimum (σ_3) stress axes close to the growing fractures instead of a rotation of the stress field (e.g. Guerriero et al., 2010).

The successive shortening (Figs. 48; 49b-d), characterized by a NE-SW direction and producing the overthrusting of the External *Dorsale Calcaire* Unit onto the Predorsalian Unit, includes (i) a $(D_1)_1^{DC}$ early layer parallel shortening (Figs. 48, 49b) producing pre-buckle thrusts, stylolites orthogonal to cherty limestone beds and clast-indentation in cherty conglomerates. (ii) A $(D_1)_2^{DC}$ shortening stage (Figs. 48, 49c) developing the Chefchaouen anticline (locally with an overturned limb) with associated several minor folds and occasionally meso-scale SW-verging thrust faults, late NE-verging back-thrusts (Fig. 48d) and an overall northeastward tilting of all allochtonous units (Hlila and Sanz de Galdeano, 1995; Michard et al., 2002; Guerrera et al., 2005; Hlila, 2005).

Pre-orogenic extensional faults can control the geometry of the new structures, related to successive shortening structures in the mountain building, by means of simple reactivation as reverse or strike-slip faults (e.g. Coward, 1994; Ziegler et al., 1995; Tavani et al., 2011a, b; Quintà and Tavani, 2012); truncation or folding by late thrust faults (e.g. Butler, 1989; Tavarnelli, 1996; Scisciani et al., 2002); localization of the new structures without a notable reactivation (e.g. Laubscher, 1976; Wiltschko and Eastman, 1982).

In the analyzed succession, the most of pre-orogenic structures were not reactivated with a reverse kinematic but rather they behaved as passive markers, such as described in other orogenic chains (e.g. Vitale et al., 2012; Uzkeda et al., 2013). Due to flexural-slip mechanism, presently, the pre-orogenic normal fault planes are characterized by dislocation along the bedding surfaces; whereas the buttressing mechanism, produced indentation between hanging wall and footwall enhanced by pressure-solution processes. Only occasionally pre-orogenic normal faults show a reverse reactivation with minor displacements (Fig. 46a).

Several geological features, such as striations along the bedding planes, stylolites and fold-related fractures, indicate shallow deformation conditions for the shortening stages, ruled by the flexural-slip mechanism, as dominant process for the fold development, preceded and accompanied by pressure-solution mechanisms. However the not abundance of veins and stylolites suggests a deficiency of fluids assisting the shortening deformation. This feature, in addition to: (i) lacking of relevant damage-zones related to inherited meso-scale normal faults able to covey fluids (Sibson, 2004); (ii) unfavorable orientation of pre-orogenic normal faults generally characterized by high-angles to the bedding and orthogonal to the shortening direction; (iii) localization of the Miocene deformation along neo-formed low-angle structures or along favorably oriented major pre-orogenic normal faults as described in other areas (e.g. Mouhssine et al, 1990; El Hatimi et al., 1991); favored the passive behavior of the pre-orogenic meso-scale structures rather than a their reactivation.

6.3. Geodynamic Evolution

High velocity anomalies (Wortel and Spackman, 2000) show a steep subducted slab under the Betic Cordillera-Rif Chain arc down to 660 km of depth. However this lithospheric panel does not continue in the eastern sector of Morocco. This deep geometry is interpreted as resulting from the tear mechanism affecting the downgoing slab from Late Oligocene to Late Miocene (Rosenbaum and Lister, 2004). The W-migration of the slab break off and the subsequent fast roll-back of the lithosphere (with a subduction rate of ca. 3.3 cm/y considering a distance of 660 km covered in ca. 20 My; Rosenbaum and Lister, 2004), allowed the Betic-Rif thrust sheet pile to traveland spread out along the present arc (e.g. Lonergan and White, 1997). Furthermore thetear lateral propagation produced differentiated displacements of contiguous sectors probably accommodated by some main transfer faults such as the Jebha-Chrafate Fault (Benmakhlouf et al., 2012) bounding the SE margin of the analyzed area (Fig.32). It is worth to note as the formation of the other large orogenic arc such as the southern Apennines-Calabria Arc (Fig. 1) was driven by means of similar tear mechanisms (e.g. Ascione et al., 2012). As regarding the ages of deformation stages, the thrusting of the *Dorsale Calcaire* Unit onto the Predorsalian Unit and the latter onto the Massylian succession, involved the Lower Burdigalian deposits of the Numidian-like sandstones. Unfortunately in the Rif Chain further geological constraints lack, such as unconformably wedge-top basin, contrarily to the corresponding Ligurian successions where the Langhian-lowermost Tortonian *Cilento* Group (Vitale et al.,2013b) confines this tectonic stage to the late Burdigalian (Ciarcia et al., 2012). However, according with the most of authors (Hlila and Sanz de Galdeano, 1995; Michard et al., 2002; Guerrera et al., 2005; Hlila, 2005), and in analogy with the tectonic evolution of the Maghrebian Flysch Basin successions in the Betic Cordillera (e.g. Serrano et al., 2007) and the LAC in southern Italy (Ciarcia et al., 2012), a Late Burdigalian age for $(D_1)_{1-2}^{MA}$, $(D_1)_{1-2}^{PD}$ and $(D_1)_{1-2}^{DC}$ tectonic stages can be hypothesized. Consequently, this orogenic event, corresponding to the *paroxismo Burdigaliense* of the Spanish authors (e.g. Hermes, 1985; Martín Algarra, 1987), was synchronous in the whole western Mediterranean domain from the southern Apennines (e.g. Vitale and Ciarcia, 2013) up to the Rif and Betic chains. For what concerns the successive shortening phase (D_2^{DC}, D_2^{PD} and D_2^{MA}), characterized by a NW-SE direction (in this sector of northern Rif), there are no confident geological data able to constrain the age of this tectonic pulse. However this event could be associated to the final compression of the Rif Chain resulting in out-of-sequence thrusts affecting the whole orogenic belt (e.g. El Mrihi, 1995, 2005; Hlila, 2005; Chalouan et al., 2006), probably Tortonian in age (Sanz de Galdeano and Vera, 1992; Hlila and Sanz de Galdeano, 1995) or younger (Plio-Quaternary) as described by (i) Ait Brahim and Chotin (1984) for the Moroccan foreland where the N-S shortening was recorded as strike-slip faulting or by (ii) Meghraoui et al. (1996) that describe a NNW-SSE transpression within the Alboran Sea domain. Although the deformation history, such as resulting from this work, regards only a small sector of the Rif Chain, we attempted to reconstruct a tectonic evolution according to the wide literature about this part of the western Mediterranean area (between others: Martín Algarra, 1987; Serrano et al., 1995; Hlila and Sanz de Galdeano, 1995; Lonergan and White, 1997; Michard et al., 2002; Rosenbaum and Lister, 2004; Guerrera et al., 2005; Hlila, 2005; Chalouan et al., 2008). The figure 50 shows the paleogeographic evolution from Early Jurassic to Middle Miocene of the western Mediterranean area and some schematic cross sections. Pre-orogenic structures, hosted in the analyzed rocks, presently indicate a NE-SW extension; however it reasonable to assume that they were successively rotated following the arching of the orogenic belt (e.g. Platzman et al., 1993; Feinberg et al., 1996). Supposing, in the Early Jurassic time (Fig. 50a), an original NW-SE direction of the extension, associated with the rifting and opening of Neotethys Ocean (e.g. Handy et al., 2010; Schettino and Turco, 2011), a counterclockwise rotation of 80-90° for this sector is inferred. These values are consistent with the paleomagnetic data carried out on the External *Dorsale Calcaire* in this area the by Platzman et al. (1993).

In the Middle Eocene-Oligocene interval (Fig. 50b) some extensional basins of the northern African margin, such as the High and Middle Atlas (Arboleya et al., 2004) and the Mesorif Suture Zone (MSZ, Michard et al., 2007), previously formed as consequence of the Neotethys rifting (e.g. Schettino and Turco, 2011), were inverted. This stage ended in the late Oligocene (Fig. 50c) about synchronously with the tectonic imbrication of some of the Internal Units (External *Dorsale Calcaire* excluded). Such as described before, in the Burdigalian (Fig. 50d, e), the External *Dorsale Calcaire*, Predorsalian, Mauretanian and Massylian Units were progressively included in the accretionary wedge forming an arcuate belt with radial displacements and extension parallel to the thrust front (Vitale et al., 2014a). Finally in the Middle Miocene (Fig. 50f) the thrust front migrated toward the external zones including the Intrarif, MSZ, Mesorif and Prerif domains (Michard et al., 2007).

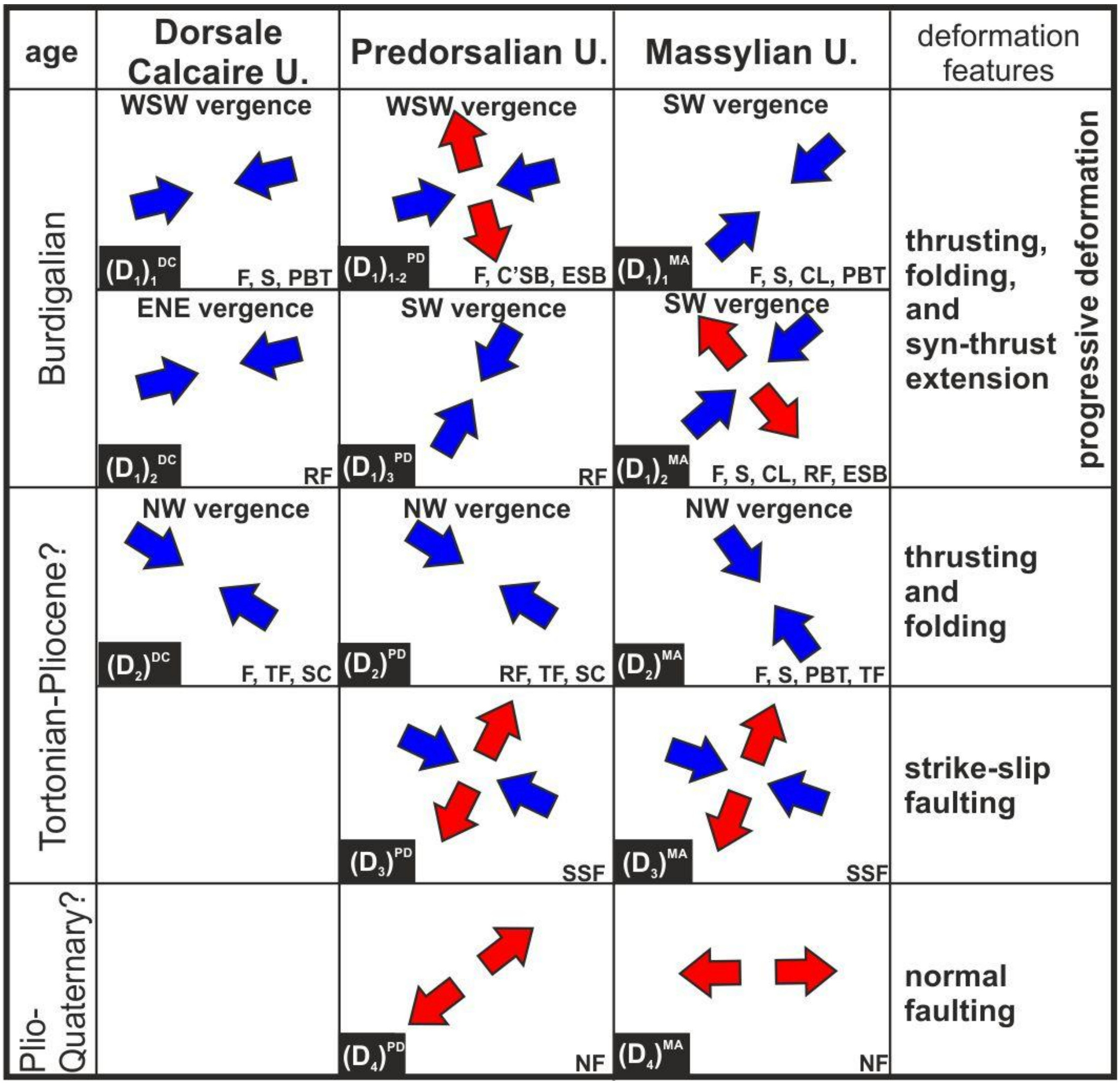

Fig. 48- Synoptic sketch showing correlation of deformation stages for the studied units. Acronym legend. C' SB, C'-type shear band; CL, crenulation lineation; ESB, conjugate extensional shear bands; F, fold; NF, normal fault; PBT, pre-buckle thrust; RF, reverse fault; S, tectonic foliation; SC, S-C structure; SSF, strike-slip fault; TF, thrust fault.

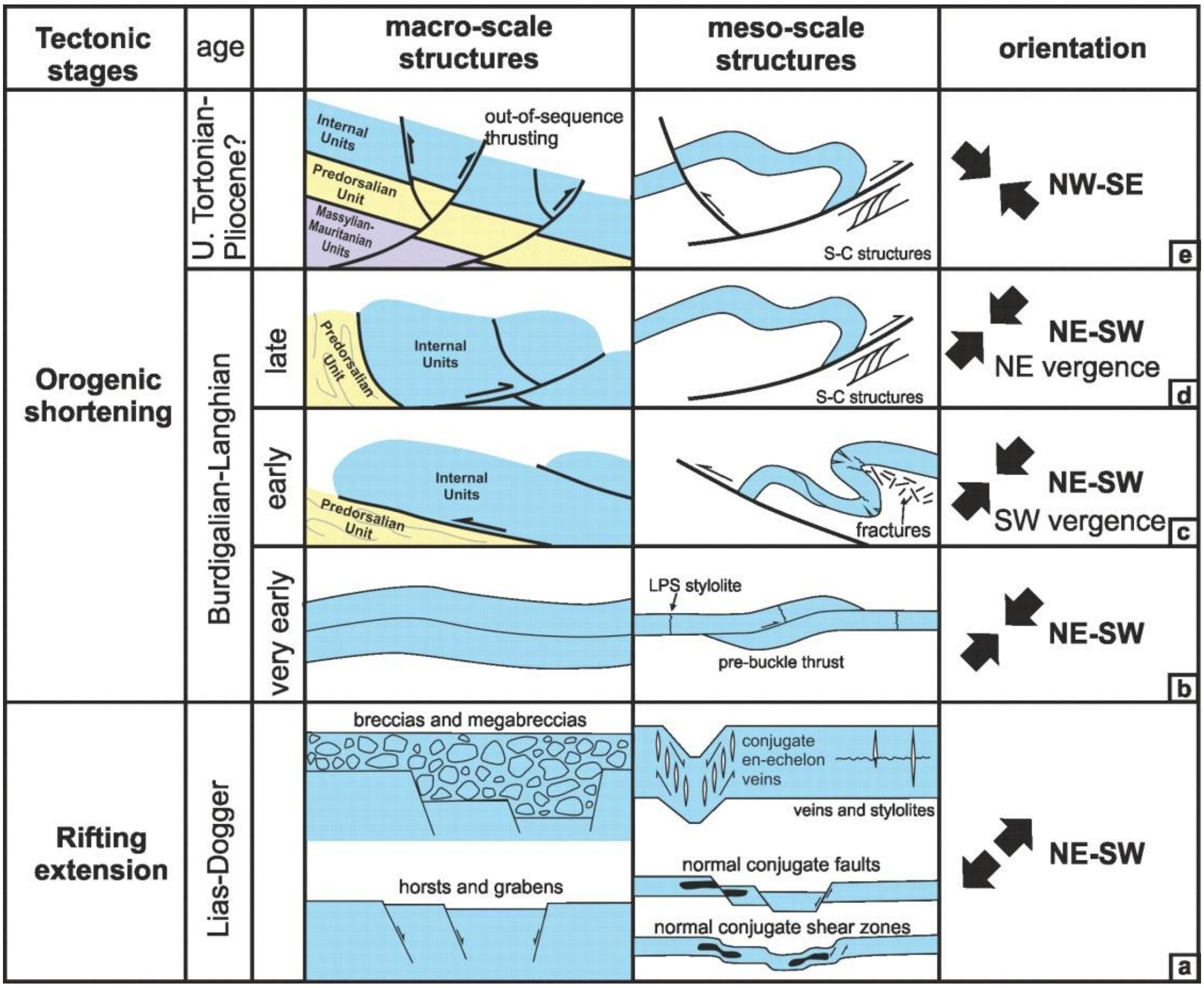

Fig. 49- Cartoon showing deformation structures at macro- and meso-scale and related deformation orientations and ages.

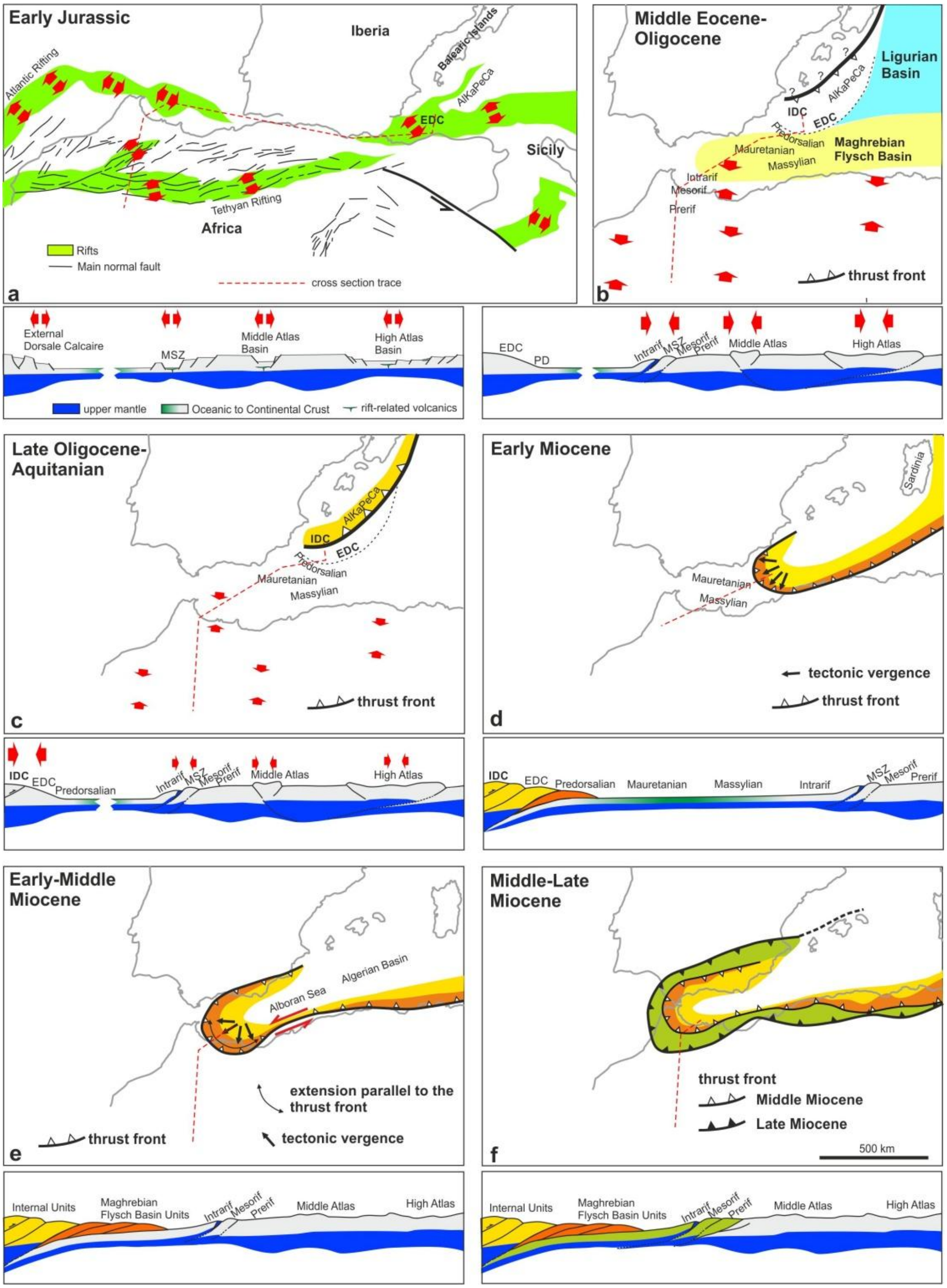

Fig. 50- Paleogeographic reconstruction and cross sections of the western Mediterranean area. Not to scale. IDC: Internal *Dorsale Calcaire*; EDC: External *Dorsale Calcaire*; MSZ: Mesorif Suture Zone.

Chapter 7 - Conclusions

7.1. Conclusions

The structural and petrographic analyses carried out on LAC both in the southern Apennines (*Frido*, *Nord-Calabrese*, *Parasicilide* and *Sicilide* Units) and northern *Calabria* (*Diamante-Terranova* Unit) allowed to reconstruct the tectonic history of this tectonic complex within the context of the Eocene to Late Miocene geodynamic evolution of the eastern sector of the proto-Central-Western Mediterranean Sea.

The *Frido* Unit represents a segment of an ocean-continent transition domain that reached HP/VLT metamorphic conditions probably during the Aquitanian and then rapidly exhumed in the late Serravallian-middle Tortonian interval. During the (i) burial; (ii) exhumation and (iii) emplacement into the obducted LAC, the *Frido* Unit experienced several deformation phases.The first two (D_1 and D_2),characterized by HP/VLT conditions, suggested by the occurrence of Fe-Mg-carpholite (X_{Mg} = 0.29–0.41), in phyllites and metapelites, aragonite in the calcshists (Spadea, 1976) and blue amphibole in metabasites. The presence of carpholite, associated to phengite, indicate an HP/VLT metamorphism characterized by pressures of ~1.2-1.4 GPa and temperatures around 350 °C. In high strain zones, fold hinges of F_2 folds, are parallel to the maximum lenghtening direction marked by the stretching lineation SL_2, with a mean NW-SE trend, whereas, in low strain zones, fold hinges are at a high angle to the maximum stretching direction. The third deformation phase (D_3) is related to the early stages of exhumation of the *Frido* Unit. This is recorded in meta-sandstones by the growth of Na-amphibole and stilpnomelane on the S_2 foliation and along extensional shear surfaces, indicating lower pressure and temperature conditions. The latter structures are frequent all around continental and oceanic crust mega-boudins, indicating extension both parallel and orthogonal to the stretching lineation SL_2. In analogy with the tectonic transport recorded by the *Lungro-Verbicaro* Unit in northern *Calabria* (Vitale and Mazzoli, 2008) and the *Nord Calabrese* and *Parasicilide* units in the *Cilento* area (Ciarcia et al., 2012; Vitale et al., 2011), a mean SE tectonic transport appears to have characterized the *Frido* Unit during the main deformation stages, leading to its final inclusion in the LAC.

The *Nord Calabrese*, *Parasicilide* and *Sicilide* Units show a similar deformation evolution characterized by the superposition of four fold and thrust sets (D_1-D_4). The first two stages show common features indicating a progressive deformation especially localized in less competent rocks, with an overall strain gradient existing from the more deformed *Nord Calabrese* Unit to lesser deformed *Parasicilide* and *Sicilide* Units. The progressive deformation was mainly recorded as two superposed fold sets (D_1-D_2), for all analyzed successions, related to the building of the thrust sheet pile in the Burdigalian time.The third fold and thrust set (D_3), affected also the wedge-top basin deposits of *Albidona* Fm. and the underlying carbonates of the *Pollino-Ciagola* Unit. It was associated to the overthrusting of the Apennine wedge onto the eastern sector of the Apulian domain and the inclusion of *Lagonegro* Units in the tectonic prism (Vitale and Ciarcia, 2013). The latter event probably occurred before the deposition of the unconformable upper Tortonian-lower Messinian wedge-top basin deposits of *Oriolo* Fm. A further deformation (D_4) was expressed by long wavelength-high amplitude folds, related to deeply rooted thrusts, deforming the whole thrust sheet pile and producing, in the easternmost sector of the analyzed area, the tectonic windows of *Valsinni* and *Rotondella*, where Numidian Sandstones (*Lagonegro-Molise*

Basin Units) crop out. This thick-skinned thrusting, synchronous with the Pliocene-Middle Pleistocene filling of the *Sant'Arcangelo* wedge-top basin, was responsible also of the uplifts of *Castroregio, Farneta* and *Monte Alpi* in the central sector of the study area. All the analyzed LAC Units show a similar stratigraphy and a strong correspondence exists between the Upper Cretaceous-Lower Miocene deposits of *Sicilide* Unit and the *Lagonegro-Molise* Basin successions (*Flysch Rosso* Fm.). This relation is probably associated with the paleogeographic evolution of this sector, where the *Panormide* Platform, that separated the Ligurian/Maghrebian Flysch and *Lagonegro-Molise/Imerese* basins, starting from the uppermost Cretaceous, drowned and allowed the joining of these two basins. Finally tectonic vergences, recorded in different thrust sheets and unconformable wedge-top basin deposits, indicate: (i) an Early-Middle Miocene mean SE tectonic transport for the LAC successions; (ii) a Late Miocene transport from NW to NE for the LAC Units, overlying *Albidona* Fm., Apennine Platform and *Lagonegro-Molise* Basin Units; and finally (iii) a constant NE-SW shortening for the tectonic structures related to the Plio-Quaternary thick-skinned thrusting.

As concerning the *Diamante-Terranova* Units, although the studies are in preliminary stages, several important considerations can carry out. The present work shed light on the complex deformation affecting the whole succession characterized by: (i) three progressive deformative stages (D_1-D_2-D_3) in blueschist facies conditions (P~0.9-1.1 GPa, T~380 °C; Liberi and Piluso, 2009), followed by a tectonic exhumation stages recorded by extensional brittle-ductile shear zones and normal faults.

The petrographic analysis provides other important information, amongst others: (i) the occurrencepre- to inter- and post-tectonic lawsonite, suggests also its continuous growth during all metamorphic path (D_1-D_2-D_3); (ii) the amphibole zonation from Na-rich blue core to Ca-rich greenish rim suggests lower pressure conditions during the tectonic exhumation (D_4).

The reconstruction of the tectono-metamorphic evolution of the LAC units both in the southern Apennines and northern *Calabria* clarified the first stages of the history of the southern Apennines/CPT system. Such Eocene-Late Miocene tectonic stages, associated with the closure of the Ligurian Ocean and coeval back-arc opening of the Ligurian-Provençal Basin, are dominated by a general E/SE-directed tectonic transport (in present-day coordinates). Later (late Tortonian to Middle Pleistocene) thrusting, coeval with back-arc opening of the Tyrrhenian Sea, was characterized by a more dispersed (i.e., radial) pattern, resulting in a mean NE-directed tectonic transport (in present-day coordinates) in the Apennines.

The study of the Chefchaouen area (Morocco), where the Internal Unit of *Dorsale Calcaire* overthrust the MFB Units, the latter corresponding to the sedimentary LAC units, allowed to reconstruct the Jurassic-Early Miocene tectonic evolution of a key-sector of the northern Rif.

The Rhaetian-Liassic portion of the External *Dorsale Calcaire* Unit, cropping out in the study area, recorded a polyphasic deformation with a wide range of structures. The first stage was characterized by an early syn-sedimentary extension related to the Liassic Neotethys rifting, whereas the two following main deformative events were related to Miocene shortening pulses. However the pre-orogenic extensional structures, such as normal faults and veins, mainly behaved as passive markers, due to: (i) scarcity of fluids and well-developed fault-related damage zones able to convey fluids; (ii) unfavorable orientation of pre-orogenic structures generally at high angle to the bedding; (iii) strain localization along neo-formed low-angle thrusts. The passive behavior of pre-orgenic structures is marked by folded, tilted and dislocated normal faults (flexural-slip), and indented by means of pressure-solution mechanisms fault planes, as a consequence of the buttressing effect. Only few meso-scale extensional structures were reactivated as reverse faults with minor displacements.

The first orogenic deformation, characterized by a NE-SW shortening, produced the tectonic superimpositions of the Internal Unit (*Dorsale Calcaire* Unit) onto Predorsalian Unit, and the latter onto the Massylian Unit. This stage was recorded by a progressive deformation expressed by early structures such as pre-buckle thrusts and LPS stylolites and subsequent meso- to macro-scale folds and thrust faults in the hanging-wall carbonate succession. In the footwall (Predorsalian Unit) the overthrusting produced a progressive deformation characterized by a wide shear zone, located close to the main regional thrust fault, hosting early isoclinal folds and, in the pelitic levels, a severe boudinage. Successively the succession was deformed by open to close folds and late reverse faults. In turn the PredorsalianUnit tectonically covered the Massylian succession where a progressive deformation was recorded by early isoclinal and late open to tight folds and thrust faults.

Late back-thrusts affected the whole thrust-sheet pile, as well as tectonic contacts among the Internal Units, frequently northeastward tilted. The subsequent deformation stage, affecting the whole thrust sheet pile and consisting of a NW-SE shortening, includes thrust faults and related folds verging both to NW and SE. Strike-slip faults crosscut all structures providing an about NW-SE shortening probably related to the last stages of the accretionary wedge building. Finally normal faults cut all successions. The Jurassic extension and the successive Miocene shortening presently show the same NE-SW direction, however assuming a Jurassic NW-SE extension (e.g. Handy et al., 2010; Schettino and Turco, 2011), a Miocene counterclockwise rotation of 80-90° results, well-fitting with paleomagnetic data for the External *Dorsale Calcaire* in this area (Platzman et al., 1993).

The reconstructed deformation evolution, joined to the wide geological knowledge about the Rif Chain, allowed to reconstruct a possible tectonic evolution from the Late Oligocene up to the Recent. The Late Oligocene paleogeography was characterized by the MFB separating the Europe continent and AlKaPeCa microplate to the north and the African continent to the south, with the Predorsalian succession deposited along the W/SW margin of the AlKaPeCa microplate. In the late Burdigalian, the most of deposits in this basin domain were completely detached from their basement and accreted in the tectonic prism by means of a dominant thin-skinned tectonics, including a NE-SW shortening for the study area. This deformation was the result of the W-migration of the thrust front as consequence of the down-going plate roll back and slab tear. The thrust front migration was accommodated by (i) a main lithospheric sinistral transfer zone; (ii) the arching and (iii) the counterclockwise rotation (for the Moroccan sector) of the orogenic belt. The radial translation was accompanied by syn-thrusting extension resulting in a ductile and brittle stretching parallel to the thrust front. This Burdigalian deformation testifies an orogenic event recorded in the most of peri-Mediterranean chains from the southern Apennines up to the Rif and Betic chains. The successive shortening stage, especially recorded in the internal sector, has occurred in the Tortonian-Pliocene interval and was characterized by out-of-sequence thrust faults, mainly verging to NW, and late strike-slip faults.

It is worth to note that the Rif chain and the southern Apennines-*Calabria* Arc (Fig. 1) were driven by means of similar tear mechanisms (e.g. Ascione et al., 2012). LAC and MFB Units, both subject of this study, recorded two main almost orthogonal fold sets as well as described in the previous paragraphs and in several recent work (Vitale et al., 2010, 2013a, b, 2014a, b; Ciarcia et al., 2012). Comparable is also the deformative style, with the deformation that, in both cases, was localized mainly in the pelitic portions and giving to these successions, sometimes, the characters of broken formations.

As regarding the ages of deformation stages, in the Rif Chain further geological constraints such as unconformably wedge-top basin, occurring in southern Apennines, lack. In the latter sector, the Langhian-Lowermost Tortonian *Cilento* Group (Vitale et al., 2013b) confines this tectonic stage to the Late Burdigalian (Ciarcia et al., 2012). In the light of these considerations and in analogy with the tectonic evolution of the MFB successions in the Betic Cordillera (e.g. Serrano et al., 2007), $(D_1)_{1\text{-}2}^{MA}$, $(D_1)_{1\text{-}2}^{PD}$ and $(D_1)_{1\text{-}2}^{DC}$ tectonic stages can be ascribed to the *paroxismo Burdigaliense* of the Spanish authors (e.g. Hermes, 1985; Martín Algarra, 1987). Also another important feature, as the extensional structures pointing out a prevalence of extension orthogonal to the shear direction, i.e. parallel to the axis of the orogenic belt, is a frequent feature in southern Apennines and Calabrian Arc (e.g. Ferranti et al., 1996) and more in general in arched mountains. In the southern Apennines, the radial displacement caused a continuous arc spreading with divergent transport directions, extension parallel to the thrust front (Piedmont Glacier model of Hindle and Burkhard, 1999) and different rotations for adjacent arc sectors.

7.2. Concluding remarks about analogies and differences between LAC and MFB Units tectonic evolution

- All sedimentary basin units were included in the tectonic wedge by frontal accretion, all detached by their Cretaceous (LAC Units) and Jurassic (MFB Units) basements;
- the main overthrusting stages occurred in the Burdigalian time (*Paroxismo Burdigaliense*) both for LAC and MFB units;
- The radial translation was accompanied by syn-thrusting extension resulting in a ductile and brittle stretching parallel to the thrust front both for LAC and MFB units;
- In the Rif, the Internal Unit of the *Dorsale Calcaire*, overthrust onto the MFB Units, such as occurred in the northern *Calabria* where the Internal Unit of Sila tectonically covered the *Diamante-Terranova* Unit, but differently from the southern Apennines where the Internal Units lack;
- In the southern Apennines several wedge-top basin deposits allowed to constraint all tectonic pulses, on the contrary in the Rif, no Miocene unconformable deposit crops out onto the MFB successions;
- In all sedimentary basin units the deformation was:

  (a) Heterogeneous and localized in the lesser competent levels often producing a chaotic tectonic facies as a "broken formation";

  (b) Progressive, characterizing the first stages of the thrusting, with brittle-ductile structures indicating shallow deformation conditions.

- The *Frido* and *Diamante-Terranova* Units show a comparable P-T-path (with higher pressures and lower temperatures for the *Frido* Unit) suggesting an origin in a common oceanic domain (Ligurian Ocean).

Reference List

Afiri, A., Gueydan, F., Pitra, P., Essaifi, A., Précigout, J., 2011.Oligo-Miocene exhumation of the Beni-Bousera peridotite through a lithosphere-scale extensional shear zone. Geodin. Acta 24 (1), 49-60.

Ait Brahim, L., Chotin, P., 1984. Mise en évidence d'un changement de direction de compression dans l'avant-pays rifain (Maroc) au cours du Tertiaire et du Quaternaire. Bull. Soc. Géol. Fr. 4, 681-691.

Alsop, G.I., Holdsworth, R.E., 2004. The geometry and topology of natural sheath folds: a new tool for structural analysis. Journal of Structural Geology 26, 1561-1589.

Alvarez, W., Cocozza, T., Wezel, F.C., 1974. Fragmentation of the Alpine orogenic belt by microplate dispersal. Nature 248, 309-314.

Amodio-Morelli, L., Bonardi, G., Colonna, V., Dietrich, D., Giunta, G., Ippolito, F., Liguori, V., Lorenzoni, S., Paglionico, A., Perrone, V., Piccarreta, G., Russo, M., Scandone, P., Zanetti-Lorenzoni, E., Zuppetta, A., 1976. L'Arco Calabro-Peloritano nell'orogene appenninico-maghrebide. Memorie della Società Geologica Italiana 17, 1-60.

Amore, O., Bonardi, G., Ciampo, G., De Capoa, P., Perrone, V., Sgrosso, I., 1988. Relazione fra «flysch interni» e domini appenninici: reinterpretazione delle formazioni di Pollica, San Mauro e Albidona nel quadro dell'evoluzione infra-miocenica delle zone esterne appenniniche. Memorie della Società Geologica Italiana 41, 285-299.

Anderson, E.M., 1951. The Dynamics of Faulting and Dyke Formation, 2nd ed. Oliver & Boyd, Edinburgh. Andrieux, J., 1971. La structure du Rif central. Notes et Mémoires du Service géologique du Maroc 235, 1-155.

Andrieux, J., Mattauer, M., 1963. Sur la présence de roches vertes à la base des nappes «ultra» du Rif. C. R. Somm. Soc. Géol. Fr. 7, 213-215.

Andrieux, J., 1971. La structure du Rif central. Notes et Mémoires du Service géologique du Maroc 235, 1-155.

Angelier, J., Mechler, P., 1977. Sur une méthode graphique de recherche des contraintes principales égalment utilisable en tectonique et en seismologie: la méthode des dièdres droits. Bull. Soc. Géol. Fr. 19, 1309-1318.

APAT, 2005. Carta Geologica d'Italia alla scala 1:50.000, Foglio 506 'S. Arcangelo', SELCA, Firenze.

Ascione, A., Ciarcia, S., Di Donato, V., Mazzoli, S., Vitale, S., 2012. The Pliocene-Quaternary wedge-top basins of southern Italy: an expression of propagating lateral slab tear beneath the Apennines. Basin Research 24, 456-474.

Arboleya, M.L., Teixell, A., Charroud, M., Julivert, M., 2004. A structural transect through the High and Middle Atlas of Morocco. J. Afr. Earth Sci. 39, 319-327.

Balanyá, J.C., García-Dueñas, V., 1988. El cabalgamiento cortical de Gibraltar y la tectónica de Béticas y Rif. II Congreso geológico de España. Simposio cinturones orogénicos. Soc. Geol. de España, 35-44.

Balanyà, J.C., Crespo-Blanc, A., Diaz-Azpiroz, M., Expòsito, I., Lujàn, M., 2007. Structural trend line pattern and strain partitioning around Gibraltar Arc accretionary wedge: insights as to the mode of orogenic arc building. Tectonics 26, TC2005, http://dx.doi.org/10.1029/2005TC.001932.

Balanyà, J.C., Crespo-Blanc, A., Diaz-Azpiroz, M., Expósito, I., Torcal, F., Pèrez-Peña, V., Booth Rea, G., 2012. Arc-parallel vs back-arc extension in the Western Gibraltar arc: is the Gibraltar forearc still active? Geol. Acta 10, 249-263.

Beccaluva L., Maciotta G., Spadea P., 1982. Petrology and geodynamic significance of the Calabria-Lucania ophiolites. Rend. Soc. It. Miner. Petrol. 38, 973-987.

Belviso, C., Lettino, A., Cavalcante, F., Fiore, S., Finizio, F., 2009. Carta Geologica delle Unità Liguridi dell'area del Pollino (Basilicata): Nuovi dati Geologici, Mineralogici e Petrografici. Carta Geologica delle Unità Liguridi dell'area del Pollino (Basilicata): Nuovi dati Geologici, Mineralogici e Petrografici. ISBN: 978-88-7522-026-6, 1-36.

Benmakhlouf, M., Galindo-Zaldívar, J., Chalouan, A., Sanz de Galdeano, C., Fedal Ahmamou, M., López-Garrido, A.C., 2012. Inversion of transfer faults: the Jebha-Chrafate fault (Rif, Morocco). J. Afr. Earth Sci. 73-74, 33-43.

Bigi, G., Cosentino, D., Parotto, M., Sartori, R., Scandone, P. (Eds.), 1992. Structural model of Italy and gravity map, scale 1:500,000, Progetto Finalizzato Geodinamica CNR, Quad. Ric. Sci. 3, 114.

Blidi, M., 1993. Les calciturbidites à silex de la Dorsale Calcaire entre Chaouen et Assifane (Rif interne, Maroc). Témoins d'un rifting liasique téthysien. Thèse Univ., Pau, pp. 232.

Blidi, M., Hervouet, Y., 1991. Dépôts de pente de bas de talus lies au rifting liasique de la Dorsale calcaire (Rif interne, Maroc): étude de formations à silex près de Chaouen. C.R. Acad. Sci. Paris 312, 1379-1384.

Bonardi, G., Ciampo, G., Perrone, V., 1985. La Formazione di Albidona nell'Appennino calabro-lucano. Bollettino della Societa Geologica Italiana 104, 539-549.

Bonardi, G., Amore, F.O., Ciampo, G., de Capoa, P., Miconnet, P., Perrone, V., 1988a. Il Complesso Liguride Auct.: stato delle conoscenze e problemi aperti sull'evoluzione pre-appenninica ed i suoi rapporti con l'arco calabro. Memorie della Società Geologica Italiana 41, 17-35.

Bonardi, G., D'Argenio, B., Perrone, V., 1988b. Carta Geologica dell'Appennino Meridionale. Memorie della Società Geologica Italiana 41, scale 1:250.000, 1 sheet.

Bonardi, G., de Capoa, P., Fioretti, B., Perrone, V., 1993. L'âge des métacalcaires de l'Unité du Frido (région calabro-lucanienne, Italie) et ses implications géodynamiques. Comptes Rendus de l'Académie des Sciences 317, 955-962.

Bonardi, G., Cavazza, W., Perrone, V., Rossi, S., 2001. Calabria-Peloritani terrane and northern Ionian Sea. In: Vai, F., Martini, I.P. (Eds.), Anatomy of an Orogen: The Apennines and Adjacent Mediterranean Basins. Kluwer Academic Publishers, Dordrecht, 287-306.

Bonardi, G., Ciarcia, S., Di Nocera, S., Matano, F., Sgrosso, I., Torre, M., 2009. Carta delle principali unità cinematiche dell'Appennino meridionale. Nota illustrativa. Bollettino della Societa Geologica Italiana 128, 47-60.

Bonini, M., Sani, F., 2000. Pliocene-Quaternary transpressional evolution of the Anzi-Calvello and Northern S. Arcangelo Basins (Basilicata, Southern Apennines Italy) as a consequence of deep-seated fault reactivation. Marine and Petroleum Geology 17, 909-927.

Bouillin, J.P., 1984. Nouvelle interprétation de la liaison Apennin-Maghrébides en Calabre; conséquences sul la paléogéographientéthysienne entre Gibraltar et les Alpes. Revue de Géologie Dynamique et de Géographie Physique 25, 321-338.

Bouillin, J.P., 1986. Le bassin maghrébin: une ancienne limite entre l'Europe et l'Afrique à l'ouest des Alpes. Bull. Soc. Geol. Fr. 2, 5547-5558.

Bousquet, J.C., 1973. La tectonique récente de l'Apennin calabro-lucanien dans son cadre géologique et géophysique. Geologica Romana 12, 1-103.

Brogi, A., Giorgetti, G., 2012. Tectono-metamorphic evolution of the siliciclastic units in the middle Tuscan Range (inner Northern Apennines): Mg-carpholite bearing quartz veins related to syn-metamorphic syn-orogenic foliation. Tectonophysics 526-529, 167-184.

Brun, J.P., Faccenna, C., 2008. Exhumation of high-pressure rocks driven by slab rollback. Earth and Planetary Science Letters 272, 1-7.

Butler, R.W.H. 1989. The influence of pre-existing basin structure on thrust systemevolution in the Western Alps.From Cooper, M. A. & Williams, G. D.

(eds), 1989, Inversion Tectonics, Geological Society Special Publications 44, 105-122.

Calvo, M., Cuevas, J., Tubıa, J.M., 2001. Preliminary paleomagnetic results on Oligocene-early Miocene mafic dykes from southern Spain. Tectonophysics 332, 333-345.

Carmignani, L., Decandia, F.A., Disperati, L., Fantozzi, P.L., Kligfield, R., Lazzarotto, A., Liotta, D., Meccheri, M., 2001. Inner Northern Apennines. In: Vai, F., Martini, I.P. (Eds.), Anatomy of an Orogen: the Apennines and Adjacent Mediterranean Basins. Kluwer Academic Publishers, Dordrecht, 197-214.

Carminati, E., Lustrino, M., Doglioni, C., 2012.Geodynamic evolution of the central and western Mediterranean: tectonic vs. igneous petrology constraints. Tectonophysics 579, 173-192. http://dx.doi.org/10.1016/j.tecto.2012.01.026.

Casero, P., Roure, F., Endignoux, L., Moretti, I., Muller, C., Sage, L., Vially, R., 1988. Neogene geodynamic evolution of the Southern Apennines. Memorie della Società Geologica Italiana 41, 109-120.

Catalano, S., Monaco, C., Tortorici, L., 1993. Pleistocene strike-slip tectonics in the Lucanian Apennine (southern Italy).Tectonics 12, 656-665.

Cello, G., Morten, L., De Francesco, A.M., 1991. The tectonic significance of the Diamante-Terranova Unit (Calabria, Southern Italy) in the alpine evolution of the northern sector of the Calabrian Arc. Bollettino della Società Geologica Italiana 110, 685-694.

Cello G., Invernizzi, C., Mazzoli, S., 1996. Structural signature of tectonic processes in the Calabrian Arc, southern Italy: Evidence from the oceanic-derived Diamante-Terranova unit. Tectonics 15, 1, 187-20.

Cello, G., Mazzoli, S., 1998. Apennine tectonics in southern Italy: a review. Journal of Geodynamics 27, 191-211.

Cesarano, M., Pierantoni, P.P., Turco, E., 2002. Structural analysis of the Albidona Formation in the Alessandria del Carretto-Plataci area (Calabro-Lucanian Apennines, Southern Italy). Bollettino della Societa Geologica Italiana 1, 669-676.

Chalouan, A., 1986. Les nappes ghomarides (Rif septentrional Maroc). Un terrain varisque dans la chaîne alpine. Univ. Louis Pasteur, Strasbourg, pp. 371 (Ph.D. thesis).

Chalouan, A., Michard, A., 1990. The Ghomarides Nappes, Rif Coastal Range, Morocco: a Variscan chip in the Alpine belt. Tectonics 9, 165-183.

Chalouan, A., Michard, A., 2004. The Alpine Rif Belt (Morocco): a case of mountain building in a subduction-subduction-transform fault triple junction. Pure Appl. Geophys. 161, 489-519.

Chalouan, A., Galindo-Zaldívar, J., Akil, M., Marín, C., Chabli, A., Ruano, P., Bargach, K., Sanz de Galdeano, C., Benmakhlouf, M., Ahmamou, M., Gourari, L., 2006. Tectonic wedge escape in the southwestern front of the Rif Cordillera (Morocco). In: Moratti, G., Chalouan, A. (Eds.), Tectonics of the Western

Mediterranean and North Africa. Geological Society of London Special Publication, London, 101-118.

Chalouan, A., Michard, A., El Kadiri, K., Negro, F., Frizon de Lamotte, D., Soto, J.I., Saddiqi, O., 2008. The Rif. In: Michard, A., Saddiqi, O., Chalouan, A., Frizon de Lamotte, D. (Eds.), Continental Evolution: The Geology of Morocco-Structure, Stratigraphy, and Tectonics of the Africa-Atlantic-Mediterranean Triple Junction. Springer, p. 424.

Chemenda, A., Mattauer, M., Bokun, A., 1996. Continental subduction and a mechanism for exhumation of high-pressure metamorphic rocks: new modelling and field data from Oman. Earth and Planetary Science Letters 143, 173-182.

Ciarcia, S., Vitale, S., Di Staso, A., Iannace, A., Mazzoli, S., Torre, M., 2009. Stratigraphy and tectonics of an Internal Unit of the southern Apennines: implications for the geodymanic evolution of the peri-Tyrrhenian mountain belt. Terra Nova 21, 88-96.

Ciarcia, S., Mazzoli, S., Vitale, S., Zattin, M., 2012. On the tectonic evolution of the Ligurian accretionary complex in southern Italy. Geological Society of America Bullettin 124, 463-483.

Ciarcia, S., Vitale, S., 2013. Sedimentology, stratigraphy and tectonics of evolving wedge-top depozone: Ariano Basin, southern Apennines, Italy. Sedimentary Geology 290, 27-46

Cifelli, F., Rossetti, F., Mattei, M., 2007.The architecture of brittle post-orogenic extension: results from an integrated structural and paleomagnetic study in

North Calabria (Southern Italy). Geological Society of American Bulletin 119, 221-239.

Cifelli, F., Mattei, M., Porreca, M., 2008. New paleomagnetic data from Oligocene-Upper Miocene Sediments in the Rif Chain (Northern Morocco): insights on the Neogene tectonic evolution of the Gibraltar Arc. J. Geophys. Res. 113, B02104.doi:10.1029/2007JB005271.

Cippitelli, G., 2007. The CROP-04 seismic profile. Interpretation and structural setting of the Agropoli-Barletta Geotraverse. Bollettino della Societa Geologica Italiana 7, 267-281.

Corrado, S., Invernizzi, C., Aldega, L., D'Errico, M., Di Leo, P., Mazzoli, S., Zattin, M., 2010. Testing the validity of organic and inorganic thermal indicators in different tectonic settings from continental subduction to collision: the case history of the Calabria-Lucania border (Southern Apennines, Italy). Journal of the Geological Society 167, 985-999.

Cosentino, D., Cipollari, P., Pipponzi, G., 2003. Il sistema orogenico dell'Appennino centrale: vincoli stratigrafici e cronologia della migrazione. In: Cipollari, P., Cosentino, D. (Eds.), Evoluzione cinematica del sistema orogenico dell'Appennino centro-meridionale: caratterizzazione stratigrafico-strutturale dei bacini sintettonici. Studi Geologici Camerti, Numero Speciale 2003, 85-99.

Coward, M., 1994. Inversion Tectonics. In: Hancock, P.L. (Ed.), Continental Deformation. Pergamon Press, Oxford, pp. 289-304.

Cristi Sansone, M.T., Rizzo, G., Mongelli, G., 2011. Petrochemical characterization of mafic rocks from the Ligurian ophiolites, southern Apennines. International Geology Review 53, 130-156.

Critelli, S., 1999.The interplay of lithospheric flexure and thrust accommodation in forming stratigraphic sequences in the southern Apennines foreland basin system, Italy. Rendiconti di Scienze Fisiche e Naturali dell'Accademia Nazionale dei Lincei 10, 257-326.

D'Argenio, B., Pescatore, T., Scandone, P., 1973. In: Schema geologico dell'Appennino meridionale (Campania-Lucania) Atti convegno Moderne vedute sulla geologia dell'Appennino. Accademia Nazionale dei Lincei, Roma 183, 49-72.

De Roever, E.W.F., 1972. Lawsonite-albite facies metamorphism near Fuscaldo, Calabria (Southern Italy), its geological significance and petrological aspects. GUA papers of geology series 1, 3, thesis, University of Amsterdam.

Dewey, J.F., Helman, M.L., Turco, E., Hutton, D.H.W., Knott, S.D., 1989. Kinematics of the western Mediterranean. In: Coward, M.P., Dietrich, D., Park, R.G. (Eds.), Alpine tectonics: Geological Society of London Special Publication, 45, 265-283.

Dietrich D., Scandone P., 1972. The position of the basic andultrabasic rocks in the tectonic units of the Southern Apennines. Atti Acc. Pont., Napoli, 21, 61-75.

Di Staso, A., Giardino, S., 2002. New integrate biostratigraphic data about the Saraceno Formation (North-Calabrian Unit; Southern Apennines). Bollettino della Societa Geologica Italiana special volume 1, 517-526.

Di Staso, A., Perrone, V., Perrotta, S., Zaghloul, M.N., Durand-Delga, M., 2010. Stratigraphy, age and petrography of the Beni Issef successions (External Rif; Morocco): insights for the evolution of the Maghrebian Chain. C. R. Geosci. 342, 718-730.

Didon, J., Durand-Delga, M., Kornprobst, J., 1973. Homologies géologiques entre les deux rives du détroit de Gibraltar. Bull. Soc. Geol. Fr. 15, 79-105.

Donzelli, G., Crescenti, U., 1962. Lembi di Flysch oligocenico affiorante a SE della Piana del Sele. Memorie della Societa Geologica Italiana 3, 569-592.

Durand-Delga, M., Hottinger, L., Marçais, J., Mattauer, M., Milliard, Y., Suter, G., 1960-1962. Actual data about the Rif structure. Mém. Soc. Géol. Fr. 1, 399-422.

Durand-Delga, M., Kornprobst, J., 1963. Esquisse géologique de la région de Ceuta (Maroc). Bull. Soc. Géol. Fr. 5, 1049-1057.

Durand-Delga, M., 1965. C. R. Reunion extraordinaire de la Societé géologique de France en Tchécoslovaquie. Bull. Soc. Géol. Fr. 7, 1027-1129.

Durand-Delga, M., Rossi, P., Olivier, P., Puglisi, D., 2000. Situation structurale et nature ophiolitique de roches basiques jurassiques associées aux flyschs Maghrébens du Rif (Maroc) et de Sicile (Italie). C. R. Acad. Sci. 331, 29-38.

El Hatimi, N., Duée, G., Hervouet, Y., 1991. La Dorsale calcaire du Haouz: ancienne marge continentale passive téthysienne (Rif, Maroc). Bull. Soc. Geol. Fr. 162, 79-90.

El Kadiri, Kh., Linares, A., Olóriz, F., 1990. Les éléments du Groupe Jbel Moussa (Chaine Calcaire, Rif, Maroc): évolution stratigraphique et géodynamique au cours du Jurassique-Crétacé. Commun. Serv. Geol. Portugal 76, 141-161.

El Kadiri, K., Linares, A., Oloriz, F., 1992. La Dorsale calcaire rifaine (Maroc septentrional): Evolution stratigraphique et géodynamique durant le Jurassique-Crétacé. Notes et Mémoires de Service Géologique du Maroc, 336, 217-265.

El Kadiri, K., Fauzi, M., 1996. Les formations carbonates massives de la Dorsale Calcaire externe (Rif interne, Maroc), un exemple de plateforme tidale sous controle géodynamique durant le Trias moyen-Lias inférieur. Mines Géologique Rabat, 55, 79-92.

El Kadiri, K., 2002. Jurassic ferruginous hardgrounds of the “Dorsale Calcaire” and the Jbel Moussa Group (internal Rif Morocco) stratigraphical context and paleoceanographic consequences of mineralization processes. Geol. Romana 36, 33-70.

El Mrihi, A., 1995. Structures alphines des zones extemes et des nappes de flysch à l’ouest de la chaîne du Haouz (Rif septentrional, Maroc). Thesis Diplôme Etudes Supèrieures. Universitè Mohammed V, Rabat.

El Mrihi, A., 2005. Structure et cinématique de mise en place des nappes de flyschs mauritaniens (Rif externe nord occidental): elaboration d’ un modèle. Université de Tetouan (Ph.D. thesis).

Faccenna, C., Davy, P., Brun, J.P., Funiciello, R., Giardini, D., Mattei, M., Nalpas, T., 1996. The dynamics of back-arc extension: an experimental approach to the opening of the Tyrrhenian Sea. Geophysical Journal International 126, 781-795

Faccenna, C., Becker, T.W., Lucente, F.P., Jolivet, L., Rossetti, F., 2001. History of subduction and back-arc extension in the Central Mediterranean. Geophysical Journal International 145, 809-820.

Fallot, P., 1937. Essai sur la géologie du Rif septentrional. Notes Mém. Serv. Géol. Maroc 40, 548.

Feinberg, H., Saddiqi, O., Michard, A., 1996. New constraints on the bending of the Gibraltar Arc from paleomagnetism of the Ronda peridotite (Betic Cordilleras, Spain). Paleomagnetism and Tectonics of Mediterranean Region. Geological Society of London Special Publication, 105, 43-52.

Ferranti, L., Oldow, J.S., Sacchi, M., 1996.Pre-Quaternary orogen-parallel extension in the Southern Apennine belt, Italy.Tectonophysics 260, 325-347.

Ferranti, L., Santoro, E., Mazzella, M.E., Monaco, C., Morelli, D., 2009. Active transpression in the northern Calabria Apennines, southern Italy. Tectonophysics 476, 226-251.

Frizon de Lamotte, D., 1985. La structure du Rif oriental (Maroc), rôle de la tectonique longitudinale et importance des fluides. Thèse de Doctoratès-Sciences, Univ. Paris VI, 85-03 (436).

García-Dueñas, V., Balanyá, J.C., Martínez-Martínez, J.M., 1992. Miocene extensional detachments in the outcropping basement of the Northern Alboran Basin (Betics) and their tectonic implications.Geo-Mar. Lett. 12, 88-95.

Gattacceca, J., Deino, A., Rizzo, R., Jones, D.S., Henry, B., Beaudoin, B., Vadeboin, F., 2007. Miocene rotation of Sardinia: new paleomagnetic and geochronological constraints and geodynamic implications. Earth and Planetary Science Letters 258, 359-377.

Guerrera, F., Martín-Algarra, A., Perrone, V., 1993. Late Oligocene-Miocene syn/late orogenic successions in Western and Central Mediterranean chains from the Betic Cordillera to the southern Apennines. Terra Nova 5, 525-544.

Guerrera, F., Martin-Martin, M., Perrone, V., Tramontana, M., 2005. Tectono-sedimentary evolution of the southern branch of the western Tethys (Maghrebian Flysch Basin and Lucanian Ocean): consequences for western Mediterranean geodynamics. Terra Nova 17, 358-367.

Guerriero, V., Iannace, A., Mazzoli, S., Parente, M., Vitale, S., Giorgioni, M., 2010. Quantifying uncertainties in multi-scale studies of fractured reservoir analogues: implemented statistical analysis of scan line data. J. Struct. Geol. 32, 1271-1276.

Guzzetta, G., Ietto, A., 1971. Relazioni tra unità strutturali e unità litostratigrafiche nel flysch del Cilento. Atti dell'Accademia Pontaniana di Napoli 20, 1-7.

Haccard, D., Lorenz, C. and Grandjacquet, C., 1972. Essai sur l'evolution tectogenetique de la liason Aipes-Apennines (de la Ligurie a la Calabrie). Mem.Soc. Geol. Ital., 11, 309-341.

Handy, M.R., Schmid, S.M., Bousquet, R., Kissling, E., Bernoulli, D., 2010. Reconciling plate-tectonic reconstructions of Alpine Tethys with the geological-geophysical record of spreading and subduction in the Alps. Earth-Science Reviews 102, 121-158.

Hermes, J.J., 1985. Algunos aspectos de la estructura de la Zona Subbética (Cordilleras Béticas, España meridional). Estudios Geol. 41, 157-176.

Hindle, D., Burkhard, M., 1999. Strain, displacement and rotation associated with the formation of curvature in fold belts: the example of the Jura Arc. J. Struct.Geol. 21, 1089-1101.

Hlila, R., Sanz de Galdeano, C., 1995. Structure, cinématique et chronologie des déformations dans la dorsale du Haouz (Rif, Maroc). Geogaceta 17, 95-97.

Hlila, R., 2005. Evolution tectono-sédimentaire tertiaire au front ouest du domained'Alboran (Ghomarides et Dorsale calcaire). Univ. de Tetouan, pp. 351 (Ph.D. thesis).

Iannace A., Boni M., Zamparelli, V., 1995. The Middle Upper Triassic of the San Donato Unit Auct. (northernCalabria): stratigraphy, paleogeography and tectonic implications. Riv. Ital. Paleont. Strat., 10113, 301-324.

Iannace, A., Garcia Tortosa, F.J., Vitale, S., 2005. The Triassic metasedimentary successions across the boundary between Southern Apennines and Calabria-Peloritani Arc (Northern Calabria, Italy).Geological Journal 40, 155-171.

Iannace, A., Vitale, S., D'Errico, M., Mazzoli, S., Di Staso, A., Maiacone, E., Messina, A., Reddy, S.M., Somma, R., Zamparelli, V., Zattin, M., Bonardi, G., 2007. The carbonate tectonic units of the northern Calabria (Italy): a record of Apulian paleomargin evolution and Miocene convergence, continental crust subduction, and exhumation of HP-LT rocks. Journal of the Geological Society 164, 1165-1186.

Ietto, A., Pescatore, T., Cocco, E., 1965. Il flysch mesozoico-terziario del Cilento occidentale. Bollettino della Società dei Naturalisti in Napoli 74, 396-402.

Ietto, A., Barillaro, A.M., 1993. L'Unita di San Donato quale margine deformato Cretacico-Paleogene del bacino di Lagonegro (Appennino meridionale-Arco Calabro). Bollettino della Societa Geologica Italiana 112, 477-496

ISPRA, 2009. Carta Geologica d’Italia alla scala 1:50.000, Foglio 535 ‘Trebisacce’, SELCA, Firenze.

Jolivet, L., Faccenna, C., Goffé, B., Mattei, M., Rossetti, F., Brunet, C., Storti, F., Funiciello, R., Cadet, J.P., D'Agostino, N., Parra, T., 1998. Mid crustal shear zones in post-orogenic extension-example from northern Tyrrhenian Sea. Journal of Geophysical Research 103 (B6), 12123-12160.

Jones, R.R., Holdsworth, R.E., Bailey, W., 1997 Lateral extrusion in transpression zones: the importance of boundary conditions Journalof Structural Geology, 19, 9, 1201-1217.

Knott, S.D., 1987. The Liguride complex of Southern Italy - a Cretaceous to Paleogene accretionary wedge. Tectonophysics 142, 217-226.

Knott, S.D., 1994. Structure, kinematics and metamorphism in the Liguride Complex, southern Appennines, Italy. Journal of Structural Geology 16, 1107-1120.

Kornprobst, J., 1974. Contribution à l'étude pétrographique et structurale de la zone interne du Rif, (Maroc septentrional). Notes et Mémoires de Service Géologique, Maroc, 251-256.

Lallam, S., Sahnoun, E., El Hatimi, N., Hervouet, Y., De Leon, J.T., 1997. Mise en évidence de la dynamique de la marge téthysienne de l’Hettangien à l’Aalénien dans la Dorsale Calcaire (Tetouan, Rif, Maroc). C. R. Acad. Sci. Paris 324 (II), 923-930.

Lanzafame, G., Zuffa, G., 1976. Geologia e petrografia del foglio Bisignano (Bacino del Crati, Calabria). Geol. Rom., 15, 223-270, con carta geologica 1:50.000.

Lanzafame, G., Spadea, P., Tortorici, L., 1979. Mesozoic ophiolites of Northern Calabria and Lucanian Apennine (Southern Italy). Ofioliti 4, 173-182.

Laubscher, H.P., 1976. Geometrical adjustment during rotation of a Jura fold limb. Tectonophysics 36, 347-365.

Leake, B.E., Woolley, A.R., Arps, C.E.S., Birch, B.D., Gilbert, M.C., Grice, J.D., Hawthorne, F.C., Kato, A., Kisch, H.J., Krivovichev, V.G., Linthout, K., Laird, J., Mandarino, J.A., Maresch, W.V., Nickel, E.H., Rock, N.M.S., Schumacher, J.C., Smith, D.C., Stephenson, N.C.N., Ungaretti, L., Wittaker, E.J.W., Youzhi, G., 1997. Nomenclature of amphiboles: report of the subcommittee on amphiboles of the International Mineralogical Association, Commission on new minerals and mineral names. The Canadian Mineralogist 35, 219-246.

Leblanc, D., 1980. L'accident du Nekor et la structure du Rif oriental (Maroc). Rev. Géol. Dynam. Géog. Phys. 22, 267-277.

Lentini, F., 1979. Le Unità Sicilidi della Val d'Agri (Appennino Lucano). Geologica Romana 18, 215-224.

Liberi, F., Morten L., Piluso, E., 2006. Geodynamic significance of ophiolites within the Calabrian Arc.Island Arc 15, 26-43

Liberi, F., Piluso, E., 2009.Tectono-metamorphic evolution of the ophiolitic sequence from Northern Calabrian Arc. Bollettino della Societa Geologica Italiana 128, 483-493.

Liotta, D., Cernobori, L., Nicolich, R., 1998. Restricted rifting and its coexistence with compressional structures: results from the Crop03 traverse (Northern Apennines, Italy). Terra Nova 10, 16-20.

Lonergan, L., White, N., 1997. Origin of the Betic-Rif mountain belt.Tectonics 16, 504-522.

Lustrino, M., Morra, V., Fedele, L., Franciosi, L., 2009. Beginning of the Apennine subduction system in central western Mediterranean: constraints from Cenozoic "orogenic" magmatic activity of Sardinia, Italy. Tectonics 28, TC5016. http://dx.doi.org/10.1029/2008TC002419.

Lustrino, M., Duggen, S., Rosenberg, C.L., 2011. The Central-Western Mediterranean: anomalous igneous activity in an anomalous collisional tectonic setting. Earth-Science Reviews 104, 1-40.

Malinverno, A., Ryan, W.B.F., 1986. Extension in the Tyrrhenian Sea and shortening in the Apennines as a result of arc migration driven by sinking of the lithosphere. Tectonics 5, 227-243.

Mantovani, E., Babbucci, D., Tamburelli, C., Viti, M., 2009. A review on the drivingmechanism of the Tyrrhenian-Apennines system: Implications for the present seismotectonic setting in the Central-Northern Apennines. Tectonophysics 476, 22-40.

Martín Algarra, A., 1987. Evolución geológica alpina del contacto entre las ZonasInternas y las Zonas Externas de la Cordillera Bética. Univ. de Granada, pp. 1171 (Ph.D thesis).

Mattauer, M., 1960. Nouvelles données sur la «Dorsale Calcaire» du Rif. C. R. Acad. Sci. Paris 250, 374-376.

Mattei, M., Speranza, F., Argentieri, A., Rossetti, F., Sagnotti, L., Funiciello, R., 1999. Extensional tectonics in the Amantea basin (Calabria, Italy): a comparison between structural and magnetic anisotropy data. Tectonophysics 307, 33-49.

Mattei, M., Cifelli, F., D'Agostino, N., 2007. The evolution of the Calabrian Arc: evidence from paleomagnetic and GPS observations. Earth and Planetary Science Letters 263, 259-274.

Mattioni, L., Shiner, P., Tondi, E., Vitale, S., Cello, G., 2006. The Argille varicolori unit of Lucania (Italy): a record of tectonic off scraping and gravity sliding in the Mesozoic-Tertiary Lagonegro Basin, southern Apennines. In: Moratti, G., Chalouan, A. (Eds.), Geology and Active Tectonics of the Western Mediterranean Region and North Africa, vol. 262. Geological Society of London, London, 277-288 (Special publication).

Mauro, A., Schiattarella, M., 1988. L’Unità Silentina di base: Assetto strutturale, metamorfico e significato tettonico nel quadro geologico dell’Appennino Meridionale. Memorie della Societa Geologica Italiana 41, 1201-1213.

Mazzoli, S., 1998. The Liguride units of southern Lucania (Italy): structural evolution and exhumation of high-pressure metamorphic rocks. Rendiconti di Scienze Fisiche e Naturali dell'Accademia Nazionale dei Lincei 9, 271-291.

Mazzoli, S., Helman, M., 1994. Neogene patterns of relative plate motions for Africa-Europe: some implications for recent central Mediterranean tectonics. Geologische Rundschau 83, 464-468.

Mazzoli, S., Martín-Algarra, A., 2011. Deformation partitioning during transpressional emplacement of a ‘mantle extrusion wedge’: the Ronda peridotites, western Betic Cordillera, Spain. Journal of the Geological Society 168, 373-382.

Meghraoui, M., Morel, J.L., Andrieux, J., Dahmani, M., 1996.Tectonique plio-quaternaire de la chaîne tello-rifaine et de la mer d'Alboran. Une zone complexe de convergence continent-continent. Bull. Soc. Géol. Fr. 167 (1), 141-157.

Menardi Noguera, A., Rea, G., 2000. Deep structure of the Campanian-Lucanian Arc (southern Apennines). Tectonophysics 324, 239-265

Michard, A., Chalouan, A., 1991. The Ghomarides nappes, Rif Coastal range, Morocco: an African terrane in the West Mediterranean Alpine belt. Bull. Geol. Soc. Grec.XXV, 117-129.

Michard, A., Goffé, B., Bouybaouene, M., Saddiqi, O., 1997. Late Hercynian-Mesozoic thinning in the Alboran domain: metamorphic data from northern Rif, Morocco. Terra Nova 9, 1-8.

Michard, A., Chalouan, A., Feinberg, H., Goffé, B., Montigny, R., 2002. How does the Alpine belt end between Spain and Morocco? Bull. Soc. Géol. Fr. 173, 3-15.

Michard, A., Negro, F., Saddiqi, O., Bouybaouene, M.L., Chalouan, A., Montigny, R., Goffé, B., 2006. Pressure-temperature-time constraints on the Maghrebide mountain building: evidence from the Rif-Betic transect (Morocco, Spain), Algerian correlations, and geodynamic implications. Compt. Rendus Geosci. 338, 92-114.

Michard, A., Negro, F., Frizon de Lamotte, D., Saddiqi, O., 2007. Serpentinite sliversand metamorphism in the External Maghrebides: arguments for an intracontinental suture in the African paleomargin (Morocco, Algeria). Rev. Soc. Geol. España 20 (3-4), 173-185.

Michard, A., Mokhtari, A., Chalouan A., Saddiqi, O., Rossi, P., Rjimati, E., 2014. New ophiolite slivers in the External Rif belt, and tentative restoration of a dual Tethyan suture in the western Maghrebides. Bull. Soc. Géol. Fr. 5, 313-328.

Minelli, L., Faccenna, C., 2010. Evolution of the Calabrian accretionary wedge (central Mediterranean). Tectonics 29, TC4004.http://dx.doi.org/10.1029/2009TC002562.

Molli, G., 2008. Northern Apennine-Corsica orogenic system: an updated review. In: Siegesmund, S., Fugenschuh, B., Froitzheim, N. (Eds.), Tectonic Aspects of the Alpine-Dinaride-Carpathian System: Geological Society of London Special Publication, 298, 413-442.

Monaco, C., Tansi, C., Tortorici, L., De Francesco, A.M., Morten, L., 1991. Analisi geologico-strutturale dell'Unità del Frido al confine calabro-lucano (Appennino meridionale). Memorie della Società Geologica Italiana 47, 341-353.

Monaco, C., Tortorici, L., 1995. Tectonic role of ophiolite-bearing terranes in the building of the Southern Apennines orogenic belt.Terra Nova 7, 153-160.

Mostardini, F., Merlini, S., 1986. Appennino centro-meridionale: sezioni geologiche e proposta di modello strutturale. Memorie della Società Geologica Italiana 35, 177-202.

Mouhssine, M., Hervouet, Y., Benyaich, A., 1990. Les Mégabréches et turbidites calcaires à silex de la Dorsale externe des Bokoya (Rif interne, Maroc) témoins du rifting liasique de la Téthys. C. R. Acad. Sci. Paris 310, 1279-1284.

Oberhänsli, R., Partzsch, J., Candan, O., Çetinkaplan, M., 2001. First occurrence of Fe-Mg-carpholite documenting a high-pressure metamorphism in metasediments of the Lycian Nappes, SW Turkey.International Journal of Earth Sciences 89, 867-873.

Ogniben, L., 1960. Nota illustrativa dello schema geologico della Sicilia nord-orientale. Riv. Min. Sicil. 11, 183-212.

Ogniben, L., 1969. Schema introduttivo alla geologia del confine calabro-lucano. Memorie della Società Geologica Italiana 8, 453-763.

Olivier, P., 1984. Évolution de la limite entre Zones Internes et Zones Externes dans l'Arc de Gibraltar (Maroc-Espagne). Thèse de l'Université Paul Sabatier, Toulouse, pp. 229.

Passchier, C.W., Trouw, R.A.J., 2005. Microtectonics, 2nd ed. Springer Verlag, pp. 366.

Patacca, E., Sartori, R., Scandone, P., 1990. Tyrrhenian basin and Apenninic arcs: kinematic relations since late Tortonian times. Memorie della Società Geologica Italiana 45, 425-451.

Patacca, E., Scandone, P., 2007. Results of the CROP project, sub-project CROP-04. Bollettino della Società Geologica Italiana 7, 75-119.

Perrone, V., Torre, M., Zuppetta, A., 1973. Il Miocene della Catena Costiera calabra. 1° contributo: zona Diamante-Bonifati-Sant'Agata d'Esaro (Cosenza). Rivista Italiana Paleontologia Stratigrafia 79, 157-205.

Piccardo, G.B., 2009. Geodynamic evolution of the Jurassic Ligurian Tethys viewed from the Mantle perspective. Italian Journal of Geosciences 128, 565-574.

Piedilato, S., Prosser, G., 2005. Thrust sequences and evolution of the external sector of a fold and thrust belt: example from the Southern Apennines (Italy). Journal of Geodynamics 39, 386-402.

Platt, J.P., Allerton, S., Kirker, A., Mandeville, C., Mayfield, A., Platzman, E.S., Rimi, A., 2003. The ultimate arc: differential displacement, oroclinal bending, and vertical axis rotation in the external Betic-Rif arc. Tectonics 22, 1017, http://dx.doi.org/10.1029/2001TC001321.

Platzman, E.S., Platt, J.P., Olivier, P., 1993. Paleomagnetic rotations and fault kinematics in the Rif arc of Morocco. J. Geol. Soc. 150, 707-718.

Platzman, E., Platt, J.P., Kelley, S.P., Allerton, S., 2000. Large clockwise rotations in an extensional allochthon, Alboran Domain (southern Spain). J. Geol. Soc. 157, 1187-1197.

Quintà, A., Tavani, S., 2012. The foreland deformation in the south-western Basque-Cantabrian Belt (Spain). Tectonophysics 576-577, 4-19.

Ramsay, J.G., 1967. Folding and Fracturing of Rocks. McGraw-Hill Book Company, New York (568 pp.).

Réhault, J.P., Honthaas, C., Guennoc, P., Bellon, H., Ruffet, G., Cotten, J., Sosson, M., Maury, R.C., 2012. Offshore Oligo-Miocene volcanic fields within the Corsica-Liguria Basin: magmatic diversity and slab evolution in the western Mediterranean Sea. Journal of Geodynamics 58, 73-95.

Reiter, F., Acs, P., 1996-2003. Tectonics FP. Software for Structural Geology Innsbruck University, Austria (http://www.tectonicsfp.com/).

Ring, U., Glodny, J., 2010. No need for lithospheric extension for exhuming (U) HP rocks by normal faulting. Journal of the Geological Society of London 167, 225-228. http://dx.doi.org/10.1144/0016-76492009-134.

Rosenbaum, G., Lister, G.S., 2004. Formation of arcuate orogenic belts in the western Mediterranean region. In: Arlo, B.W., Sussman, A. (Eds.), Orogenic Curvature: Integrating Paleomagnetic and Structural Analyses, vol. 383. Geological Society of America Special Paper, 41-56.

Rossetti, F., Faccenna, C., Goffé, B., Monié, P., Argentieri, A., Funiciello, R., Mattei, M., 2001a. Alpine structural and metamorphic signature of the Sila Piccola Massif nappe stack (Calabria, Italy): insights for the tectonic evolution of the Calabrian Arc. Tectonics 20, 112-133.

Rossetti, F., Faccenna, C., Jolivet, L., Funiciello, R., Goffé, B., Tecce, F., Brunet, C., Monié, P., Vidal, O., 2001b. Structural signature and exhumation P-T-t path of the Gorgonia blueschist sequenze (Tuscan Arcipelago, Italy). Ofioliti 26, 175-186.

Rossetti, F., Faccenna, C., Goffé, B., Funiciello, R., Monié, P., 2002. Tectono-metamorphic evolution of the ophiolite-bearing HP/LT Gimigliano-Monte Reventino unit (Gimigliano, Sila Piccola): Insights for the tectonic evolution of the Calabrian Arc. Bollettino della Societa Geologica Italiana 121, 56-67.

Rossetti, F., Goffé, B., Monié, P., Faccenna, C., Vignaroli, G., 2004. Alpine orogenic P-T-t deformation history of the Catena Costiera area and surrounding regions (Calabrian Arc, southern Italy): the nappe edifice of Northern Calabria revised with insights on the Tyrrhenian–Apennine system formation. Tectonics 23, TC6011. http://dx.doi.org/10. 1029/2003TC001560.

Roure, F., Casero, P., Vially, R., 1991. Growth processes and melange formation in the southern Apennines accretionary wedge. Earth and Planetary Science Letters 102, 395-412.

Russo, M., Zuppetta, A., Guida, A., 1995. Alcune precisazioni stratigrafiche sul Flysch del Cilento (Appennino meridionale). Bollettino della Società Geologica Italiana 114, 353-359.

Saddiqi, O., Feinberg, H., Elazzab, D., Michard, A., 1995. Paléomagnètisme des Pèridotites des Beni Boussera (Rif interne, Maroc): Conséquences pour l’évolution Miocene de l’Arc de Gibraltar. C.R. Acad. Sci 321, 361-368.

Sanz de Galdeano, C., Vera, J.A., 1992. Stratigraphic record and paleogeographical context of the Neogene basins in the Betic Cordillera, Spain. Basin Res. 4, 21-26.

Savelli, C., 2002. Time-space distribution ofmagmatic activity in the western Mediterranean and peripheral orogens during the past 30 Ma (a stimulus to geodynamic considerations).Journal of Geodynamics 34, 99-126.

Scandone, P., 1967. Studi di geologia lucana: la serie calcareo-silico-marnosa ed i suoi rapporti con l'Appennino calcareo. Bollettino della Società Naturalisti in Napoli 76, 301-469.

Scandone, P., 1972. Studi di Geologia lucana: carta dei terreni della serie calcareo-silico-marnosa e note illustrative. Bollettino della Società Naturalisti in Napoli, 81, 225-300.

Schettino, A., Turco, E., 2011. Tectonic history of the western Tethys since the late Triassic. Geol. Soc. Am. Bull. 123, 89-105.

Scisciani, V., Tavarnelli, E., Calamita, F., 2002. The interaction of extensional and contractional deformations in the outer zones of the Central Apennines, Italy. J. Struct. Geol. 24, 1647-1658.

Searle, M.P., Warren, C.J., Parrish, R.R., Waters, D.J., 2004. Structural evolution, metamorphism and restoration of the Arabian continental margin, Saih Hatat region, Oman Mountains.Journal of Structural Geology 26, 451-473.

Selli, R., 1957. Sulla trasgressione del Miocene nell'Italia meridionale. Giornale di Geologia 26, 1-54.

Selli, R., 1962. Il Paleogene nel quadro della geologia dell'Italia meridionale. Memorie della Società Geologica Italiana 3, 737-790.

Serrano, F., Sanz de Galdeano, C., Delgado, F., Lopez-Garrido, A.C., Martìn-Algarra,A., 1995. The Mesozoic and Cenozoic Complex in the Malaga area: a Paleogene olistostrome-type chaotic complex (Betic Cordillera, Spain). Geol. Mijnb. 74, 105-116.

Serrano, F., Guerra-Merchán, A., El Kadiri, K., Sanz de Galdeano, C., López-Garrido, A., Martín-Martín, C., Hlila, M.R., 2007. Tectono-sedimentary setting of the Oligocene-early Miocene deposits on the Betic-Rifian Internal Zone (Spain and Morocco). Geobios 40, 191-205.

Shimabukuro, D.H., Wakabayashi, J., Alvarez, W., Chang, S., 2012. Cold and old: the rock record of subduction initiation beneath a continental margin, Calabria, southern Italy. Lithosphere 4, 524-532. http://dx.doi.org/10.1130/L222.1.

Shiner, P., Beccacini, A., Mazzoli, S., 2004. Thin-skinned versus thick-skinned structural models for Apulian carbonate reservoirs: constraints from the Val D'Agri fields. Marine and Petroleum Geology 21, 805-827.

Sibson, R.H., 2004. Controls on maximum fluid overpressure defining conditions for mesozonal mineralization. J. Struct. Geol. 26, 1127-1136.

Spadea, P., 1976. I carbonati nelle rocce metacalcaree della Formazione del Frido della Lucania. Ofioliti 1, 431-456.

Spadea, P., Tortorici, L. and Lanzafame, G., 1980. Ophiolites of Lucanian Apennine. In: Field Guide to 4th OphioliteField Conference, Italy.

Spadea, P., 1982. Continental crust rocks associated with ophiolites in Lucanian Appennine (southern Italy). Ofioliti 2 (3), 501-522.

Stöckhert, B., Wachmann, M., Küster, M., Bimmermann, S., 1999. Low effective viscosity during high pressuremetamorphismdue to dissolution precipitation creep: the record of HP-LT metamorphic carbonates and siliciclastic rocks from Crete. Tectonophysics 303, 299-319.

Suter, G., 1965. La région du Moyen Ouerrha (Rif, Maroc): étude préliminaire sur la tectonique et la stratigraphie. Notes et Mémoires du Service géologique du Maroc, 24, 7-17.

Suter, G., 1980. Carte structurale de la chaîne rifaine au 1:500,000. Notes et Mémoires du Service géologique du Maroc 245p.

Tavani, S., Mencos, J., Bausà, J., Muñoz, J.A., 2011a. The fracture pattern of the Sant Corneli Bóixols oblique inversion anticline (Spanish Pyrenees). J. Struct. Geol. 33(11), 1662-1680.

Tavani, S., Quintá, A., Granado, P., 2011b. Cenozoic right-lateral wrench tectonics in the Western Pyrenees (Spain): the Ubierna Fault System. Tectonophysics 509, 238-253.

Tavarnelli, E., 1996. The effects of pre-existing normal faults on thrust ramp development: an example from the northern Apennines, Italy. Geol. Rundsch. 85, 363-371.

Thomson, S.N., 1998. Assessing the nature of tectonic contacts using fission-track thermochronology: an example from the Calabrian Arc, southern Italy. Terra Nova 10, 32-36.

Thomas, M.F.H., Bodin, S., Redfern, J., Irving, D.H.B., 2010. A constrained African craton source for the Cenozoic Numidian Flysch: implications for the paleogeography of the western Mediterranean basin. Earth Sci. Rev. 101, 1-23.

Turco, E., Macchiavelli, C., Mazzoli, S., Schettino, A., Pierantoni, P.P., 2012. Kinematic evolution of Alpine Corsica in the framework of Mediterranean mountain belts. Tectonophysics 579, 193-206.

Uzkeda, H., Bulnes, M., Poblet, J., García-Ramos, J.C., Piñuela, L., 2013. Buttressing and reverse reactivation of a normal fault in the Jurassic rocks of the Asturian Basin, NW Iberian Peninsula. Tectonophysics 599, 117-134.

Vezzani, L., 1966. La sezione Tortoniana di Perosa sul fiume Sinni presso Episcopia. Geologica Romana 5, 263-290.

Vezzani, L., 1968. Distribuzione, facies e stratigrafia della Formazione del Saraceno (Albiano-Daniano) nell'area compresa tra il Mare Ionio ed il Torrente Frido. Geologica Romana 7, 229-276.

Vignaroli, G., Faccenna, C., Rossetti, F., Jolivet, L., 2009. Insights from the Apennines metamorphic complexes and their bearing on the kinematics evolution of the orogen. Geological Society Special Publication 311, 235-256.

Vignaroli, G., Minelli, L., Rossetti, F., Balestrieri, M.L., Faccenna, C., 2012. Miocene thrusting in the eastern Sila Massif: Implication for the evolution of the Calabria-Peloritani orogenic wedge (southern Italy). Tectonophysics 538-540, 105-119.

Vitale, S., White, J.C., Iannace, A., Mazzoli, S., 2007. Ductile strain partitioning inmicritic limestones, Calabria, Italy: the roles and mechanisms of intracrystalline and intercrystalline deformation. Can. J. Earth Sci. 44, 1587-1602.

Vitale, S., Mazzoli, S., 2010. Strain analysis of heterogeneous ductile shear zones based on planar markers. J. Struct. Geol. 32, 321-329.

Vitale, S., Mazzoli, S., 2008. Heterogeneous shear zone evolution: the role of shear strain hardening/softening. Journal of Structural Geology 30, 1363-1395.

Vitale, S., Mazzoli, S., 2009. Finite strain analysis of a natural ductile shear zone in limestones: insights into 3-D coaxial vs. non-coaxial deformation partitioning. Journal of Structural Geology 31, 104-113.

Vitale, S., Ciarcia, S., Mazzoli, S., Iannace, A., Torre, M., 2010. Structural analysis of the ‘Internal’ Units of Cilento, Italy: new constraints on the Miocene tectonic evolution of the southern Apennine accretionary wedge. Comptes Rendus Geosciences 342, 475-482.

Vitale, S., Ciarcia, S., Mazzoli, S., Zaghloul, M.N., 2011. Tectonic evolution of the ‘Liguride’ accretionary wedge in the Cilento area, southern Italy: a record of early Appennine geodynamics. J. Geodynamics 51, 25-36.

Vitale, S., Dati, F., Mazzoli, S., Ciarcia, S., Guerriero, V., Iannace, A., 2012. Modes and timing of fracture network development in poly-deformed carbonate reservoir analogues, Mt. Chianello, southern Italy. J. Struct. Geol. 37, 223-235.

Vitale, S., Ciarcia, S., 2013. Tectono-stratigraphic and kinematic evolution of the southern Apennines/Calabria-Peloritani Terrane system (Italy). Tectonophysics 583, 164-182.

Vitale, S., Ciarcia, S., Tramparulo, F.D.A., 2013a. Deformation and stratigraphic evolution of the Ligurian Accretionary Complex in the southern Apennines (Italy). J. Geodyn. 66, 120-133.

Vitale, S., Fedele, L., Tramparulo, F.D.A., Ciarcia, S., Mazzoli, S., Novellino, A., 2013b. Structural and petrological analyses of the Frido Unit (southern Italy): new insights into the early tectonic evolution of the southern Apennines-Calabrian Arc system. Lithos 168-169, 219-235.

Vitale, S., Zaghloul, M.N., Tramparulo, F.D.A., El Ouaragli, B., 2014a. Deformation characterization of a regional thrust zone in the northern Rif (Chefchaouen, Morocco). J. Geodyn. 77, 22-38.

Vitale, S., Zaghloul, M.N., Tramparulo, F.D.A., El Ouaragli, B., 2014b. From Jurassic extension to Miocene shortening: An example of polyphasic deformation in the External Dorsale Calcaire Unit (Chefchaouen, Morocco) Tectonophysics 633, 63-76.

Wildi, W., Nold, M., Uttinger, J., 1977. La Dorsale Calcaire entre Tetouan et Assifane (Rif interne, Maroc). Eclogae Geol. Helv. 70, 371-415.

Wildi, W., 1983. La chaîne tello-rifaine (Algérie, Maroc, Tunisie): structure, stratigraphie et évolution du Trias au Miocène. Rev. Géol. Dyn. Géogr. Phys. 24, 201-297.

Wiltschko, D.V., Eastman, D.B., 1982. Role of basement warps and faults in localizing thrust-fault ramps. Geol. Soc. Am. Mem. 158, 177-190.

Wortel, M.J.R., Spackman, W., 2000. Subduction and slab detachment in the Mediterranean-Carpathian region. Science 290, 1910-1917.

Zaghloul, M.N., 1994. Les Unités Federico septentrionales (Rif interne, Maroc): Inventaire des deformations et leur contexte géodynamique dans la chaine Bético-Rifaine (MSc Thesis) Mohammed V University, Rabat, Morocco (218 pp.).

Zaghloul, M.N., Di Staso, A., El Moutchou, B., Gigliuto, L.G., Puglisi, D., 2005. Sedimentology, provenance and biostratigraphy of the Upper Oligocene-Lower Miocène terrigenous deposits of the internal «DorsaleCalcaire» (Rif, Morocco): paleogeographic and geodynamic implications. Boll. Soc. Geol. It. 124, 437-454.

Ziegler, P.A., Cloetingh, S., Van Wees, J.D., 1995. Dynamics of intraplate compressional deformation: the Alpine foreland and other examples. Tectonophysics 252, 7-59.

Zuppetta, A., Russo, M., Turco, E., 1984. Alcune osservazioni sulle Tufiti di Tusa nell'area compresa tra la Valsinni e Rocca Imperiale (confine calabro-lucano). Boll. Soc. Geol. It., 103, 623-627.

Zuppetta A., Mazzoli S., 1997. Deformation history of a synorogenic sedimentary wedge, northern Cilento area, southern Apennines thrust and fold belt, Italy. Geological Society of America Bulletin, 109: 698-708.